TECHNICAL REPORT STANDARD TITLE PAGE

1. Report Number	2. Government Accession No.	3. Recipient's Catalog No.
FHWA/TX-92/1165-2F		

4. Title and Subtitle	5. Report Date
EFFECTIVENESS OF CONTROLLING PAVEMENT ROUGHNESS DUE TO EXPANSIVE CLAYS WITH VERTICAL MOISTURE BARRIERS	November 1992 Revised May 1993
	6. Performing Organization Code

7. Author(s)	8. Performing Organization Report No.
Ranasinghege Jayatilaka, Derek A. Gay, Robert L. Lytton, W. Kent Wray	Research Report 1165-2F

9. Performing Organization Name and Address	10. Work Unit No.
Texas Transportation Institute The Texas A&M University System College Station, Texas 77843-3135	11. Contract or Grant No. Study No. 2/11/8-88-1165

12. Sponsoring Agency Name and Address	13. Type of Report and Period Covered
Texas Department of Transportation Transportation Planning Division P. O. Box 5051 Austin, Texas 78763	Final Report - Sept. 1987 November 1992
	14. Sponsoring Agency Code

15. Supplementary Notes

Research performed in cooperation with the Texas Department of Transportation and the U.S. Department of Transportation, Federal Highway Administration.

16. Abstract

This report summarizes the results and conclusions of a five year study of the effectiveness of vertical moisture barriers in controlling the roughness of pavements resting on expansive clay subgrades. During the study, vertical moisture barriers were installed at six sites in three of the seven climatic zones in Texas. Site maps are given for each site showing the location of the moisture barriers and the moisture sensors relative to the pavements along which they were placed. The moisture (suction) was monitored on both sides of the barrier for the remainder of the period of this study. In addition, the surface profiles of these pavements in each lane were measured every six months with the TxDOT GM profilometer. Samples of the soil were taken and laboratory tests of the Atterberg limits, grain size distribution and suction vs. water content relations were made.

A finite element program, FLODEF, which couples moisture flow and elasticity was calibrated to reproduce the field observations of suction in each of the locations. The program was then used to perform a study of the effects of climatic zone (five cities across Texas were used), degree of cracking in the soil, depth of the root zone, depth of the moisture barrier (4 depths were tried), and lateral drainage condition (3 conditions were used) on the rate of increase of pavement roughness. The program shows the conditions under which moisture barriers will be effective and other conditions in which moisture barriers will have little effect. Sites in wet and semi-arid climates, with cracked clay soils and shallow root zones, will show the greatest benefit from using vertical moisture barriers.

Measured pavement roughness as indicated by the serviceability index, International roughness index, and bump height are compared with the same values predicted using the computer program and show that realistic trends can be predicted.

Appendices show how to measure suction with filter paper and record all of the field measurements of suction and pavement roughness that have been made in this study.

17. Key Words	18. Distribution Statement
Vertical Moisture Barriers, Expansive Clays, Suction, Pavement Roughness, Suction-vs-Water Content Relations, Thornthwaite Moisture Index, Suction Compression Index, Diffusivity, Serviceability Index, International Roughness Index, Maximum Bump Height	No Restrictions. This document is available to the public through the National Technical Information Service, 5285 Port Royal Road Springfield, Virginia 22161

19. Security Classif.(of this report)	20. Security Classif.(of this page)	21. No. of Pages	22. Price
Unclassified	Unclassified	224	

Form DOT F 1700.7 (8-69)

EFFECTIVENESS OF CONTROLLING PAVEMENT ROUGHNESS DUE TO EXPANSIVE CLAYS WITH VERTICAL MOISTURE BARRIERS

Research Study No. 2/11-8-88-1165

by

Ranasinghege Jayatilaka

Derek A. Gay

Robert L. Lytton

W. Kent Wray

Sponsored by the

Texas Department of Transportation

Texas Transportation Institute
Texas A&M University System
College Station, Texas 77843-3135

and

Texas Tech University
Lubbock, Texas 79409

Revised May 1993

METRIC (SI*) CONVERSION FACTORS

APPROXIMATE CONVERSIONS TO SI UNITS

Symbol	When You Know	Multiply By	To Find	Symbol
LENGTH				
in	inches	2.54	centimetres	cm
ft	feet	0.3048	metres	m
yd	yards	0.914	metres	m
mi	miles	1.61	kilometres	km
AREA				
in²	square inches	645.2	centimetres squared	cm²
ft²	square feet	0.0929	metres squared	m²
yd²	square yards	0.836	metres squared	m²
mi²	square miles	2.59	kilometres squared	km²
ac	acres	0.395	hectares	ha
MASS (weight)				
oz	ounces	28.35	grams	g
lb	pounds	0.454	kilograms	kg
T	short tons (2000 lb)	0.907	megagrams	Mg
VOLUME				
fl oz	fluid ounces	29.57	millilitres	mL
gal	gallons	3.785	litres	L
ft³	cubic feet	0.0328	metres cubed	m³
yd³	cubic yards	0.0765	metres cubed	m³

NOTE: Volumes greater than 1000 L shall be shown in m³.

TEMPERATURE (exact)

°F	Fahrenheit temperature	5/9 (after subtracting 32)	Celsius temperature	°C

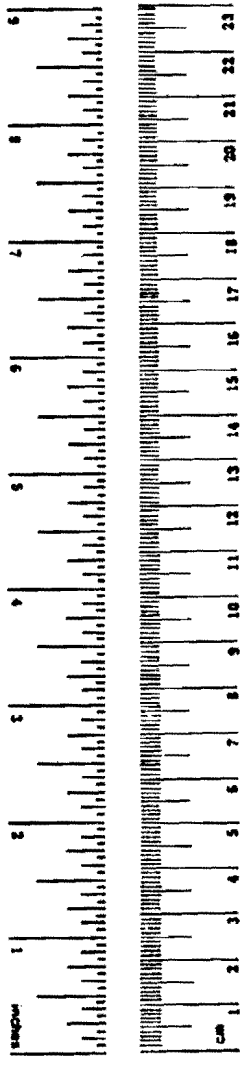

APPROXIMATE CONVERSIONS TO SI UNITS

Symbol	When You Know	Multiply By	To Find	Symbol
LENGTH				
mm	millimetres	0.039	inches	in
m	metres	3.28	feet	ft
m	metres	1.09	yards	yd
km	kilometres	0.621	miles	mi
AREA				
mm²	millimetres squared	0.0016	square inches	in²
m²	metres squared	10.764	square feet	ft²
km²	kilometres squared	0.39	square miles	mi²
ha	hectores (10 000 m²)	2.53	acres	ac
MASS (weight)				
g	grams	0.0353	ounces	oz
kg	kilograms	2.205	pounds	lb
Mg	megagrams (1 000 kg)	1.103	short tons	T
VOLUME				
mL	millilitres	0.034	fluid ounces	fl oz
L	litres	0.264	gallons	gal
m³	metres cubed	35.315	cubic feet	ft³
m³	metres cubed	1.308	cubic yards	yd³

TEMPERATURE (exact)

°C	Celsius temperature	9/5 (then add 32)	Fahrenheit temperature	°F

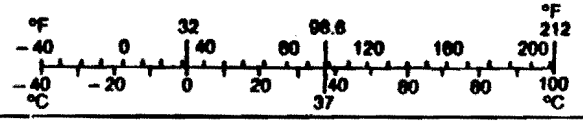

These factors conform to the requirement of FHWA Order 5190.1A.

* SI is the symbol for the International System of Measuremsnts

IMPLEMENTATION STATEMENT

This report contains a comprehensive study to determine the conditions across the State in which vertical moisture barriers will effectively control the rate at which pavement roughness due to expansive soils will develop. These findings should be reviewed when considering whether to place a moisture barrier and how deep it should go. The following are characteristics of sites where vertical moisture barriers will usually prove effective:

1. Climatic area: wet to semi-arid
2. Depth of barrier: deeper than root depth
3. Lateral drainage conditions: wet, normal, or dry
4. Soil condition: cracked or moderately cracked

In the arid zones of the States, moisture barriers will improve performance when the lateral drainage condition is wet.

The results of this study should be implemented by reviewing the conclusions of this report when any pavement site on expansive clay is being considered for a moisture barrier at both District and residency level.

There are three more findings that are implementable. The first is that a thorough site investigation including soils borings should be conducted prior to installing a moisture barrier. The borings should be twice as deep as the expected depth of the moisture barrier. The soils data should include water content, Atterberg limits, and suction measurements with depth in each boring. Suction can be measured using filter paper according to the method described in Appendix A. This permits a determination of how effective the moisture barrier will be once it is installed.

The second finding is to carry the moisture barriers to a depth equal to the greatest depth where root fibers were found in any boring.

The third finding is to crown and pave all median strips in expansive clay areas wherever that is possible in order to reduce the roughness caused by water entering the subgrade in the median.

DISCLAIMER

The contents of this report reflect the view of the authors who are responsible for the opinions, findings, and conclusions presented herein. The contents do not necessarily reflect the official view or policies of the Texas Department of Transportation or the Federal Highway Administration. This report does not constitute a standard, specification, or regulation.

There is no invention or discovery conceived or first actually reduced to practice in the course of or under this contract, including any art, method, process, machine, manufacture, design or composition of matter, or any new and useful improvement thereof, or any variety of plant which is or may be patentable under the patent law of the United States of America or any foreign country. This report is not intended for construction, bidding or permit purposes.

ACKNOWLEDGEMENTS

Acknowledgements are due to a number of TTI employees who have contributed to the completion of this study and its final report. Special thanks to Mary Anne Reese-Rodriguez; Dr. Keith Wallace, Professor of Civil Engineering at Queensland University of Technology, Brisbane, Queensland, Australia; and Andrzej Wojtasik, Fulbright Scholar from Poznan, Poland; all of whom contributed significantly to the work reported here.

TABLE OF CONTENTS

PAGE

LIST OF TABLES

LIST OF TABLES (Continued)

LIST OF TABLES (Continued)

LIST OF FIGURES

LIST OF FIGURES (Continued)

LIST OF FIGURES (Continued)

LIST OF FIGURES (Continued)

LIST OF FIGURES (Continued)

LIST OF FIGURES (Continued)

LIST OF FIGURES (Continued)

LIST OF FIGURES (Continued)

CHAPTER I

INTRODUCTION

GENERAL

Expansive soils are clay soils which exhibit significant volume changes with changes in their ambient environment. If an expansive soil gains moisture, it swells and upward movement results. On the other hand, if it loses moisture, the soil shrinks and settlement occurs. The volume change of a clay soil due to changes in water content is caused by interaction between clay minerals and water (1).

The magnitude of volume change is dependent upon the in situ soil properties and site conditions, and the environmental conditions (2). The soil properties include the type and amount of clay, the thickness and location of potentially expansive clay layers, and the depth of the active zone. Montmorillonite is the predominant clay mineral found in most of the highly expansive soils (3). However, the other clay minerals such as kaolinite, illite, vermiculite, and chlorite also exhibit some degree of expansiveness. Rainfall, evapotranspiration, site drainage and location, and type of vegetation are the environmental factors that affect the magnitude of volume change of expansive soils. Vegetation will cause the soil to dry much more rapidly, thus enhancing the shrinkage of soil (4). Due to the variation of moisture conditions and soil properties, the magnitude of volume change may be different from point to point. This condition results in differential movement of soil which is detrimental for structures built on shallow foundations, such as buildings, highway pavements, and airport pavements.

In the United States, approximately 20 percent of the area is underlain by moderately to highly expansive soils (5). These soils cause at least 2.3 billion dollars worth of damage annually, which is more than the combined damages caused by natural catastrophes such as earthquakes, tornadoes, hurricanes, and floods (6). More than half of this estimated damage is attributed to highways and streets.

The most common types of distress modes observed in highway pavements built on expansive soils are as follows:

1. Surface unevenness distributed over a considerable length of road
2. Longitudinal cracks
3. Excessive deformations in locations such as pipe culverts where moisture concentration occurs

When a pavement is built on an expansive soil, the existing moisture flow pattern will be altered (7). The moisture condition at the center of the pavement will remain virtually unchanged, while at the edge, moisture fluctuations will occur in response to rainfall and evapotranspiration. This moisture variation causes the lateral differential pavement movement of the pavement. Differential movement is the main source of roughness development in pavement structures on expansive soils. The major effects of the development of roughness are the loss of riding comfort and road-holding ability, a reduction in pavement service life, and costly rehabilitation (8).

The greatest challenge of researchers dealing with expansive soils is the invention of successful methods to mitigate damages associated with expansive soils. Various methods (3,9,10,11) with varying degrees of success have been attempted in the past. All these

methods can be grouped into two categories:

1. Alteration of expansive material by mechanical, chemical or physical means
2. Control of subgrade moisture conditions

Mechanical alteration includes ripping, scarifying and then compacting the soil with moisture and/or density control. The subexcavation and replacement with granular or non swelling or chemically treated materials can also be grouped in this category. The third method in this category is the use of fills over expansive soils in order to reduce heave as a result of the external load. The physical alteration method requires the mixing of expansive soil with granular or non swelling material. Chemical alteration refers to the addition of chemical compounds to alter the characteristics of clay minerals. Lime is the most extensively used chemical for modification of expansive soils.

The control of the subgrade moisture condition is achieved by prewetting the subgrade or by introducing a physical barrier enclosing the subgrade soil. The idea of prewetting or ponding a subgrade prior to the construction of a pavement is to minimize the volume change after the construction by allowing preswelling of the subgrade as a result of the increased moisture condition. The stabilization of subgrade moisture condition can be achieved by a physical barrier. The following methods have been attempted in the past:

1. Sprayed asphalt membrane over the subgrade, ditches, verge slope and backslope

2. Full-depth asphalt pavement with a sprayed asphalt or synthetic fabric membrane beneath the ditch
3. Full-depth asphalt pavement with paved ditches in cut sections
4. Vertical synthetic impermeable fabric membrane cutoffs

Prewetting a subgrade before the pavement placement and the horizontal membrane technique have shown promising results in improving the pavement performance (12,13). The limitation of the ponding method and the horizontal membrane method is that they can only be used as a preconstruciton measure.

Unlike the methods described above, a vertical moisture barrier can be used either before or after the placement of a pavement. Therefore, a vertical moisture barrier seems to be a better solution for the mitigation of damage in highway pavements caused by expansive soils.

SCOPE OF THE STUDY

The objectives of this research are to (a) evaluate the effectiveness of vertical moisture barriers in reducing the development of roughness in pavements on expansive soils, (b) recommend suitable moisture control installations for various drainage, soil, and climatic conditions, and (c) recommend suitable site investigation practices for the design of vertical moisture barriers.

To begin the study, the existing literature on vertical moisture barriers and related subjects was reviewed and is presented in chapter II of this report.

In order to investigate the effectiveness of vertical moisture

barriers in highway pavements, a total of eleven pavement test sections from six locations in three climatic regions in Texas, were selected to satisfy the following requirements:

1. Have an expansive soil subgrade
2. Have a history of repeated maintenance requirements
3. Roadway in a cut, at natural grade or at minimum fill
4. Have a distressed length at least 0.25 mile long

There were three test sections at Snyder, two sections each at Wichita Falls, Dallas, and Ennis, and one section each at Seguin and Converse.

Calibrated instruments for the measurement of in situ soil suction were installed at all of the selected test sites. Thermal moisture sensors or thermocouple psychrometers were placed at different depths of subgrade inside and outside of barriers. The thermocouple psychrometers were installed in sections at Snyder and Wichita Falls, while the test sections at other locations were instrumented with the thermal moisture sensors.

Vertical moisture barriers were installed along both edges of the pavement at eight of the selected test sections. These were at Dallas (two sections), Snyder (three sections), and one section each at Wichita Falls, Converse and Seguin.

In order to characterize the subgrade soils in test sections, disturbed soil samples from all test sites were collected and tested in the laboratory. Testing included the Atterberg limits, grain size distribution, and laboratory suction using pressure plate apparatus. Periodic readings of in situ soil suction were taken from the moisture measuring devices. In addition, profilometer readings were taken on a

bi-annual basis in order to measure the roughness development on pavements. A detailed description of the test sites and test results are presented in Chapter III of this report.

In Chapter IV of this report, estimates are made of the expansive properties and flow properties of subgrade soils using soil test results and existing empirical methods (14,15,16). In addition, the flow and deformation(FLODEF) program (17) is used to predict the suction values at different depths of test pavement sections inside and outside of the barriers. The measured suction values are then compared with these predicted values.

A parametric study was carried out in order to estimate the vertical movement in highway pavements in different climatic regions under different drainage and soil conditions. The FLODEF program was used in this respect. The estimated vertical movements are then used to predict the roughness development in the pavement. These results are presented and discussed in Chapter V.

Chapter VI contains the final conclusions of this research study and the recommendations that result from them.

CHAPTER II

REVIEW OF EXISTING LITERATURE

INTRODUCTION

The study of the effectiveness of vertical moisture barriers in reducing the development of roughness in pavements on expansive soils requires the evaluation of (a) climatic condition of the locality, (b) expansive properties of the subgrade soil, (c) moisture variation under the pavement structure, and (d) roughness development on pavement surface. An indication of the climatic condition of a particular area can be obtained from the value of the Thornthwaite Moisture Index (18) of that area.

Most expansive soils encountered in engineering problems are in an unsaturated state. Knowledge of the moisture condition of such soil is best obtained by measuring soil suction (15). The most commonly used methods of measuring soil suction include the thermal moisture sensor, thermocouple psychrometer,and filter paper. The filter paper method works well for all ranges of moisture content, while the psychrometer is accurate only when the soil is drier than the plastic limit. The thermal moisture sensors are accurate in measuring soil suction above -1 bar but lose sensitivity below that level of suction (19).

This chapter reviews the existing literature on (a) vertical moisture barriers, (b) characterization of expansive soils, and (c) measurement of roughness on pavements.

VERTICAL MOISTURE BARRIERS

A vertical moisture barrier can be used in highway pavements to

minimize the roughness development on pavements by minimizing the subgrade moisture changes beneath the pavement structure. The Texas Department of Transportation (TxDOT) installed two deep vertical fabric moisture barriers on Interstate Highway Loop 410 and on Interstate Highway 37 in San Antonio, Texas in 1978 and 1979 (20,21,22). Base on previous observations that the depth of active zone was between 8-10 feet in the San Antonio area, these barriers were installed to a depth of 8 feet. Both sites showed less roughness development over time than companion control sections.

Based on these limited results alone, it is not possible to conclude that the vertical moisture barrier is the best solution for the problem of expansive soils. There are many factors that affect the effectiveness of vertical moisture barriers. The main factors determining the effectiveness of a barrier are rainfall and evapotranspiration (23). Drainage condition, cracked pattern and soil properties play an important role in determining the amount of water in the subgrade. Therefore, it is necessary to consider all these factors in the design of a vertical moisture barrier.

Picornell (24) developed a design procedure that would allow the determination of the depth of a barrier needed for a particular site based on its climatic condition and the subsoil characteristics. This approach assumed that the barrier performs different roles depending on the moisture condition of the subsoil at the time of installation of barrier. Two basic assumptions made in this procedure were (a) if the soil is at an advanced stage of desiccation, the barrier will prevent the access of free water to the shrinkage crack fabric, and (b) if the subsoil is initially very wet, the crack fabric is closed and it does

not allow the movement of water. The role of the barrier in this condition is the prevention of excessive drying of the soil under the edges of the pavement.

From both points of view, the worst drought condition governs the design is associated with the worst intensity of the drought that seems possible at a particular site. A statistical analysis of existing records of meteorological data was made to evaluate the worst drought condition of a particular site for a return period equal to the design life of a pavement.

Since the pavements are essentially impermeable, the rainfall that falls on the pavement runs off towards the uncovered ground surface between the shoulder and the drainage ditch. The effect of this extra supply of water available for infiltration was taken into account by multiplying the direct rainfall by a Rainfall Multiplying Factor (RMF). In that study, the coefficient RMF was treated as a parameter that ranges between 1 and 5. The RMF values for a particular highway section were chosen based on the relative width of the pavement, the uncovered soil profile adjacent to the pavement edge, and the geometric characteristics of the roadway cross section. The finite element method was used in the modelling of moisture flow and in the analysis of non linear elastic deformation of the soil.

This procedure allows the determination of the depth of a barrier for a particular climatic environment and site condition by two criteria: the edge distortion criterion and the maximum crack depth criterion. In the edge distortion criterion, the barrier depth is chosen as the smaller depth that would maintain an angular distortion of 1/360 or less at the edge of the pavement. When the moisture barrier

is intended to prevent the development of roughness, the criterion should be the maximum crack depth. In that case, the barrier should be extended to the maximum crack depth expected with the hydrologic regime imposed by the pavement or to the crack depth existing at the time of construction, whichever is larger.

Picornell suggests that the edge distortion criterion be used to determine the depth of a barrier if the initial soil conditions are at its equilibrium condition or wetter than the equilibrium condition. The crack depth criterion is suggested when the initial moisture condition is drier than the equilibrium condition. Based on this study, Picornell and Lytton (24) suggested that a barrier be placed to the depth of the roots in order to stop longitudinal cracking and about 25 percent deeper than the root depth to stop the development of roughness.

Gay (17) used the development of roughness on pavements to study the performance of vertical moisture barriers using data collected on ten expansive clay sites in three different climatic regions in Texas. The findings of this study include the following:

1. Highway sections with median drains in which no moisture barriers were installed showed an increased level of roughness in the inside lanes of 2 to 4 times over the outside lanes. Sections in which moisture barriers were present showed a similar trend but the difference between the inside and outside lanes was approximately 2 times.
2. A low level of roughness development was observed in the pavement sections which were rehabilitated after significant damage from expansive clay activity. This suggests that the vertical moisture barriers help to

maintain the soil moisture condition over time in subgrade soils in which an equilibrium moisture condition has been attained.

3. Moisture barrier sections in which equilibrium conditions had not been reached showed roughness development rates similar to that of sections without barriers.
4. A little difference of overall performance was observed between the moisture barriers placed to depths of 6 ft and 8 ft. However, the 8 ft deep barrier was more efficient in accelerating roughness development.

In that study, the roughness data was collected on several pavement sections with and without barriers for up to ten years and analyzed. Roughness prediction models were developed through the regression analysis of the rates of roughness development and the expected value of vertical movement. The expected value of vertical movement for each site was estimated by integrating over depth the changes in vertical movement as a function of the change in matrix suction between the expected wet and dry suction profiles. The wet, dry, and equilibrium suction profiles were obtained by applying a monthly moisture balance procedure to historical records of weather data. These roughness prediction models allow the estimation of roughness development on pavements with paved or sodded medians, and in pavements where the barriers are present or where there are no barriers installed.

CHARACTERIZATION OF EXPANSIVE SOILS

A reliable and efficient method for the identification and

classification of expansive soils is important in the design of any type of remedial measures for expansive soils. Many attempts have been made in the past to find an universal system for the identification and classification of expansive soils. Snethen (3,26) reviewed the then existing identification and classification techniques and divided them into three broad categories; indirect, direct, and combination.

In indirect techniques, one or more of the related intrinsic properties of expansive soils are measured and indicators of potential volume change are provided. Five indicator groups that comprise the indirect techniques are the soil composition, physiochemical properties, physical properties, index properties, and currently used soil classification systems. The most widely used indicator group is the index property group which involves properties such as liquid limit, plasticity index, and shrinkage limit.

The direct techniques include all of those methods which quantitatively assess the volume change characteristics of expansive soils. The measurement of these characteristics is accomplished by the use of odometer-type testing procedures.

The combination category is an extension of the index property group, and involves the correlation of indirect and direct techniques, either directly or by statistical reduction. The most widely used parameters are the liquid limit, plasticity index, shrinkage limit, colloidal content, activity, and swell or swelling pressures from odometer-type tests.

Presently available techniques for the quantitative characterization of expansive soils are (a) odometer tests, (b) soil suction tests, and (c) empirical methodology. The soil suction concept

and associated testing and prediction procedures provide a better characterization of the behavior of expansive soils and a more reliable estimate of anticipated volume change for selected conditions based on comparisons with measured field behavior (27).

Soil suction is a macroscopic property of soil which indicates the intensity with which a soil will attract water. The total suction is the negative gauge pressure relative to the external gas pressure on the soil water to which a pool of pure water must be subjected in order to be in equilibrium through a semi permeable membrane with the soil water (28). From a thermodynamic standpoint, the total suction can be written as (29):

$$\psi = -\frac{RT}{v_{wo}\omega_v} \ln \frac{u_v}{u_{vo}} \qquad (1)$$

Where

ψ = total suction (kPa)

R = universal (molar) gas constant (i.e., 8.31432 J/(mol K))

T = absolute temperature (i.e., T = 273.16+t^o) (K)

t^o = temperature (^oC)

v_{wo} = specific volume of water (i.e., $1/\rho_w$) (m^3/kg)

ρ_w = water density (i.e., 998 kg/m^3 at t^o =20^oC)

ω_v = molecular mass of water vapor (i.e., 18.016 kg/kmol)

u_v = partial pressure of pore-water vapor (kPa)

u_{vo} = saturation pressure of pore-water vapor over a flat surface at the same temperature (kPa)

The term u_v/u_{vo} is referred to as the relative humidity. The total suction is considered to be composed of matrix suction (u_a-u_w) and

osmotic (solute) suction (π) and can be expressed as:

$$\psi = (u_a - u_w) + \pi \qquad (2)$$

Where

u_a = pore-air pressure

u_w = pore-water pressure

Matrix suction is defined as the negative gauge pressure relative to the external gas pressure on the soil water, to which a solution identical in composition with the soil water must be subjected in order to be in equilibrium through a porous permeable wall with the soil water. The osmotic suction is the negative gauge pressure to which a pool of pure water must be subjected in order to be in equilibrium through a semipermeable (i.e., permeable to water molecules only) membrane with a pool containing a solution identical in composition with the soil water (28).

Numerous methods are available for the measurement of soil suction (27,28,29,30,31,32,33,34,35,36,37). Some of these methods are the (a) filter paper method (b) thermocouple psychrometer (c) thermal moisture sensor (d) pressure plate apparatus. The pressure plate apparatus can be used in the laboratory to obtain the relationship between moisture content and soil suction. The other methods can be used to measure in situ soil suction.

The filter paper method can be used to measure the total suction as well as the matrix suction. The filter paper is equilibrated with soil water, either through vapor phase or through combined liquid and vapor phase. The soil suction is obtained by measuring the water content of filter paper and using a filter paper calibration curve.

The matrix suction can be measured by placing a dry filter paper in contact with a soil specimen and reaching equilibrium through a combined liquid and vapor phase. On the other hand, the total suction is measured by placing a dry filter paper not in contact with a soil specimen and reaching equilibrium through a vapor phase. A detailed description of the procedure for measuring soil suction with filter paper is presented in Appendix A.

Thermocouple psychrometers are used to measure the total suction in a soil by determining the relative humidity in the soil using a Peltier cooling technique. By sending a small direct current of about 4 to 8 milliamperes through the thermocouple junction for about 15 seconds in the correct direction, this junction will cool and water will condense on it when the dew point temperature is reached. Condensation of this water prevents further cooling of the junction, and the voltage developed between the thermocouple and reference junction is measured by a microvoltmeter. The voltage outputs of the psychrometer are calibrated with total suction by tests with salt solutions, such as potassium chloride, that produce a given relative humidity for known concentrations. The total suction is related to relative humidity in accordance with Equation 1.

The thermal moisture sensor, which measures matrix suction in a soil, consists of a porous ceramic block containing a temperature sensing element and a miniature heater. Measurements are made by inserting the sensor into the soil and allowing the matrix suction in the ceramic block to come to equilibrium with the matrix suction in the soil. The equilibrium matrix suction is related to the water content in the porous block. To measure the water content in the porous block, a

controlled amount of heat is generated inside the porous block and the temperature rise after a fixed period of time is measured. The temperature rise is inversely proportional to the water content in the porous block. As a result, the measured temperature rise can be calibrated to measure the matrix suction in the soil.

Lytton (38) proposed the suction compression index to characterize the behavior of expansive soils. This index is expressed as:

$$\gamma_h = \frac{-\frac{\Delta V}{V_i}}{\log \frac{h_f}{h_i}} \qquad (3)$$

Where

γ_h = suction compression index

ΔV = volume change

V_i = initial volume

h_f = final value of soil suction

h_i = initial value of soil suction

McKeen (14,16) developed a chart method to estimate the value of γ_h with the use of clay content, plasticity index, and cation exchange capacity. Knowing the suction compression index and the expected suction variation through a soil column, it is possible to predict the heave of the soil column. This method has proven to be efficient and fairly reliable for the prediction of expansive properties of soil.

MEASUREMENT OF ROUGHNESS ON PAVEMENTS

Roughness characteristics of a pavement can be evaluated from following three methods (39):

1. profile based measurements and statistics
2. response type road roughness measuring systems
3. subjective panel ratings

Profile-Based Measurements and Statistics

In this method of roughness evaluation, relative elevations are measured at discrete intervals of a pavement, which are then used to obtain the parameters that describe the roughness characteristics of the pavement. The elevation measurements may be obtained from rod and level surveys, rolling wheel devices, or from non-contact computerized equipment such as GM profilometer. The Fourier transform techniques or numerical evaluation of first or second order derivatives using specified base lengths can be applied to obtain profile statistics. The Fourier amplitude spectrum has been used by Velasco and Lytton (40) in order to characterize roughness patterns on expansive clay. Gay and Lytton (41) used the amplitude versus wave length curve in order to introduce the Maximum Expected Bump Height to measure the roughness on pavements.

Response Type Road Roughness Measuring Systems (RTRRMS)

In this method of roughness evaluation, vehicle response to the pavement roughness is measured, and the measured response is translated to a value on a pre-calibrated scale. The measurements may be obtained from devices such as Mays Ride Meter. Mathematically modelled quarter car simulations which simulate vehicle dynamics based on road profile elevation may also be used to measure the roughness pattern. The International Roughness Index (IRI) is based on this quarter car simulation.

Subjective Panel Ratings

The Present Serviceability Rating (PSR) from the AASHO road test is a number between 0 and 5 returned by a rating panel, based on the perceived riding quality of test sections traversed in a vehicle of their choice. A predictive model, the Present Serviceability Index (SI), was developed to reproduce the PSR based on physical characteristics of the pavement surface.

CHAPTER III

DATA COLLECTION

INTRODUCTION

For this study, a total of eleven pavement sections founded on expansive soils were selected from six locations in three different climatic regions in Texas. There are seven different climatic regions in Texas as shown in Figure 1. There were three test sections at Snyder, two sections each at Wichita Falls, Dallas, and Ennis, and one section each at Seguin and Converse. The locations of these sites are shown in Figure 2. All of these eleven pavement sections were instrumented with suction measuring devices. A typical detailed layout of suction measuring devices is shown in Figure 3. In eight pavement sections, moisture barriers were installed along both edges of the pavement. The construction of a moisture barrier involves the (a) excavating of a one foot wide trench using an excavator, (b) placing of a fabric membrane, (c) backfilling the trench with sand or gravel, and (d) placing of a cement stabilized base cap over the backfill material. A typical cross section of a roadway with a vertical moisture barrier is shown in Figure 4. The exact locations and the details regarding moisture barriers and moisture measuring devices at each test pavement section are presented in Table 1. The site plans of the test sections are shown in Figures 5 through 10.

The rest of the sections in this chapter present a description of the test sites and a description of subsurface soil properties, in situ soil suction measurements, and the results of profilometer measurements.

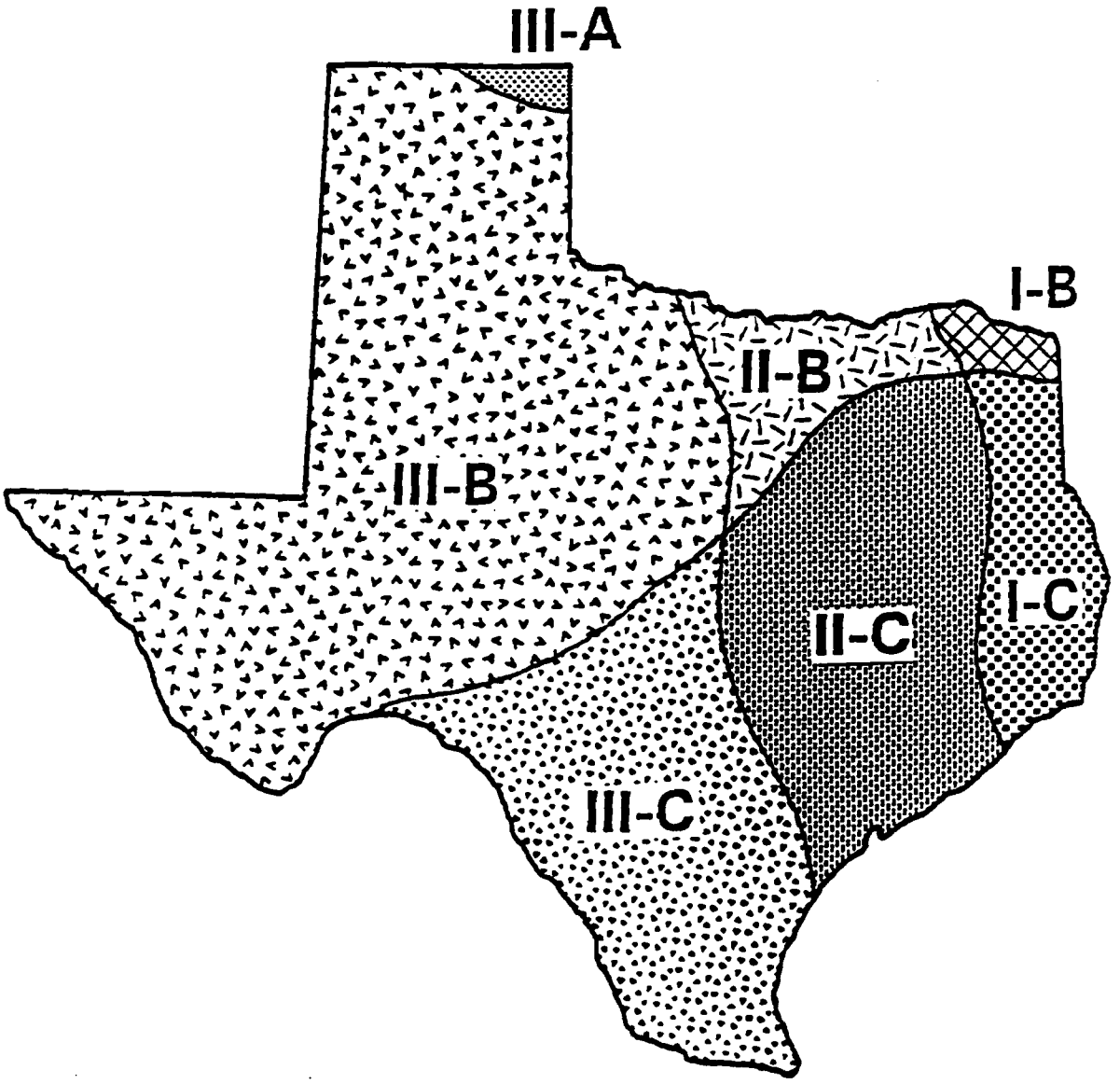

Figure 1. Climatic Zones in Texas

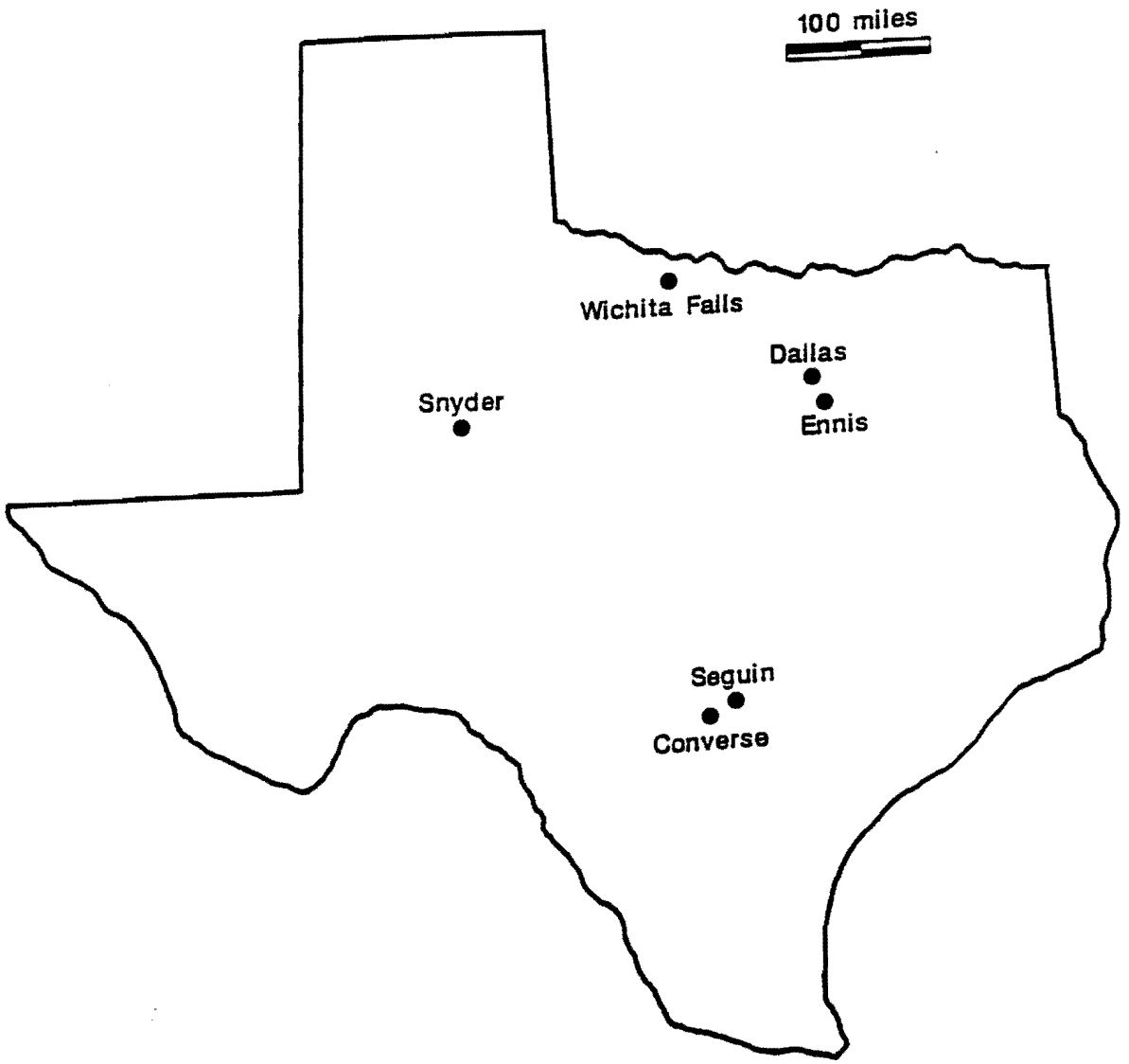

Figure 2. Location map of Test Sites

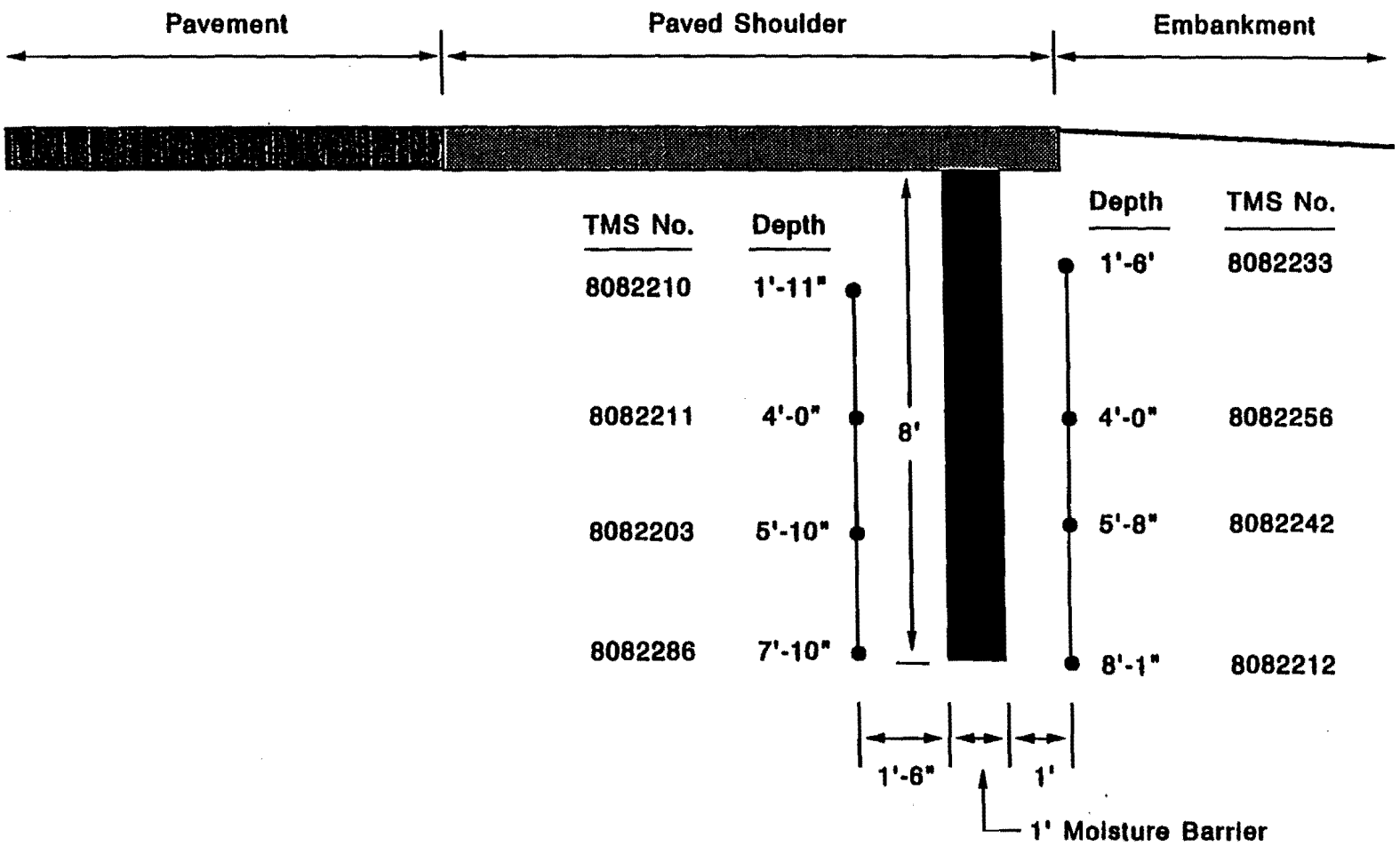

Figure 3. A Typical Layout of Suction Measuring Devices

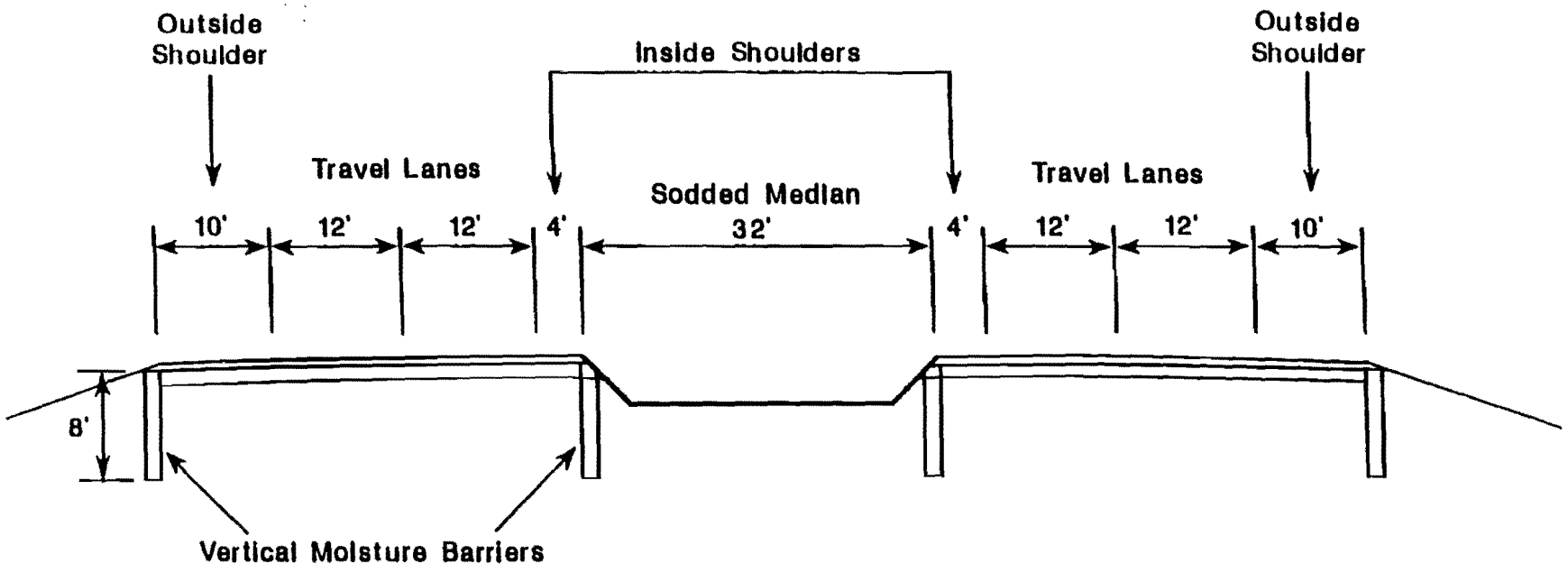

Figure 4. A Typical Cross Section of a Pavement with Vertical Moisture Barriers

Table 1. Moisture Barrier Site Configuration Summary

Test site	Name of Roadway	Climatic Region	Details of Moisture Barrier			Details of Moisture Measuring Device	
			Date of Installation	Type of Barrier	Length (ft)	Date of Installation	Device Type
Dallas 1	IH 635 Westbound	II-B	Sept., 1990	Vertical Fabric	600	Sept., 1990	Thermal Moisture Sensor
Dallas 2	IH 635 Eastbound	II-B	Dec., 1991	Vertical Fabric	600	Dec., 1991	Thermal Moisture Sensor
Ennis 1	Northbound Frontage IH 45	II-B	--	--	--	Aug., 1990	Thermal Moisture Sensor
Ennis 2	Northbound Frontage IH 45	II-B	--	--	--	Aug., 1990	Thermal Moisture Sensor
Seguin	IH 10 Westbound	III-C	Nov., 1988	Vertical Fabric	13200	Nov., 1988	Thermal Moisture Sensor
Converse	FM 1516	III-C	Nov., 1989	Vertical Fabric	7300	June, 1989	Thermal Moisture Sensor
Snyder 1	US 84 Northbound	III-B	June, 1990	Vertical Fabric	500	June, 1989	Psychrometer

Table 1. (Continued)

Test site	Name of Roadway	Climatic Region	Details of Moisture Barrier			Details of Moisture Measuring Device	
			Date of Installation	Type of Barrier	Length (ft)	Date of Installation	Device Type
Snyder 2	US 84 Northbound	III-B	June, 1990	Vertical Fabric	2500	Feb., 1991	Psychrometer
Snyder 3	US 84 Northbound	III-B	June, 1990	Vertical Fabric	1500	Feb., 1991	Psychrometer
Wichita Falls 1	IH 44 NorthBound	III-B	April, 1989	Sloping Fabric	1400	April, 1989	Psychrometer
Wichita Falls 2	IH 44 Southbound	III-B	--	--	--	April, 1989	Psychrometer

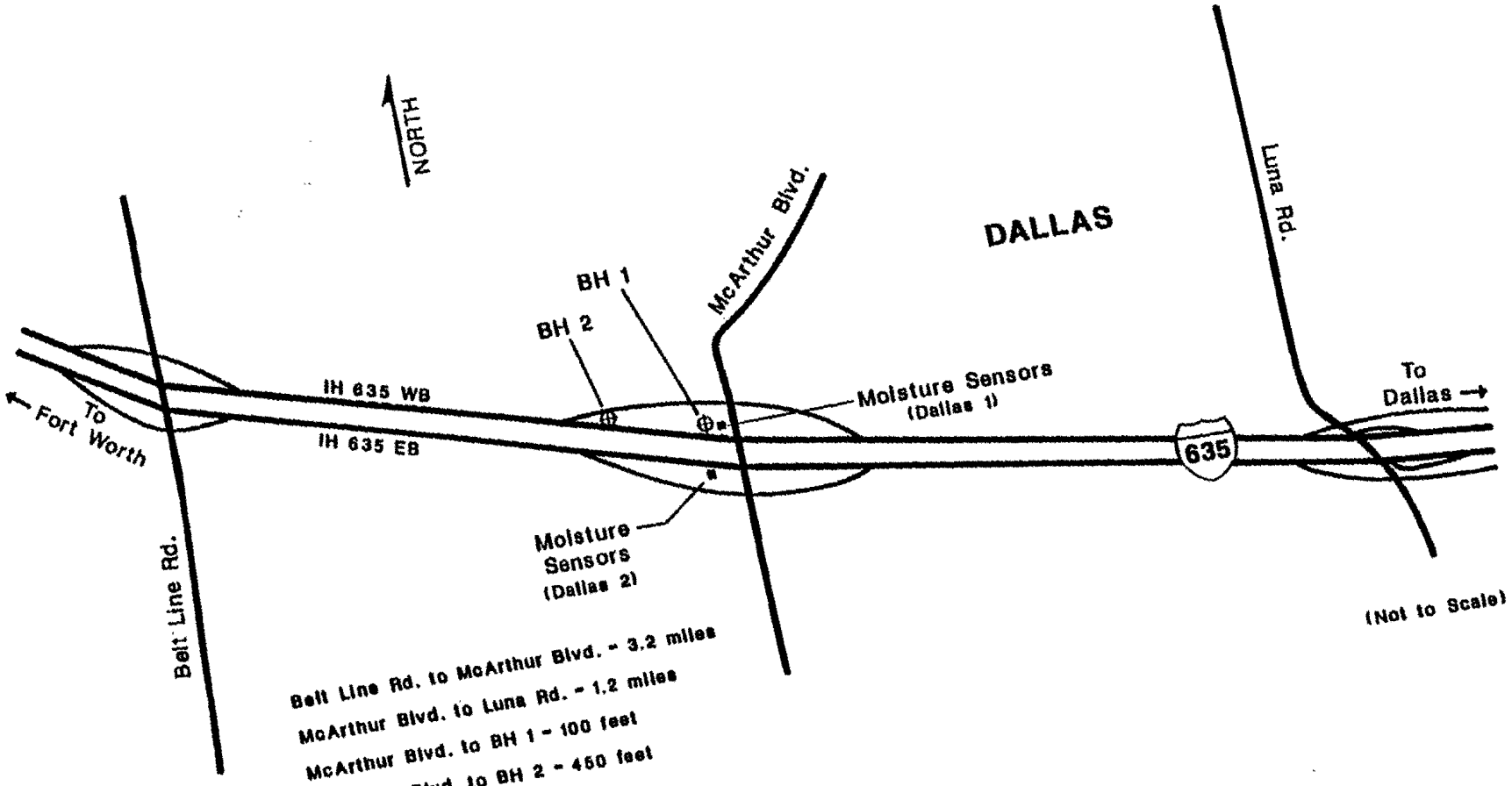

Figure 5. Site Plan of Test Sections at Dallas, IH 635

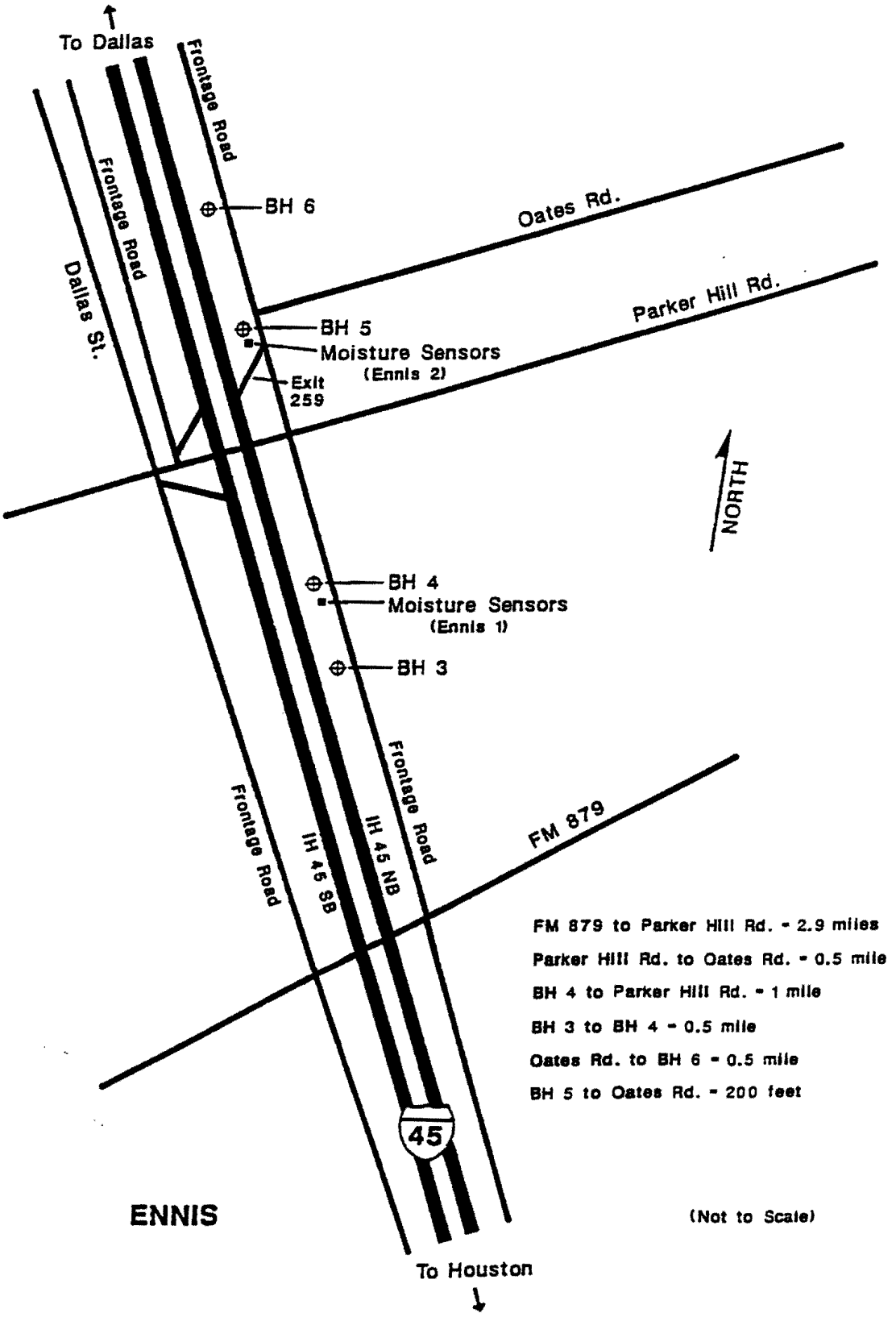

Figure 6. Site Plan of Test Section at Ennis, IH 45 Frontage Road

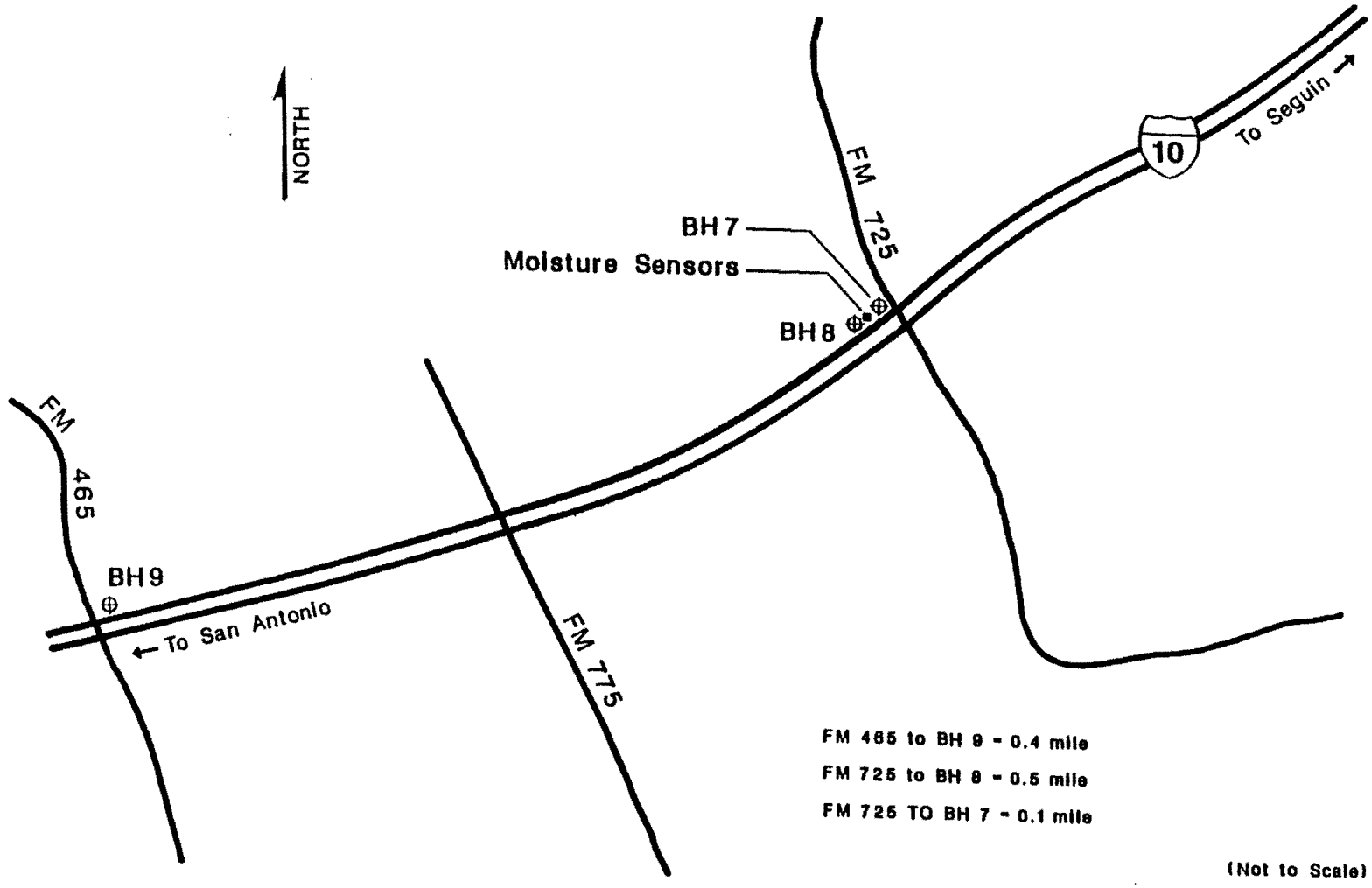

Figure 7. Site Plan of Test Section at Seguin, IH 10

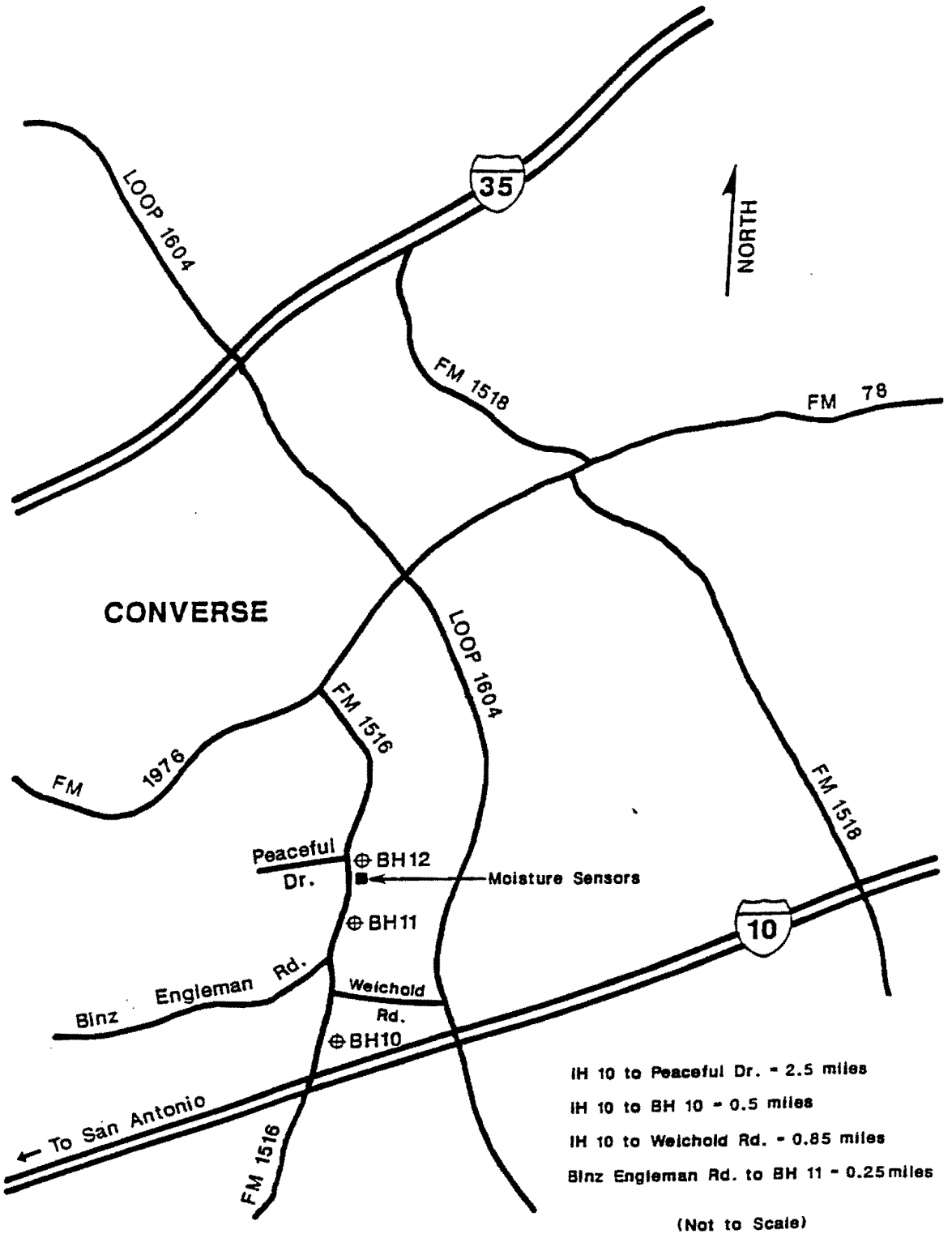

Figure 8. Site Plan of Test Section at Converse, FM 1516

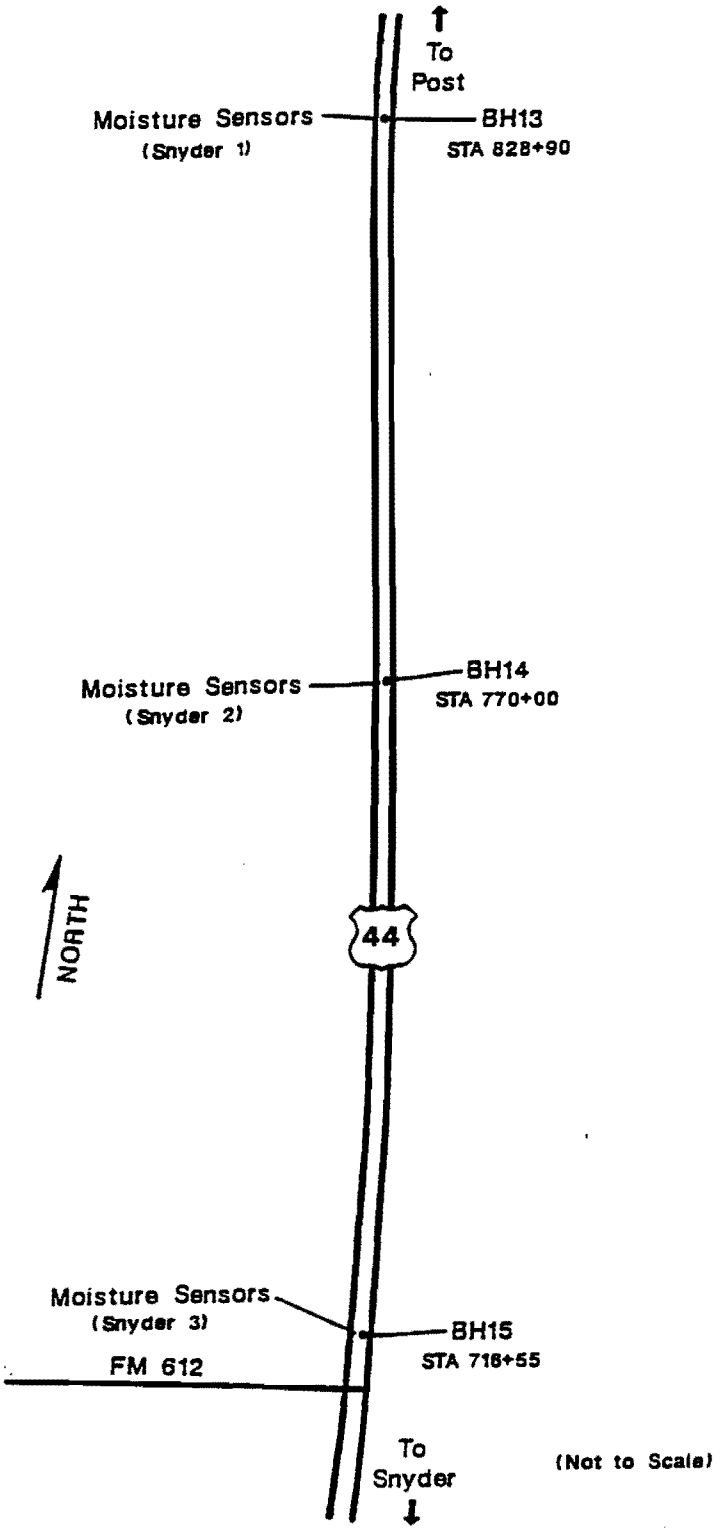

Figure 9. Site Plan of Test Sections at Snyder, US 84

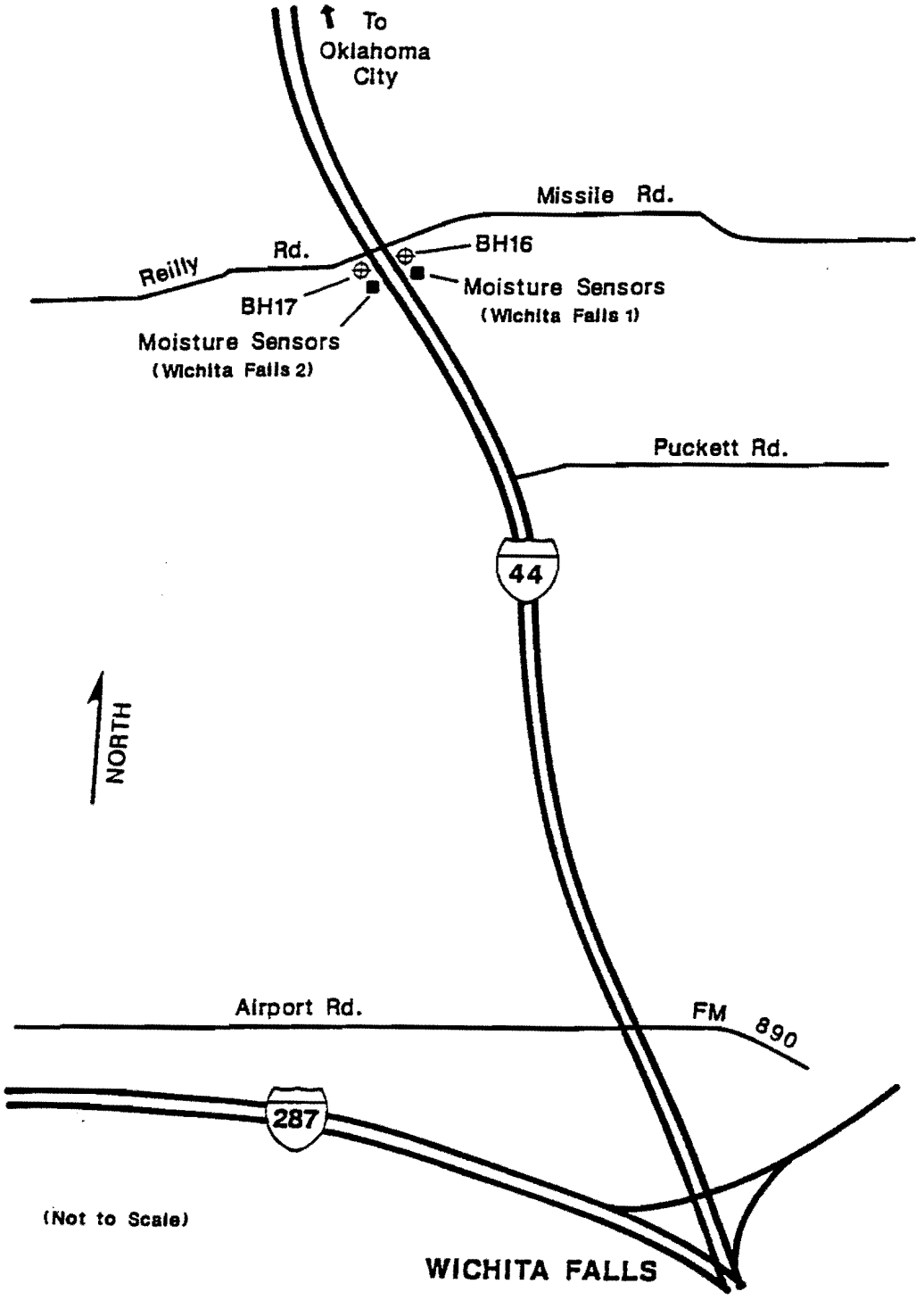

Figure 10. Site Plan of Test Sections at Wichita Falls, IH 44

SITE DESCRIPTION

Dallas, IH 635

This moisture barrier site is located along the IH 635 in Dallas County approximately four miles west of the intersection of IH 35E. The barrier is placed for a length of 600 ft along the roadway. This roadway is a six lane divided highway with paved shoulders. The eastbound and westbound roadways are separated by a 118 ft wide sodded median. Each roadway comprises a 12 ft wide outside shoulder, a 10 ft wide inside shoulder and three 12 ft wide travelway lanes. The two test sections are located at westbound and eastbound roadways opposite to each other and are named as Dallas 1 and Dallas 2 respectively.

The westbound and eastbound roadways were rehabilitated in September 1990 and December 1991, respectively. The rehabilitation work consisted of installing a 8 ft deep polypropylene fabric vertical moisture barrier at the edge of the paved shoulder along both sides of the roadway, and then placing an asphalt concrete overlay over the existing pavement structure. Thermal moisture sensors were installed inside and outside of the barriers at the outside edge of the roadways. The moisture sensors in the westbound and eastbound roadways were placed in September 1990 and December 1991 respectively.

Ennis, IH 45

Ennis 1 and Ennis 2 sites are located approximately 29 and 27.5 miles south of Dallas, respectively. Thermal moisture sensors were installed beneath the pavement at two locations of the northbound frontage road of IH 45 in Ellis County in August 1990. The two sites are named as Ennis 1 and Ennis 2. The roadway comprises two 11 ft wide

travelway lanes. The shoulders of this roadway are unpaved. Moisture barriers have not been provided for this roadway.

Seguin, IH 10

This moisture barrier site is located in the westbound Interstate Highway 10 in Guadalupe County approximately 33 miles east of San Antonio. The polypropylene fabric vertical moisture barrier was constructed to a depth of 8 ft along with an asphalt overlay over the existing pavement structure in November 1988. The test section extends from the intersection of FM 725 to the intersection of FM 465. The barrier was constructed in four separate segments with a total length of 13,200 ft on both sides of the roadway. This section of IH 10 is a four lane divided highway with paved shoulders. The roadway is separated by a 66 ft wide sodded median. Each roadway is comprised of a 10 ft wide outside shoulder, a 4-6 ft wide inside shoulder and two 12 ft wide travelway lanes. Thermal moisture sensors were installed inside and outside of the barrier at the outside edge of the roadway in November 1988.

Converse, FM 1516

This moisture barrier test section extends from the intersection of Interstate Highway 10 to approximately 1600 ft north of Peaceful Drive on Farm to Market 1516 in Bexar County. The barrier was constructed in three separate segments with a total length of 7300 ft on either side of the roadway. The roadway consists of two 12 ft wide travelway lanes, and 8 ft wide paved shoulders on both sides. The rehabilitation work consisted of the placement of polypropylene fabric vertical moisture barriers to a depth of 8 ft, and an asphalt concrete

overlay over the existing pavement structure. Thermal moisture sensors were installed inside and outside of the barrier in June 1989.

Snyder, US 84

There are three test pavement sections available at this site. These sites are located along US 84 in Snyder in Scurry County, and are named as Snyder 1, Snyder 2, and Snyder 3. The roadway is a four lane highway with paved shoulders and a sodded median. The vertical moisture barriers were placed to a depth of 8 ft and to the lengths of 500 ft, 2500 ft, and 1500 ft at Snyder 1, Snyder 2, and Snyder 3 sites, respectively, in June 1990. All of these test sections are located along the northbound roadway. Snyder 1 was instrumented with thermocouple psychrometers in June 1989 prior to the construction of the moisture barrier. The other two test sections were instrumented with thermocouple psychrometers in February 1991. In all test sections, the psychrometers were installed both inside and outside of barriers.

Wichita Falls, IH 44

The two test sections of this site are located along Interstate Highway 44 in Wichita Falls in Wichita County. The roadway is a four lane divided highway with paved shoulders. The northbound and southbound roadways are separated by a sodded median. Each roadway has an 11 ft wide outside shoulder, 6 ft wide inside shoulder, and two 12 ft wide travelway lanes. The two test sections are located on the northbound and southbound roadways opposite to each other and are named as Wichita Falls 1 and Wichita Falls 2, respectively. These test sections were instrumented with thermocouple psychrometers in April, 1989. The test section in the northbound roadway is provided with a

5 ft deep sloping fabric barrier to a length of 1400 ft along the outside edge of the paved shoulder. The moisture barrier was installed in April, 1989. The test section in southbound roadway has not been provided with a barrier and acts as the control section.

SUBSURFACE SOIL CONDITIONS

The subsurface soil properties in all test sections were investigated through the disturbed soil samples recovered from the test sections. The approximate locations of the bore holes in each test section are shown in Figures 5 through 10. The samples recovered from the borings were tested in the laboratory for identification purposes and to determine the engineering properties of the soils. The laboratory tests included the following:

1. Atterberg limits
2. Percentage passing No. 200 sieve
3. Percent of fine clay (grain size less than 0.002 mm)
4. Natural gravimetric moisture content
5. Filter paper suction
6. Laboratory suction using pressure plate apparatus

The gravimetric moisture contents were obtained from the weights of samples in the natural state and after having been oven dried. The grain size distributions were obtained from the weight of the material retained on the No. 200 sieve and by performing a hydrometer analysis. The liquid limit, plasticity index, and grain size distribution were performed as per the AASHTO standard T 89-86, T 90-86, and T 88-86, respectively. The filter paper suction, laboratory suction, and in situ suction were carried out according to the procedures described in

Chapter II and Appendix A.

The results of grain size distribution for the soils from Dallas, Seguin and Ennis show that the majority of the samples have more than 90 percent passing the No. 200 sieve. The average percentage passing No. 200 sieve for Converse, Snyder, and Wichita Falls are 88, 64, and 84 respectively. The majority of soil samples show a 40% or more clay fraction for the soils from Dallas, Seguin, Ennis, and Converse, while the clay fraction for Snyder and Wichita Falls averages to 34% and 38% respectively. The Atterberg limits have been plotted in the Unified Classification System plasticity chart and they are shown in Figure 11. The liquid limit of soils ranges from 24% to 98%, and the plasticity index ranges from 10% to 64%. The Federal Highway Administration classifies the swell potential of soil based on Atterberg limits as follows (3).

LL (%)	PI (%)	Potential swell
> 60	> 35	High
50-60	25-35	Marginal
< 50	< 25	Low

According to this classification, the majority of soils from the test sections are highly or marginally active soils.

The laboratory suction test was performed for soils recovered from bore hole nos. BH1, BH4, BH5, BH8, BH11 and samples recovered from Snyder and Wichita Falls at the preliminary stage of the project. These results are shown in Figures 12 through 28. A summary of the other test results are presented in Tables 2 through 10.

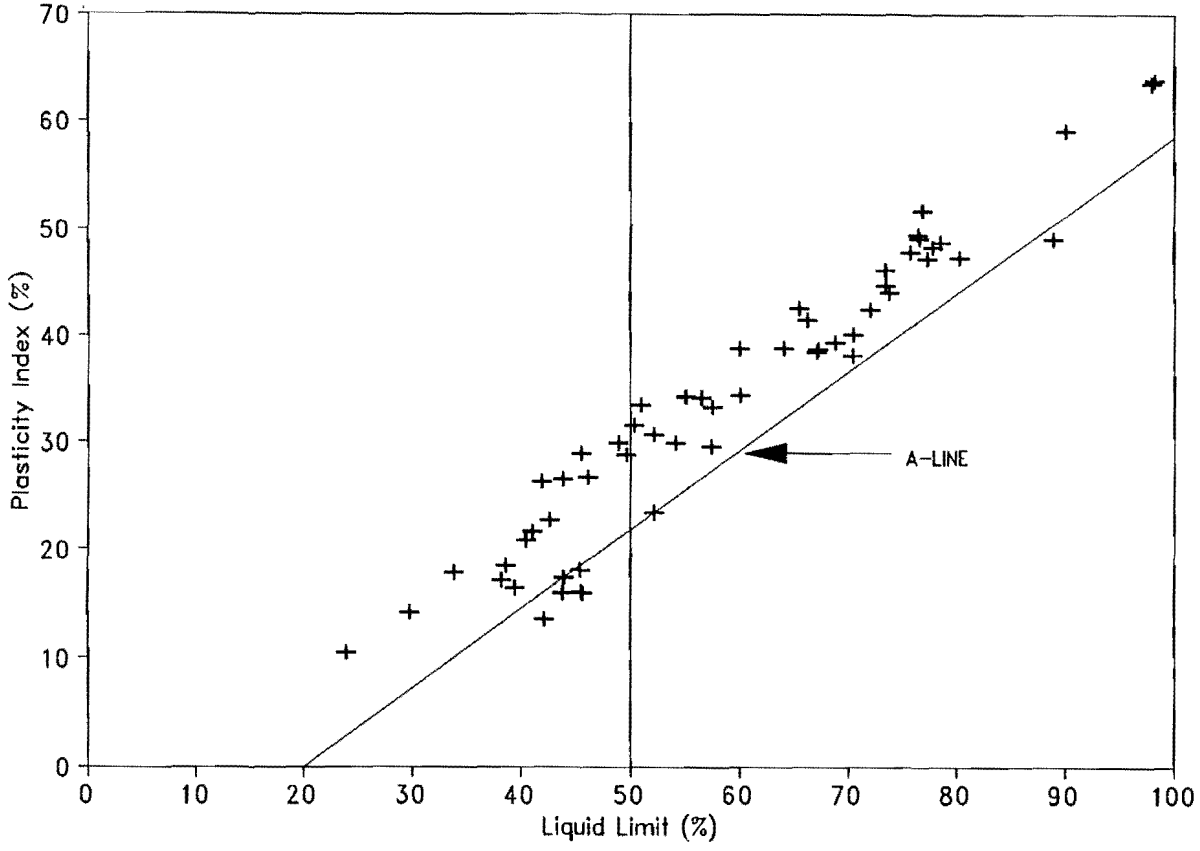

Figure 11. Atterberg Limits of the Soils at Test Sections

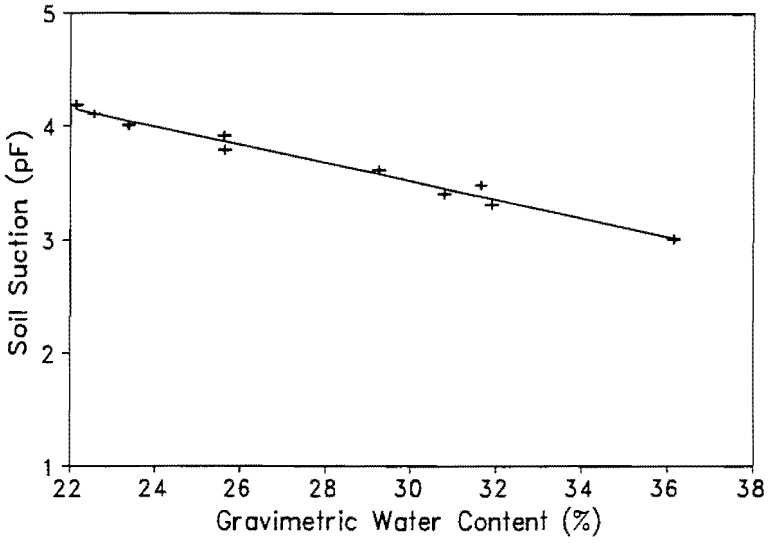

Figure 12. Desorption Relationship for the Soils from Bore Hole BH1 (0-3 ft deep)

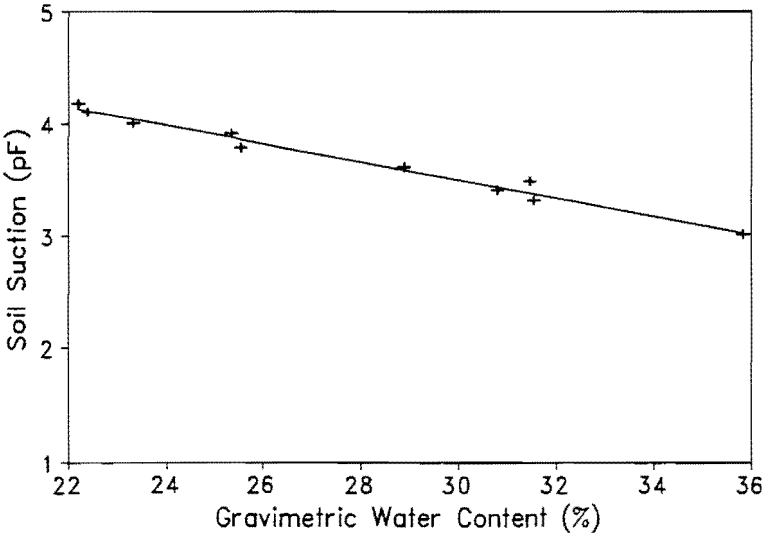

Figure 13. Desorption Relationship for the Soils from Bore Hole BH1 (4-7 ft deep)

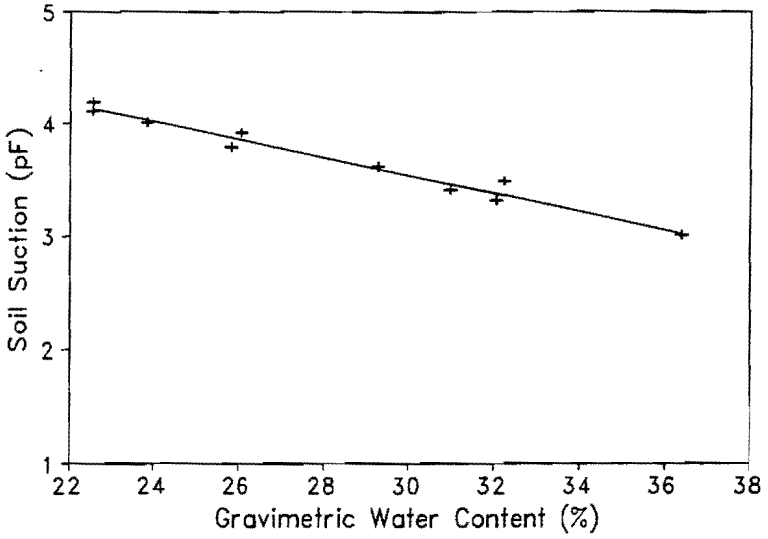

Figure 14. Desorption Relationship for the Soils from Bore Hole BH1 (7-10 ft deep)

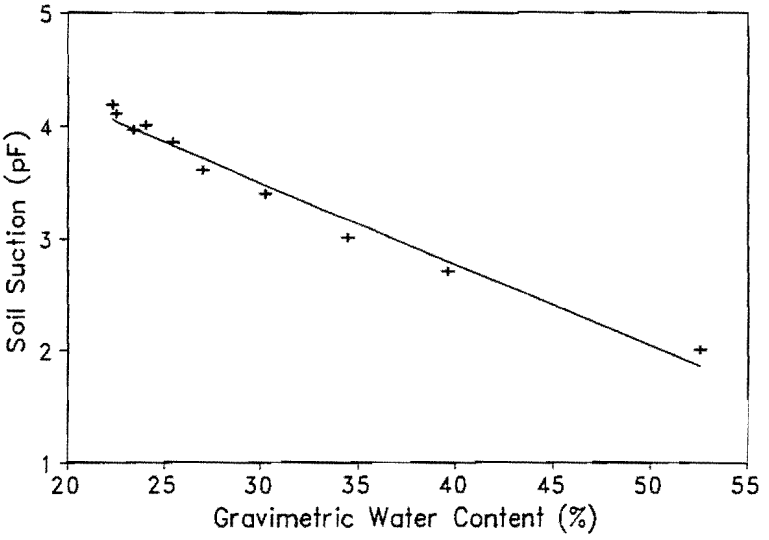

Figure 15. Desorption Relationship for the Soils from Bore Hole BH4 (0-4 ft deep)

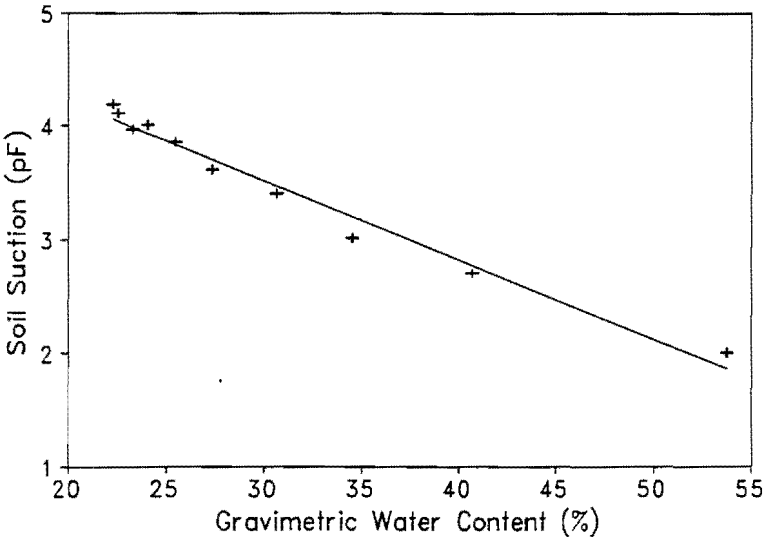

Figure 16. Desorption Relationship for the Soils from Bore Hole BH4 (5-7 ft deep)

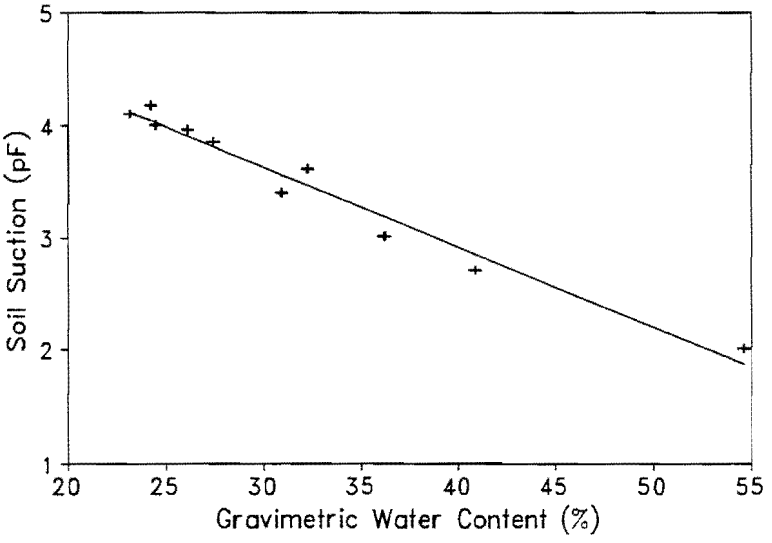

Figure 17. Desorption Relationship for the Soils from Bore Hole BH5 (0-3 ft deep)

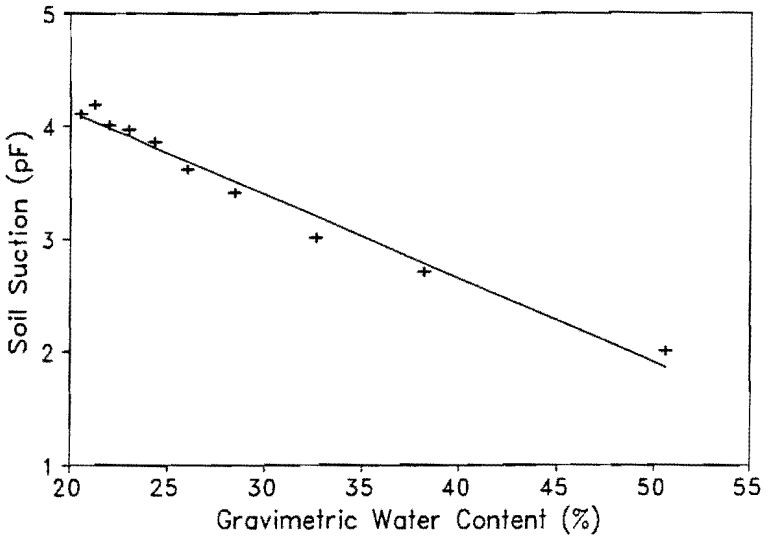

Figure 18. Desorption Relationship for the Soils from Bore Hole BH5 (4-6 ft deep)

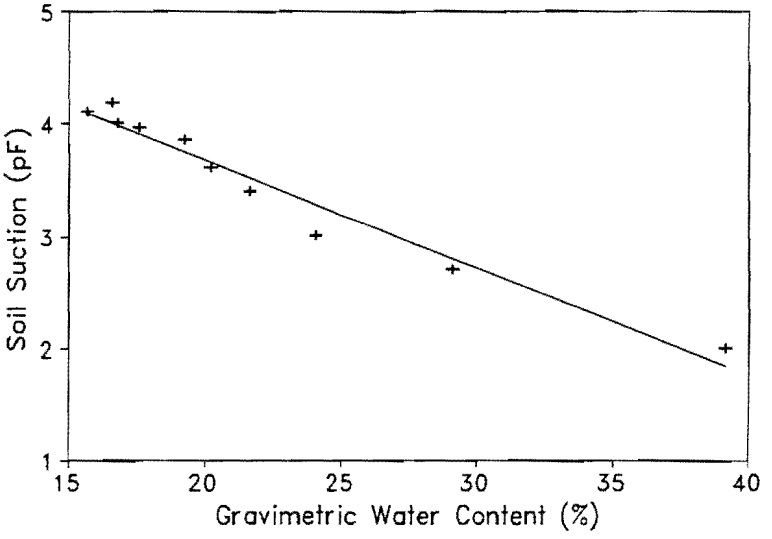

Figure 19. Desorption Relationship for the Soils from Bore Hole BH5 (6-10 ft deep)

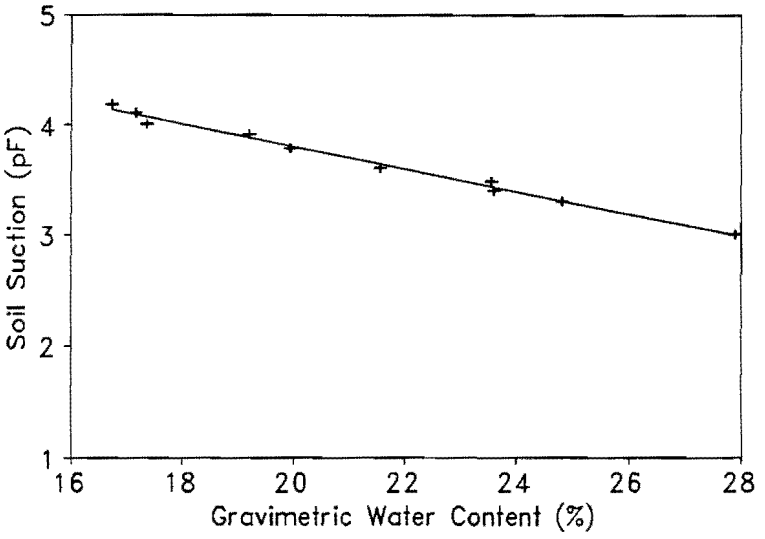

Figure 20. Desorption Relationship for the Soils from Bore Hole BH8 (2-3 ft deep)

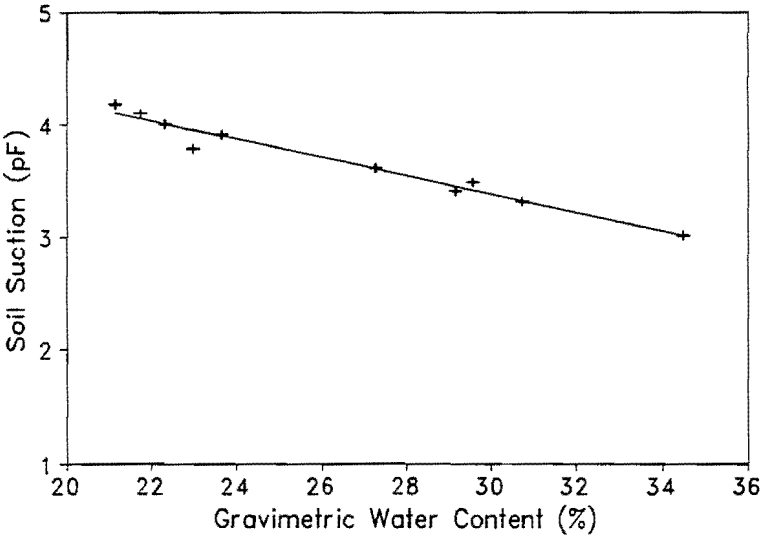

Figure 21. Desorption Relationship for the Soils from Bore Hole BH8 (4-6 ft deep)

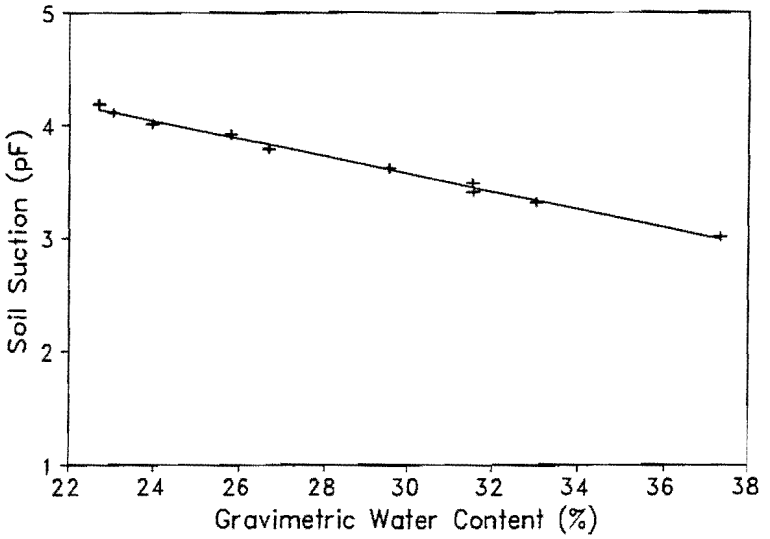

Figure 22. Desorption Relationship for the Soils from Bore Hole BH8 (6-9 ft deep)

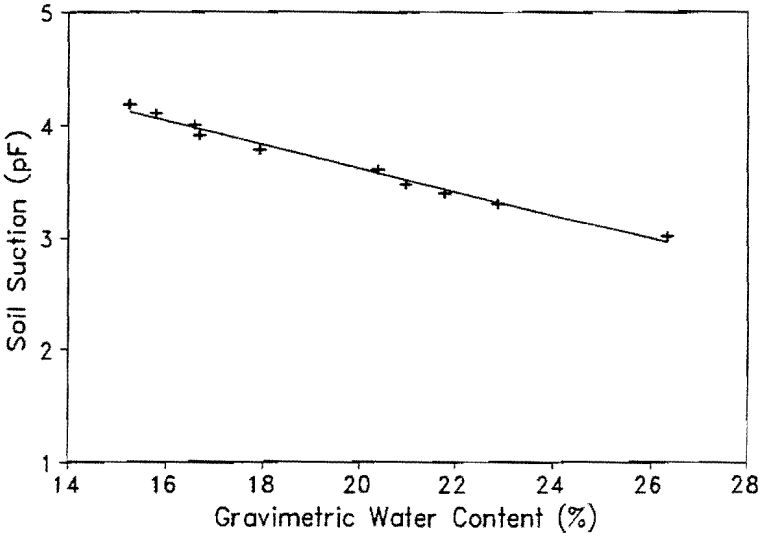

Figure 23. Desorption Relationship for the Soils from Bore Hole BH11 (0-3 ft deep)

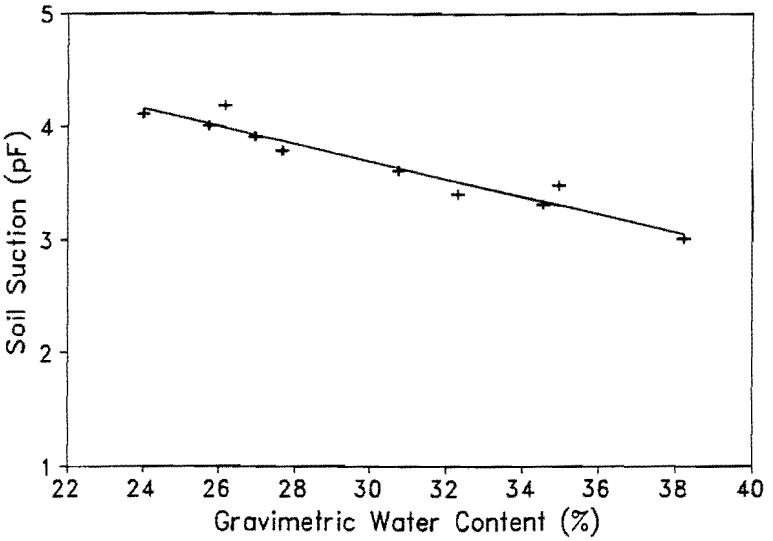

Figure 24. Desorption Relationship for the Soils from Bore Hole BH11 (3-7 ft deep)

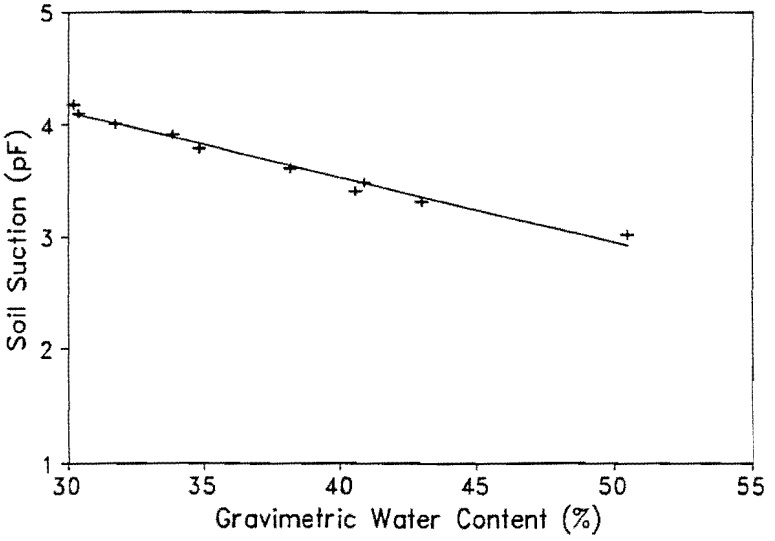

Figure 25. Desorption Relationship for the Soils from Bore Hole BH11 (7-10 ft deep)

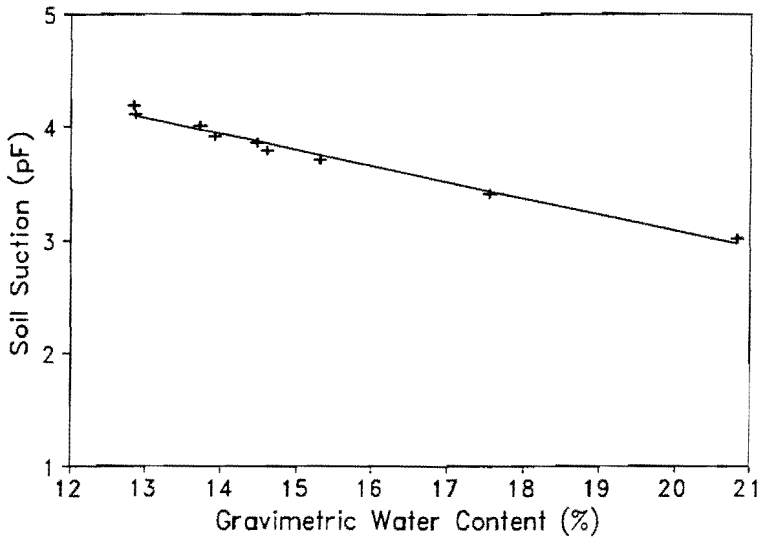

Figure 26. Desorption Relationship for the Soils from Snyder (0-3 ft deep)

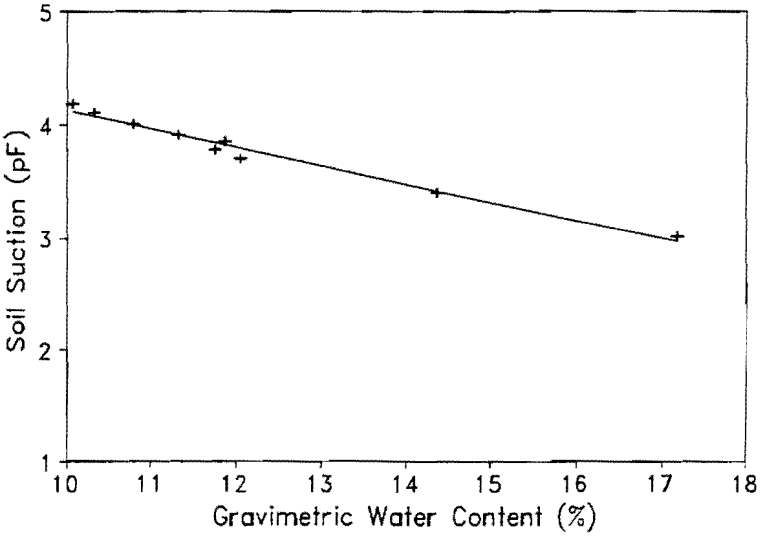

Figure 27. Desorption Relationship for the Soils from Snyder (4-5 ft deep)

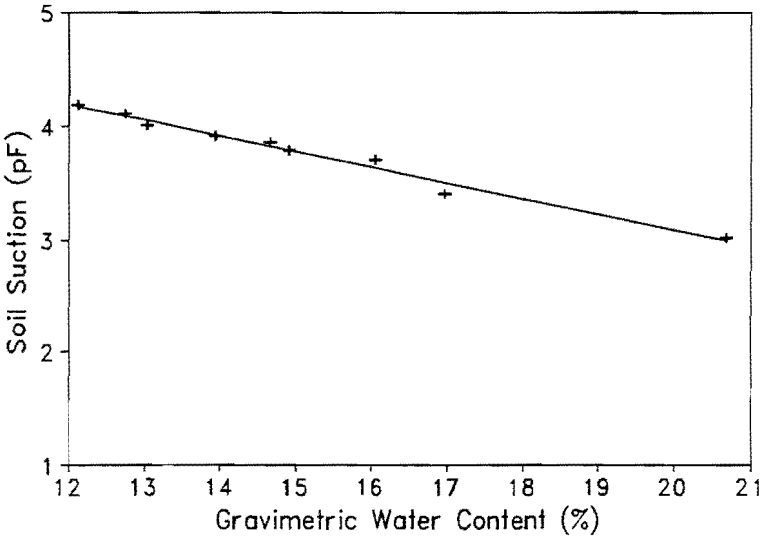

Figure 28. Desorption Relationship for the Soils from Wichita Falls (0-3 ft deep)

Table 2. Test Results for the Soils from IH 635 in Dallas

Boring No.	Sample Depth (ft)	Natural Moisture Content (%)	Filter Paper Suction (pF)	Liquid Limit (%)	Plasticity Index (%)	Passing No. 200 Sieve (%)	Fine Clay Content (%)
BH1	0-3	21.85	4.15	73.9	43.9	99.1	59.4
	4-7	23.98	3.83	73.6	46.0	99.0	57.7
	7-10	21.27	3.98	75.9	47.7	99.1	63.3
BH2	2-4	25.12	3.82	77.9	48.2	97.0	55.5
	6-9	25.28	3.60	73.5	44.6	99.4	54.7
	11-13	21.07	4.01	76.6	49.4	97.9	57.2

Table 3. Test Results for the Soils from IH 10 in Seguin

Boring No.	Sample Depth (ft)	Natural Moisture Content (%)	Filter Paper Suction (pF)	Liquid Limit (%)	Plasticity Index (%)	Passing No. 200 Sieve (%)	Fine Clay Content (%)
BH7	2-3.5	25.21	3.17	77.4	47.1	86.7	51.5
	7-9	25.79	3.14	80.3	47.3	94.0	52.8
	10-13	18.45	3.88	56.6	34.1	93.7	46.9
BH8	2-3	25.22	3.39	55.2	34.2	95.2	35.1
	4-6	29.63	3.44	57.6	33.3	91.3	42.3
	6-9	30.37	3.74	70.5	38.1	92.1	49.6
BH9	2.5-4	22.12	3.54	66.4	41.4	82.2	49.1
	4-7	19.70	3.91	49.7	28.8	85.6	42.2
	11-13	22.14	3.98	77.0	51.7	99.4	54.4

Table 4. Test Results for the Soils from Northbound Frontage Road of IH 45 in Ennis

Boring No.	Sample Depth (ft)	Natural Moisture Content (%)	Filter Paper Suction (pF)	Liquid Limit (%)	Plasticity Index (%)	Passing No. 200 Sieve (%)	Fine Clay Content (%)
BH3	1-3	20.09	4.11	45.6	29.0	78.8	42.2
	4-7	24.22	3.77	51.0	33.5	76.0	42.9
	9-12	31.70	3.36	46.2	26.7	79.2	40.0
BH4	0-4	45.59	2.43	70.6	40.1	96.9	51.0
	5-7	49.41	2.18	72.2	42.4	96.6	49.6
BH5	0-3	31.82	3.46	67.2	38.4	96.8	40.0
	4-6	29.38	3.55	65.6	42.5	96.2	40.0
	6-10	22.05	3.67	42.7	22.8	92.4	37.1
BH6	3-5	27.50	3.68	78.7	48.7	94.6	48.4
	6-8	17.83	3.94	60.2	34.3	99.2	45.5
	11-13	20.56	3.80	60.1	38.8	99.1	48.6

Table 5. Test Results for the Soils from FM 1516 in Converse

Boring No.	Sample Depth (ft)	Natural Moisture Content (%)	Filter Paper Suction (pF)	Liquid Limit (%)	Plasticity Index (%)	Passing No. 200 Sieve (%)	Fine Clay Content (%)
BH10	3-5	24.80	3.26	64.2	38.8	83.6	44.4
	5-8	14.13	4.12	43.9	26.6	79.4	43.5
	9-11	14.26	4.06	41.9	26.3	78.1	40.0
BH11	0-3	11.90	4.18	50.4	31.6	83.4	40.6
	3-7	28.82	3.67	76.7	49.0	90.9	43.6
	7-10	42.47	2.96	98.2	63.7	93.4	60.6
BH12	3-5	32.10	3.47	90.1	59.1	88.7	52.5
	5-10	30.97	3.54	98.0	63.5	98.0	52.9
	10-13	32.68	3.66	89.0	49.0	95.3	50.6

Table 6. Test Results for the Soils from US 84 in Snyder 1

Boring No.	Sample Depth (ft)	Natural Moisture Content (%)	Filter Paper Suction (pF)	Liquid Limit (%)	Plasticity Index (%)	Passing No. 200 Sieve (%)	Fine Clay Content (%)
BH13	0-1	18.20	3.51	39.5	22.0	77.7	--
	1-2	16.90	3.72	42.0	19.4	76.0	--
	2-3	20.80	3.73	40.4	20.9	72.8	32.5
	3-4	19.30	3.70	40.6	18.7	82.0	--
	4-5	13.80	3.68	35.7	20.0	78.0	--
	5-6	16.70	3.70	49.0	29.9	62.8	28.3
	6-7	18.20	3.92	54.4	34.9	69.6	--
	7-8	12.10	4.10	40.8	23.7	61.0	--
	8-9	10.60	4.10	34.4	19.5	64.2	--
	9-10	10.10	4.09	38.2	17.2	62.7	12.5
	10-11	9.40	4.03	34.2	19.3	57.6	--
	11-12	11.00	4.19	35.1	19.9	63.2	--

Table 7. Test Results for the Soils from US 84 in Snyder 2

Boring No.	Sample Depth (ft)	Natural Moisture Content (%)	Filter Paper Suction (pF)	Liquid Limit (%)	Plasticity Index (%)	Passing No. 200 Sieve (%)	Fine Clay Content (%)
BH14	1-2	24.30	3.60	45.7	15.9	52.3	23.4
	2-3	21.30	3.80	49.8	23.8	67.4	--
	3-4	21.70	3.70	42.5	15.1	59.9	--
	4-5	20.00	3.70	44.0	17.4	68.5	43.4
	5-6	I9.70	3.80	42.8	16.0	59.0	--
	6-7	20.00	3.70	45.4	18.1	41.7	25.6
	7-8	19.00	3.60	53.5	22.7	60.6	--
	8-9	21.70	3.80	43.9	15.9	83.4	57.4
	9-10	20.00	3.80	44.2	14.7	84.5	--
	10-11	18.70	3.90	42.1	13.6	26.2	21.0
	11-12	19.00	3.90	48.2	18.1	59.8	--
	12-13	19.00	4.00	43.1	14.2	49.4	--
	13-14	19.50	4.00	45.6	16.1	54.1	38.5
	14-15	19.00	3.90	45.3	16.3	37.9	--

Table 8. Test Results for the Soils from US 84 in Snyder 3

Boring No.	Sample Depth (ft)	Natural Moisture Content (%)	Filter Paper Suction (pF)	Liquid Limit (%)	Plasticity Index (%)	Passing No. 200 Sieve (%)	Fine Clay Content (%)
BH15	1-2	6.50	3.30	39.5	16.4	75.2	35.1
	2-3	23.70	3.40	49.1	23.5	60.6	--
	3-4	20.00	3.50	57.5	29.6	51.7	23.3
	4-5	21.30	3.50	61.2	35.1	52.7	--
	5-6	21.00	3.60	56.9	34.8	51.6	--
	6-7	27.30	3.70	68.9	39.4	78.5	62.4
	7-8	27.30	3.70	64.8	36.9	77.5	--
	8-9	28.70	3.70	67.3	38.7	69.0	44.5
	9-10	26.00	3.80	54.8	26.0	76.2	--
	10-11	26.70	3.80	55.6	23.8	69.0	--
	11-12	21.00	3.70	52.2	23.5	58.1	29.1

Table 9. Test Results for the Soils from IH 44 in Wichita Falls 1

Boring No.	Sample Depth (ft)	Natural Moisture Content (%)	Filter Paper Suction (pF)	Liquid Limit (%)	Plasticity Index (%)	Passing No. 200 Sieve (%)	Fine Clay Content (%)
BH16	0-1	16.30	3.91	33.9	17.9	78.5	37.3
	1-2	15.30	4.00	37.2	19.0	77.6	--
	2-3	14.00	4.20	38.0	18.6	85.8	--
	3-4	14.10	4.38	42.2	22.9	89.0	--
	4-5	13.50	4.32	38.6	18.8	90.8	--
	5-6	15.60	4.00	42.5	19.4	97.0	--
	6-7	15.70	4.13	41.0	21.7	95.3	35.1
	7-8	16.10	4.02	44.1	23.2	85.4	--
	8-9	12.70	4.14	40.7	19.5	87.4	--
	9-10	14.30	4.38	49.8	28.6	95.1	--
	10-11	12.10	4.11	36.5	15.5	98.2	--
	11-12	12.10	3.99	39.1	13.6	98.0	--
	12-13	12.20	4.20	45.1	21.4	93.8	--
	13-14	14.40	4.29	57.6	35.1	94.0	--
	14-15	16.10	4.41	52.3	30.7	92.3	38.9

Table 10. Test Results for the Soils from IH 44 in Wichita Falls 2

Boring No.	Sample Depth (ft)	Natural Moisture Content (%)	Filter Paper Suction (pF)	Liquid Limit (%)	Plasticity Index (%)	Passing No. 200 Sieve (%)	Fine Clay Content (%)
BH17	0-1	11.00	3.65	--	NP	23.2	12.1
	1-2	13.20	3.37	28.0	13.8	56.7	--
	2-3	13.60	3.27	24.0	10.4	61.3	29.2
	3-4	12.30	3.64	36.5	21.2	76.9	--
	4-5	13.80	3.70	34.1	17.2	74.6	--
	5-6	14.40	4.09	43.3	20.9	83.0	--
	6-7	13.90	4.41	29.7	14.2	84.7	56.9
	7-8	15.90	4.00	35.6	16.7	81.2	--
	8-9	13.80	4.08	39.7	18.4	82.3	--
	9-10	12.50	4.02	35.2	17.3	84.8	--
	10-11	13.10	4.20	38.6	18.4	91.9	43.6
	11-12	16.10	4.39	50.0	25.7	95.0	--
	12-13	18.10	3.84	48.1	24.9	95.4	--
	13-14	19.20	4.02	50.9	24.9	90.0	--
	14-15	18.40	4.36	54.2	29.9	89.5	48.4

MEASUREMENT OF IN SITU SOIL SUCTION

The field suction measurements were made at instrumented sites periodically and they are presented in Appendix B. The frequent failures of both thermal moisture sensors and thermocouple psychrometers hampered the continuous collection of data. Also, the instruments at Ennis 2 site were damaged in July 1991 when the Highway Department widened the pavement on IH 45, and no measurements have been made at this site since then.

MEASUREMENT OF ROUGHNESS ON PAVEMENTS

The profilometer measurements were made on pavement sections on IH 635 westbound, IH 635 Eastbound, Seguin and Converse on a bi-annual basis in order to measure the roughness development of pavements. In addition to the moisture barrier sections, there were control sections at these sites except for the site at Converse. At each site, the control section was situated adjacent to the moisture barrier section. The profilometer measurements were made on both the moisture barrier and control sections. The Serviceability Index, International Roughness Index, and Maximum Expected Bump Height were estimated for each day of measurement at these sites and are given in Appendix C.

CHAPTER IV

METHODS OF ANALYSIS AND RESULTS

INTRODUCTION

In this chapter, the measured in situ soil suction at each test site is compared with the values that can be predicted from the flow and deformation (FLODEF) program (17) which is described in the next section of this chapter. The input data required for the analysis are computed from the methods available in the existing literature. The measured soil properties are used for this purpose.

FINITE ELEMENT PROGRAM FLODEF

The finite element flow and deformation (FLODEF) program developed by Gay (17) computes the transient unsaturated moisture flow and deformation in an expansive clay domain using a sequential analysis of flow and deformation. The flow is modelled through a finite element model developed by Mitchell (42) by converting the transient non-linear partial differential equation describing unsaturated moisture flow into an ordinary differential equation. The non-linear partial differential equation (modified Darcy's law) is given by:

$$C(\phi)\frac{\partial \phi}{\partial t} = \frac{\partial}{\partial x_i}\left[K_{ij}(\phi)\left[\frac{\partial \phi}{\partial x_j} + \frac{\partial z}{\partial x_j}\right]\right] - Q(\phi, x_i, t) \qquad i,j=1,2 \qquad (4)$$

Where

$C(\phi)$ = the slope of the desorption curve

$K_{ij}(\phi)$ = the permeability tensor

$Q(\phi, x_i, t)$ = a source or sink term that may be described as a variable function of matrix potential ϕ, spatial coordinates and time

The two main assumptions made by Mitchell in the conversion of the differential equation are (a) the unsaturated permeability is linearly related to the reciprocal of total suction, and (b) the desorption relationship is linear when the matrix potential is expressed in terms of pF. The moisture flow through unsaturated soil is defined by:

$$v = -K_o \frac{h_o}{h} \frac{dh}{dx} \tag{5}$$

Where

v = velocity of flow (cm/sec)

K_o = saturated permeability (cm/sec)

h_o = total suction (approximately 100 cm)

h = suction in cm of water

Soil suction is conveniently measured in logarithmic units of pF, where

$$u(pF) = \log_{10} h = 0.4343 \log_e h \tag{6}$$

Because

$$\frac{d}{dx}(u) = \frac{0.4343}{h} \frac{dh}{dx} \tag{7}$$

then

$$v = \frac{k_o h_o}{0.4343} \frac{d}{dx}(u) \tag{8}$$

i.e.

$$v = -P \frac{du}{dx} \tag{9}$$

where

$$P = \frac{k_o h_o}{0.4343} \tag{10}$$

Through the application of Darcy's law and equations of continuity of moisture flow, the following diffusion equation was obtained to describe the unsaturated moisture flow.

$$\frac{\partial^2 u}{\partial x^2} + \frac{\partial^2 u}{\partial y^2} + \frac{\partial^2 u}{\partial z^2} + \frac{f(x,y,z,t)}{P} = \frac{1}{\alpha}\frac{\partial u}{\partial t} \tag{11}$$

$$\alpha = \frac{\gamma_w P}{\gamma_d c} \tag{12}$$

Where

α = diffusion coefficient

γ_w = density of water

γ_d = dry density of soil

c = inverse slope of log suction vs. gravimetric water content curve

P = unsaturated permeability

Mitchell modelled the effects of rainfall and evapotranspiration by a sinusoidal change in suction with time at the soil surface. This is given by:

$$u(0,t) = U_e + U_0 \cos 2\pi nt \tag{13}$$

Where

U_e = equilibrium matrix potential

U_0 = amplitude of matrix potential

n = frequency

u(0,t) = suction at the surface at time t

For this boundary condition, the suction u(y,t) at any time t and depth y can be determined through the analytical solution of the diffusion equation given by:

$$u(y,t) = U_e + U_0 \exp\left[-\left(\frac{n\pi}{\alpha}\right)^{0.5} y\right] \cos\left[2\pi nt - \left(\frac{n\pi}{\alpha}\right)^{0.5} y\right] \tag{14}$$

In the FLODEF program, the two dimensional soil deformation is modelled using a finite element approach based on quadratic isoparametric elements. The volumetric strain at each node is obtained through the swelling coefficient method (25) and is described by:

$$\frac{\Delta V}{V} = -\gamma_\sigma \log_{10}(\sigma_{oct}/\sigma_{tr}) - \gamma_h \log_{10}(\phi_m/\phi_{tr}) \qquad (15)$$

Where

$\Delta V/V$ = the shrinkage volumetric strain referred to a maximum hypothetical volume

γ_σ = the compressibility constant assumed to be constant

γ_h = the swelling coefficient assumed to be constant

σ_{oct} = the octahedral compressive stress applied or σ_{tr}, whichever is larger

σ_{oct} = $(\sigma_x+\sigma_y+\sigma_z)/3$, where $\sigma_z = \nu(\sigma_x+\sigma_y)$ for plain strain conditions in which ν = Poisson's ratio

σ_{tr} = a threshold compressive octahedral stress, the minimum stress above which soil swell is restricted

ϕ_m = the matrix potential of the elemental volume of soil

ϕ_{tr} = the minimum potential when the soil is drying; the maximum potential when the soil is wetting up

The vertical linear shrinkage is calculated as one third of the volumetric strain.

CHARACTERIZATION OF SUBGRADE SOIL

The suction compression index (SCI) is used to characterize the subgrade soil in pavement test sections. By the chart method developed by McKeen (14), the SCI can be estimated knowing the plasticity index (PI), cation exchange capacity (CEC), and the clay content of soil. This method allows the estimation of the SCI of a soil as a function of the activity of soil (PI/%fine clay) and cation exchange activity (CEC/%fine clay). The percentage of fine clay is obtained by dividing the percentage clay content by percentage passing No. 200 sieve. The cation exchange capacity can be estimated from a laboratory test. However, for this study, the cation exchange capacity is obtained by the following relationship (43).

$$CEC = (PL\%)^{1.17} \text{ meq/100 gm} \qquad (16)$$

Where

CEC = cation exchange capacity

PL = plastic limit

Table 11 shows the SCI values of soils with 100% clay content and which plot in the eight different regions of the chart in Figure 29. The SCI value for any given soil can be estimated by multiplying the SCI obtained from the chart by the fine clay percentage as a decimal of the soil. The activity and the cation exchange activity for each soil sample in the test sections were calculated and plotted in the chart shown in Figure 29. Almost all the soils lie within regions IV A, III B, and II. The SCI values of these soils have been estimated with the correction for the actual clay content, and they are presented in Table 12. The estimated SCI values range between 0.04 and 0.11. This shows

Table 11. SCI values for a Soil with 100% Clay Content

Region	SCI
I	0.220
II	0.163
III A	0.096
III B	0.096
IV A	0.061
IV B	0.061
V A	0.033
V B	0.033

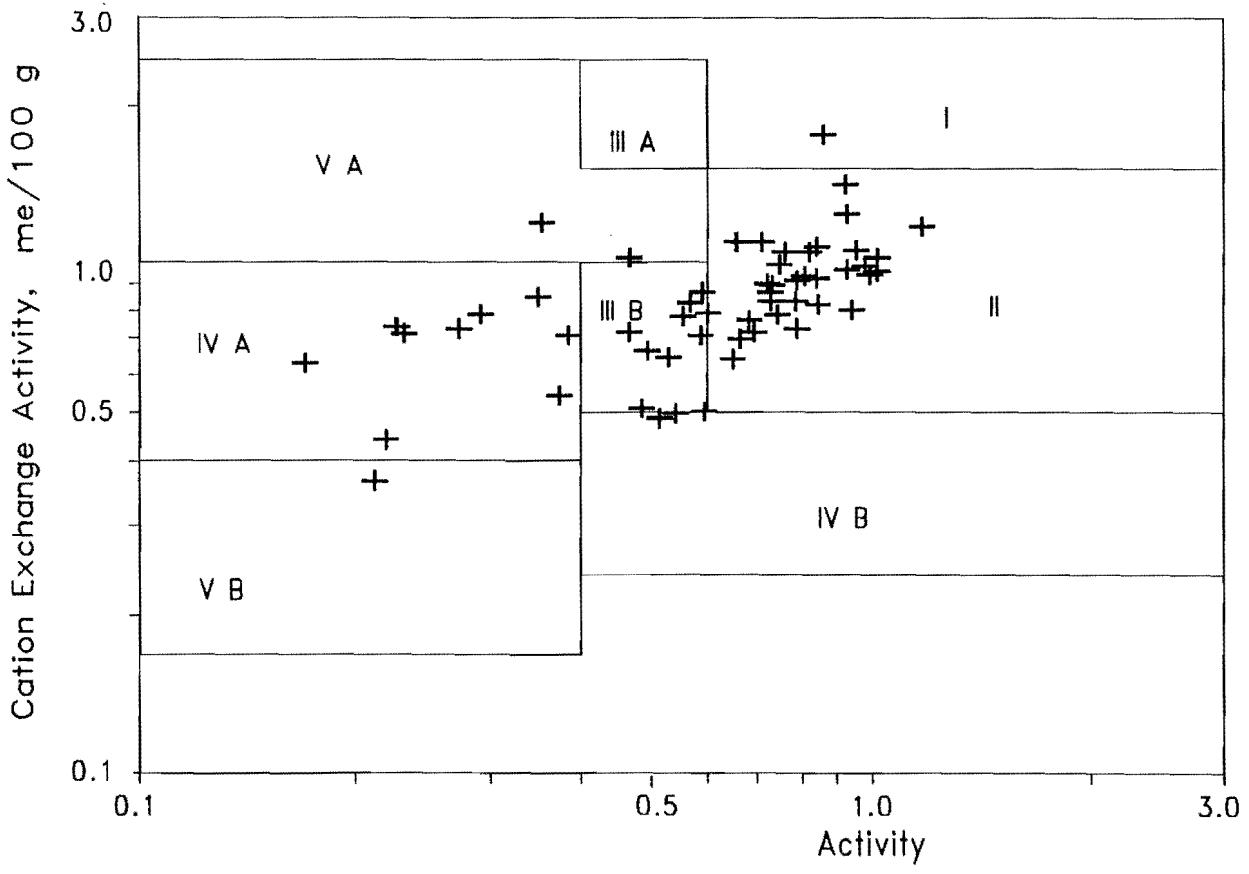

Figure 29. Chart for the Prediction of Suction Compression Index

Table 12. Estimated SCI Values from McKeen Chart

Boring No.	Sample Depth (ft)	Region	SCI for 100 % Clay	Fine Clay (%)	SCI
BH1	0-3	II	0.163	59.9	0.10
	4-7	II	0.163	58.3	0.10
	7-10	II	0.163	63.9	0.10
BH4	0-4	II	0.163	52.6	0.09
	5-7	II	0.163	51.3	0.08
BH5	0-3	II	0.163	41.3	0.07
	4-6	II	0.163	41.6	0.07
	6-10	III B	0.096	40.2	0.04
BH8	2-3	II	0.163	36.9	0.06
	4-6	II	0.163	46.3	0.08
	6-9	II	0.163	53.9	0.09
BH11	0-3	II	0.163	48.7	0.08
	3-7	II	0.163	48.0	0.08
	7-10	II	0.163	64.9	0.11

that the subgrade soil in all test sections are highly expansive.

COMPARISON OF MEASURED SUCTION WITH PREDICTED SUCTION

In this section, the measured in situ soil suction values are compared with the values that are predicted from the flow and deformation (FLODEF) program. The input data required for this program include the suction compression index (SCI), unsaturated permeability (P), and diffusion coefficient (α). Also a time dependent matrix suction variation at the exposed boundary of the pavement has to be specified.

The study was done for the test sites at Dallas 1, Ennis 1, Ennis 2, Seguin, Converse, Snyder 1, and Wichita Falls 2. Sufficient suction measurements were not available for other sites, therefore this study was not done on them.

For each site, a separate finite element mesh was prepared to represent the actual cross section at each site and to obtain nodal points at exact locations of suction measuring devices. The pavement section considered for this study consisted of a 45 cm deep combined subbase and surface layer and a 450 cm deep subgrade soil layer. The finite element mesh used for the site at Dallas is shown in Figure 30.

Even though the fabric used in the vertical moisture barriers is considered to be impermeable, in fact, this material has a permeability of 1.0×10^{-10} cm/sec (24). The actual width of fabric material is approximately 0.05 cm. Due to the consideration of numerical stability involved in modelling with such relatively narrow elements, a wide element size has to be used to represent the barrier. The permeability of the elements representing the barrier is adjusted by assuming the

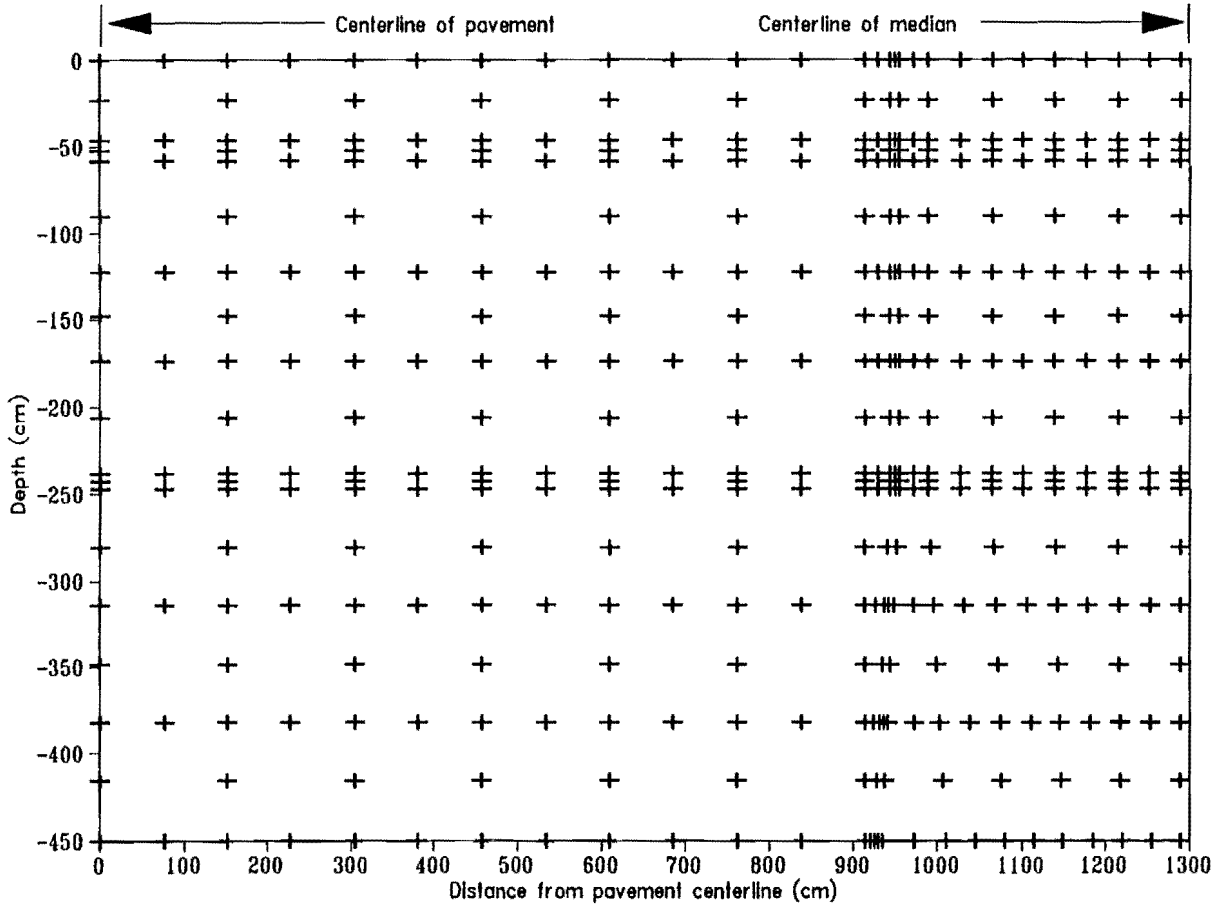

Figure 30. Finite Element Mesh used for the Comparision of Soil Suction at Dallas 1

change in head across the two different widths remains the same. This results in an effective permeability of 2 x 10^{-8} cm/sec for a 10 cm wide barrier (17).

Since no appreciable differences were observed in material properties at different depths at all of the sites, a single material for each site was used to represent the subgrade soil condition.

The study for each site was begun by assuming a combined sinusoidal and step function to represent the matrix suction variation with time at the exposed boundary, an initial moisture condition of the subgrade soil, a value for the diffusion coefficient, and a value for the unsaturated permeability. These initially assumed input data were adjusted in successive runs so that the predicted values of suction are equal to the measured values. Considering the fact that the soil surface can become extremely wet or extremely dry in response to the climatic conditions, the soil suction in the exposed boundary was assumed to range between 1.5 pF and 6.0 pF in all of the test sections. The material properties used for the comparison of the measured and predicted suctions are shown in Table 13. The combined subbase and surface layer was assumed to have an unsaturated permeability of 0.001 cm^2/sec and a diffusion coefficient of 0.001 cm^2/sec.

Table 13. Material Properties used for the Comparison

Material	Dry Density (g/cm^3)	Suction Compression Index
Combined subbase and surface layer	2.1	0.010
Subgrade soil	1.8	0.080
Fabric barrier	2.1	0.001
Backfill	2.1	0.010

The results of this study show that there is a significant difference between measured and predicted suction values in some of the data points. The possible reasons for this difference are as follows.

1. The modelling of the surface suction distribution with time as a combined step and sinusoidal function may not accurately represent daily or weekly variations of suction with time.
2. The actual evapotranspiration varies according to both temperature and wind speed, neither of which is modelled in the FLODEF program.
3. Variation of flow and material properties in different locations than in the assumed section
4. Measurement errors with the thermocouple psychrometers and thermal moisture sensors
5. The possibility of measuring soil suction adjacent to a crack in the soil where there is either more water and lower suction than in the intact soil or less water and higher suction. In the first case, measured suction will

always be numerically smaller than the computed value. In the second case, the measured value will always be larger than the computed value. Due to this reason, it is not surprising to obtain a relationship between the measured and predicted suction like the pattern shown in Figure 31.

The initial conditions given in the form of Equation 14 and the subgrade flow properties which gave the best fit of measured and predicted in situ suction are presented in Table 14. The matrix suction variation with time used to get the best fit are shown in Figures 32 through 38. The plots of measured suction vs. predicted suction are shown in Figures 39 through 45.

The simplified procedure developed by Mitchell (42) to model the moisture flow through unsaturated soil allows the estimation of diffusion coefficient (α) through Equation 12 using the value of unsaturated permeability (P) obtained from the comparison of measured and predicted suction, the slope of suction vs. gravimetric water content, and a typical value of dry density of soil. For this study, the dry density of soil is assumed as 1.8 gm/cm^3. The suction-water-content slopes for the soils for which the laboratory suction tests were performed are obtained by computing simple linear regression between gravimetric water content and soil suction. The fitted straight lines for these sites are shown in Figures 12 through 28 and the regression results are shown in Table 15. Knowing the unsaturated permeability, the saturated permeability can be estimated from Equation 10. For this purpose, the value of h_0 can be assumed as 100 cm.

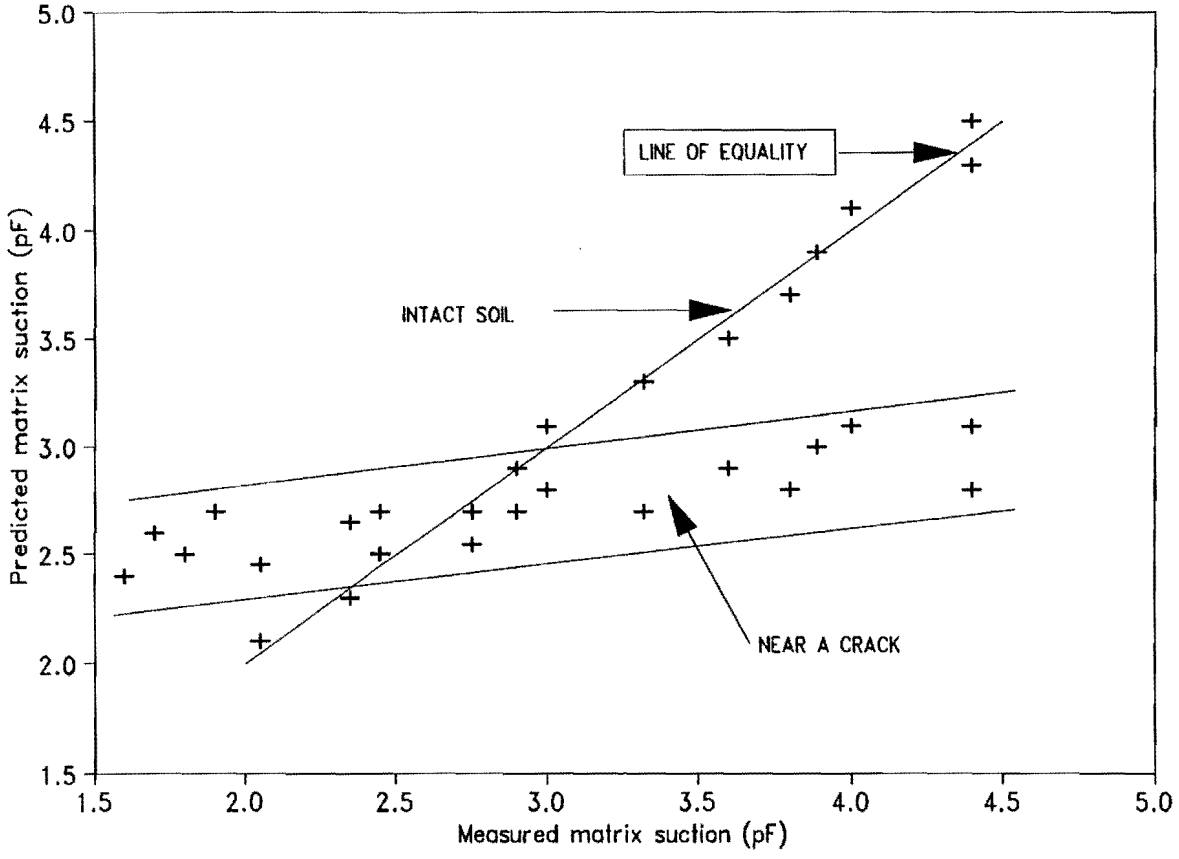

Figure 31. A Typical Pattern of Measured Soil Suction vs. Predicted Soil Suction

Table 14. Subgrade Flow Properties and Initial conditions used for the Comparison.

Site	Flow Properties		Initial Conditions			
	Unsaturated Permeability, P (cm^2/sec)	Diffusion Coefficient, α (cm^2/sec)	Equilibrium Matrix Potential (pF)	Amplitude of Matrix Potential (pF)	Phase	Frequency (cycles/yr)
Dallas 1	0.00069	0.0030	3.1	2.9	0.75	2
Ennis 1	0.00081	0.0032	2.6	1.1	0.00	2
Ennis 2	0.00083	0.0037	2.5	1.0	0.00	2
Seguin	0.00042	0.0024	3.3	2.7	0.60	2
Converse	0.00058	0.0026	3.7	1.0	0.50	2
Snyder	0.00059	0.0050	4.3	2.2	0.00	1
Wichita Falls	0.00059	0.0045	3.5	1.0	0.00	1

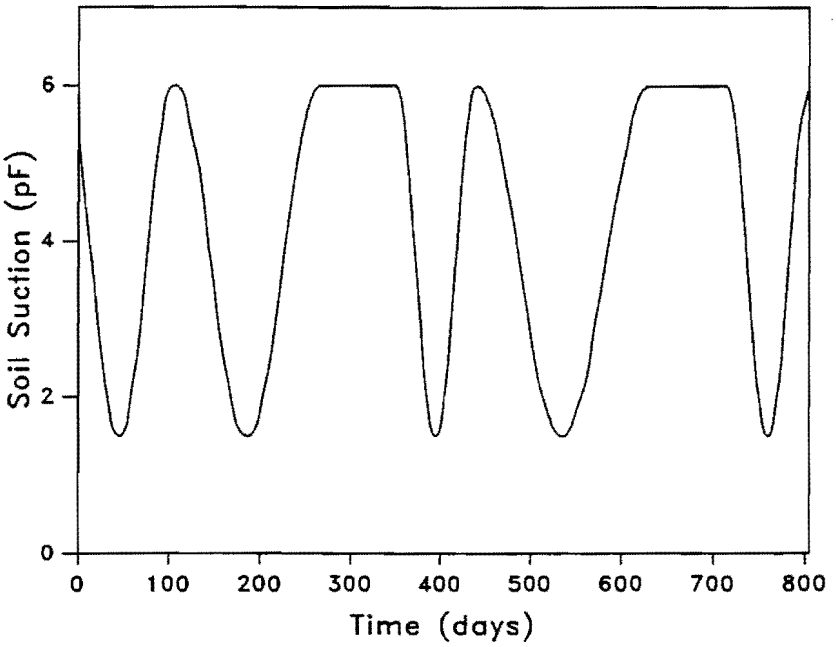

Figure 32. Surface Suction Variation with Time at Dallas 1

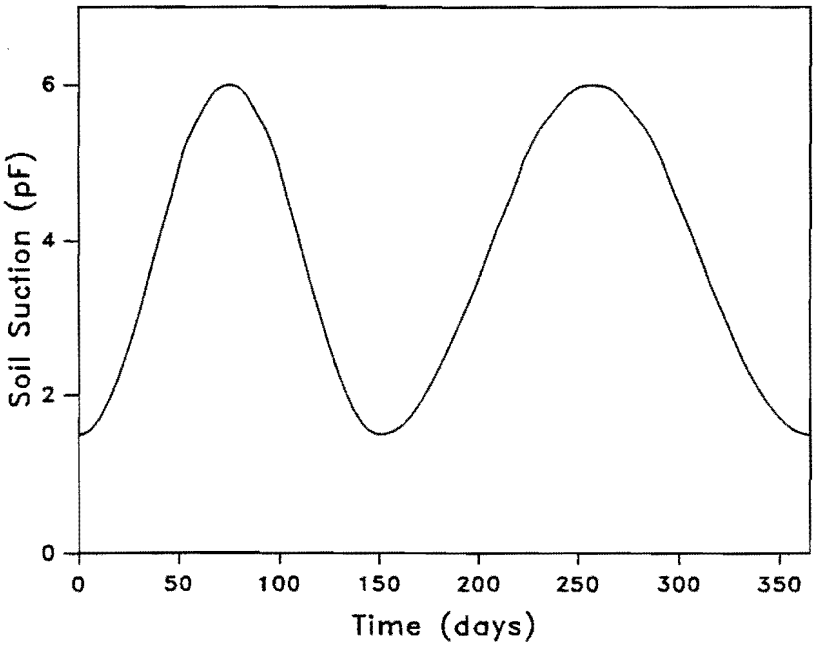

Figure 33. Surface Suction Variation with Time at Ennis 1

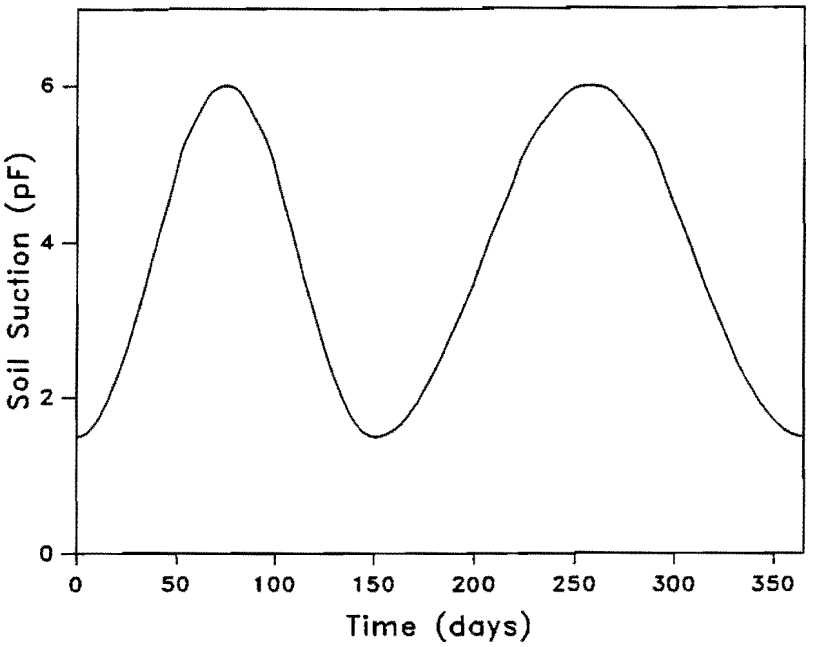

Figure 34. Surface Suction Variation with Time at Ennis 2

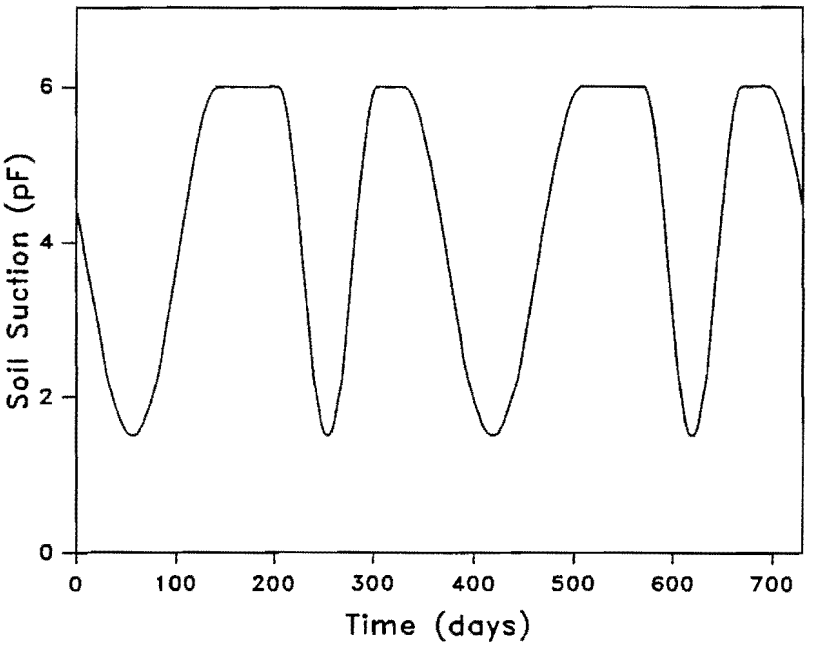

Figure 35. Surface Suction Variation with Time at Seguin

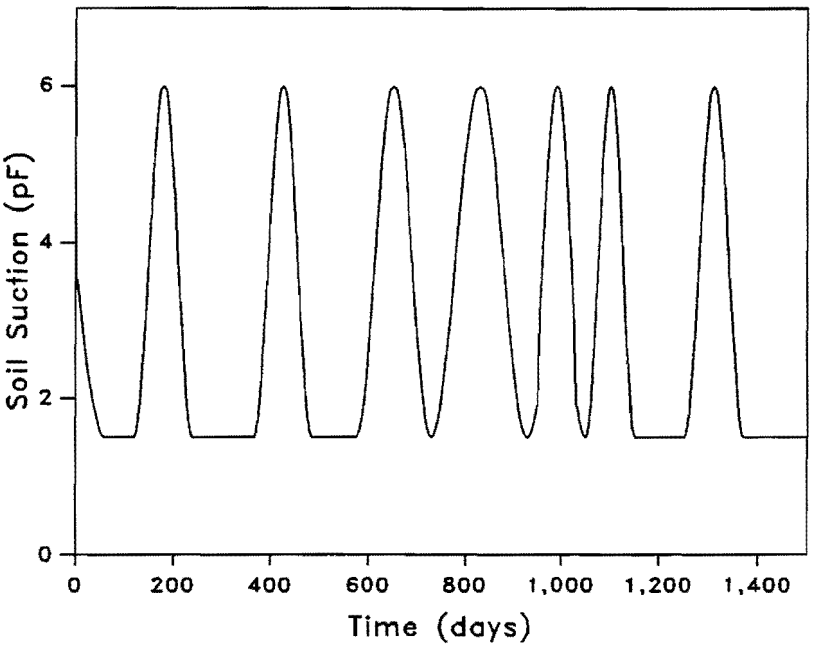

Figure 36. Surface Suction Variation with Time at Converse

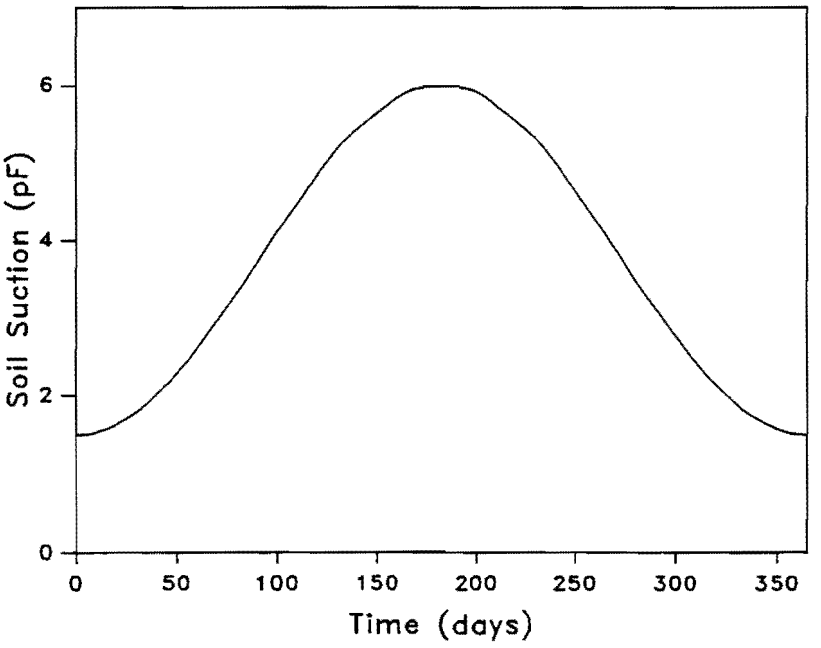

Figure 37. Surface Suction Variation with Time at Snyder 1

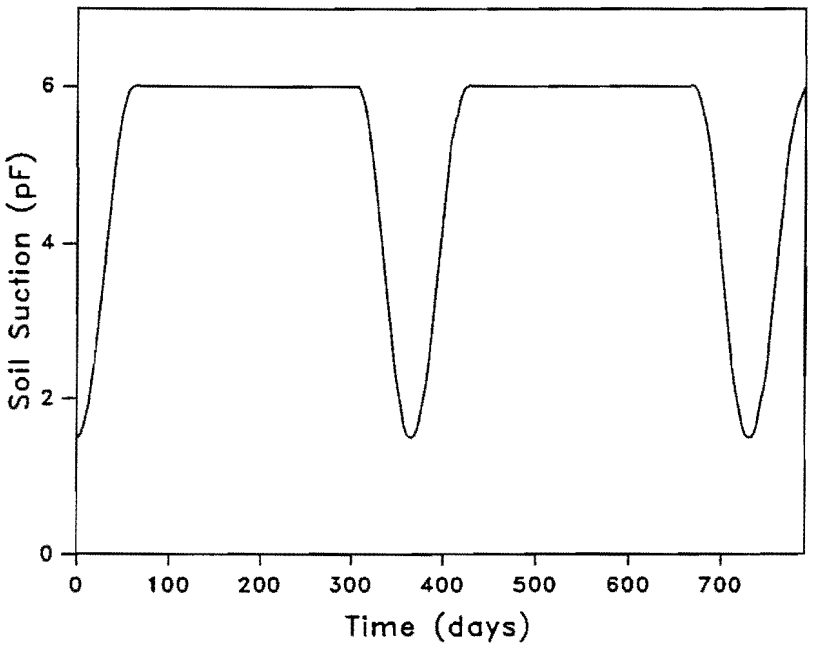

Figure 38. Surface Suction Variation with Time at Wichita Falls 2

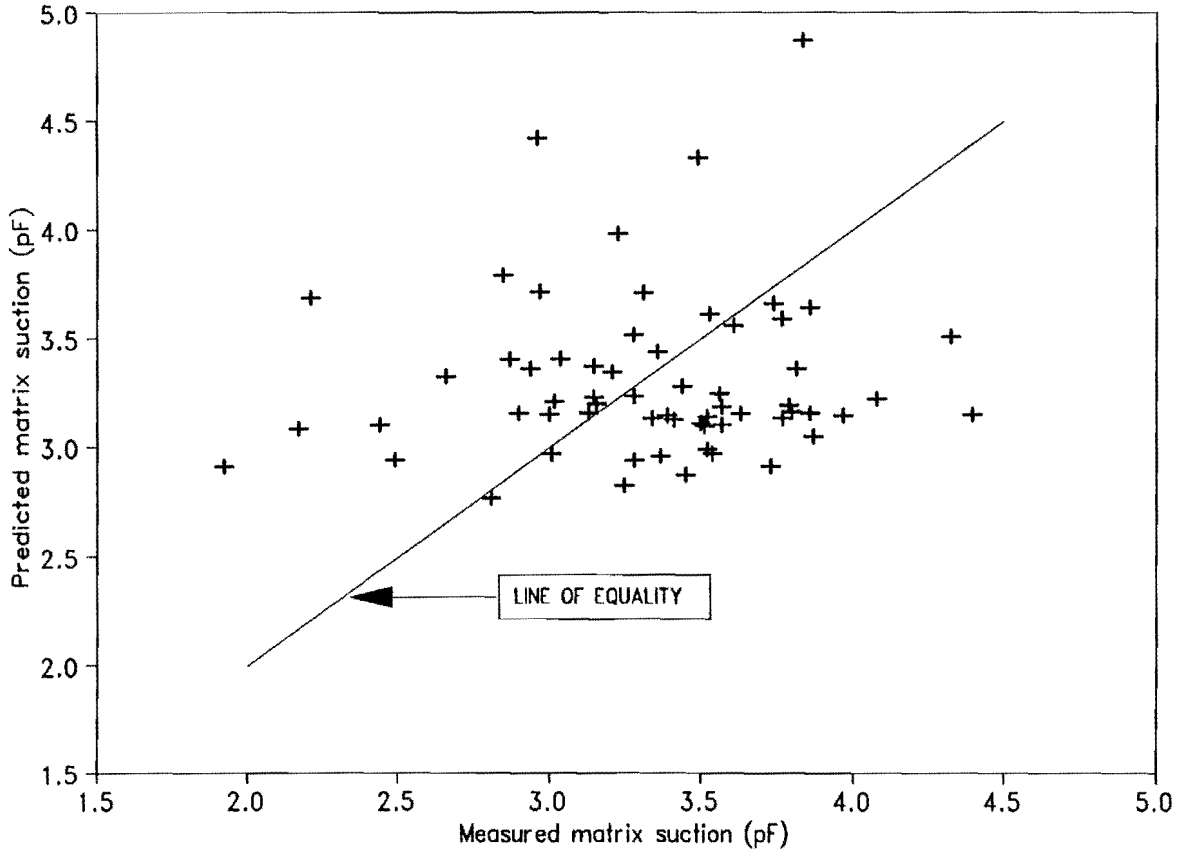

Figure 39. Measured Soil Suction vs. Predicted Soil Suction at Dallas 1

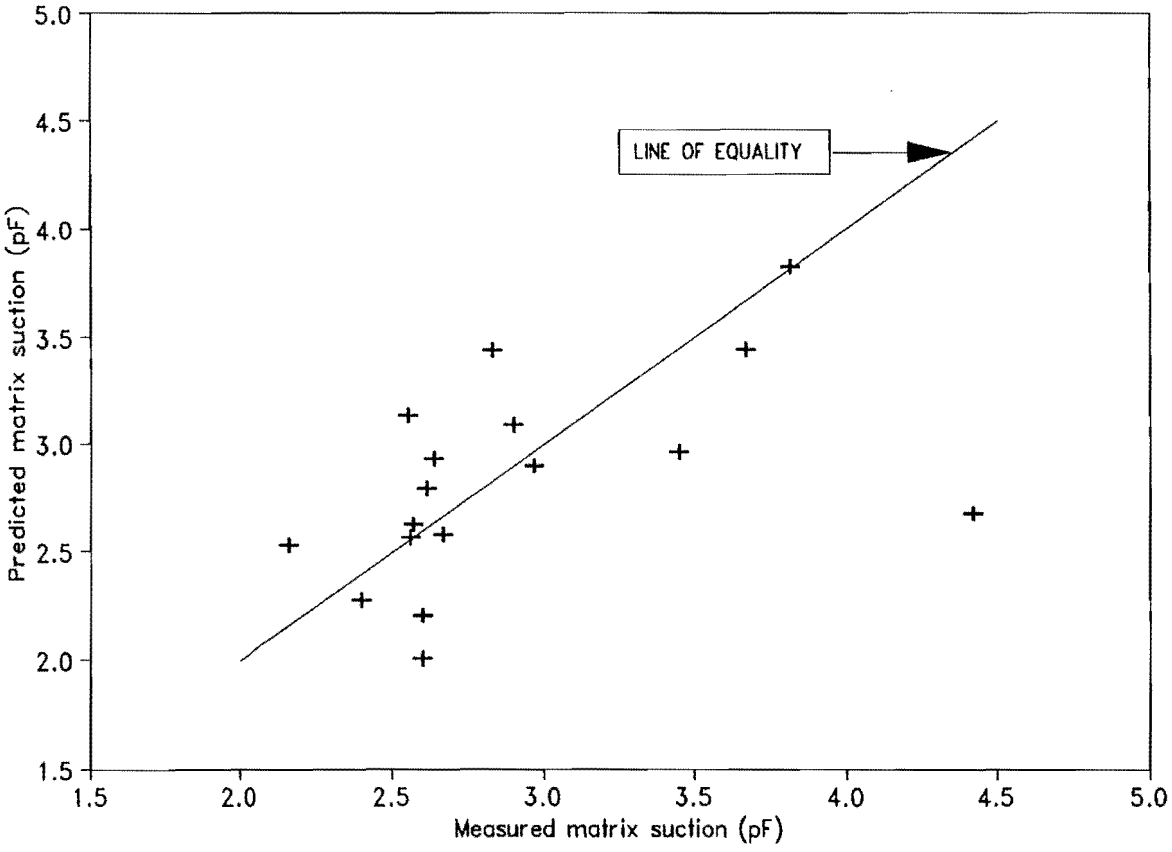

Figure 40. Measured Soil Suction vs. Predicted Soil Suction at Ennis 1

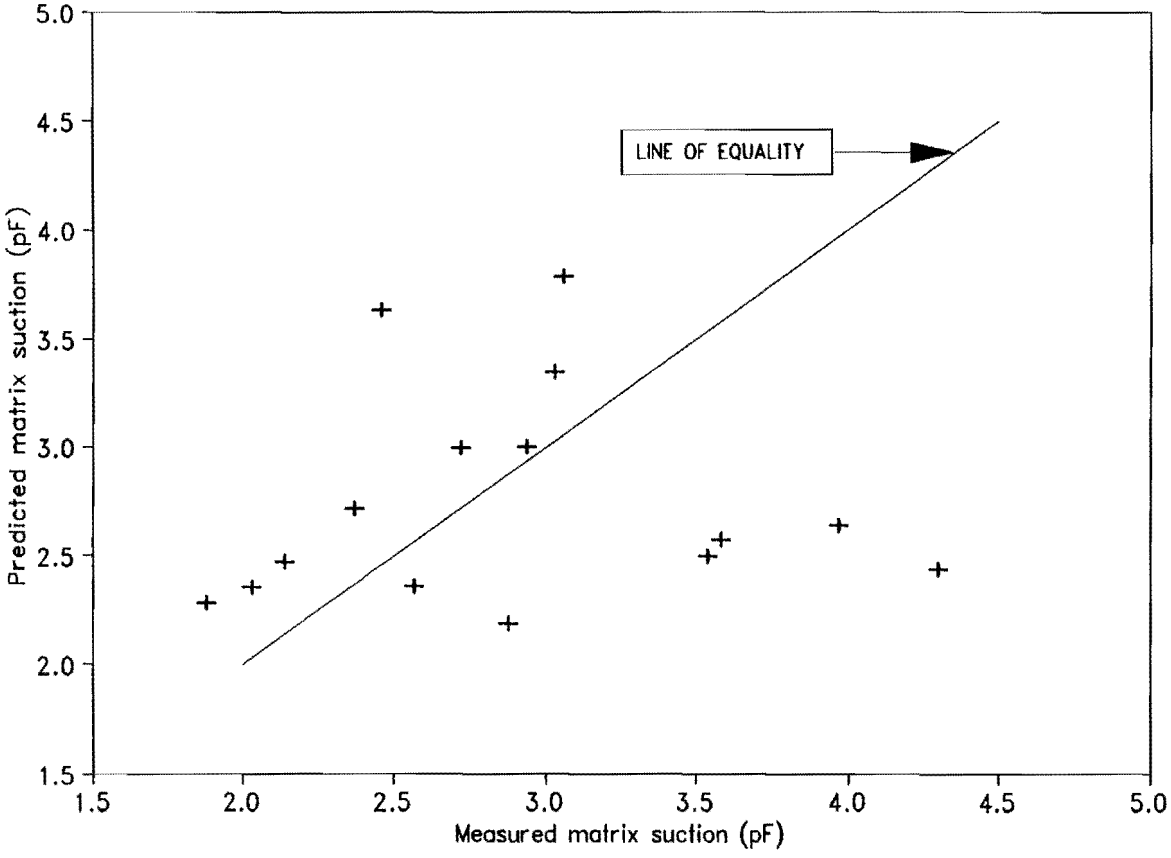

Figure 41. Measured Soil Suction vs. Predicted Soil Suction at Ennis 2

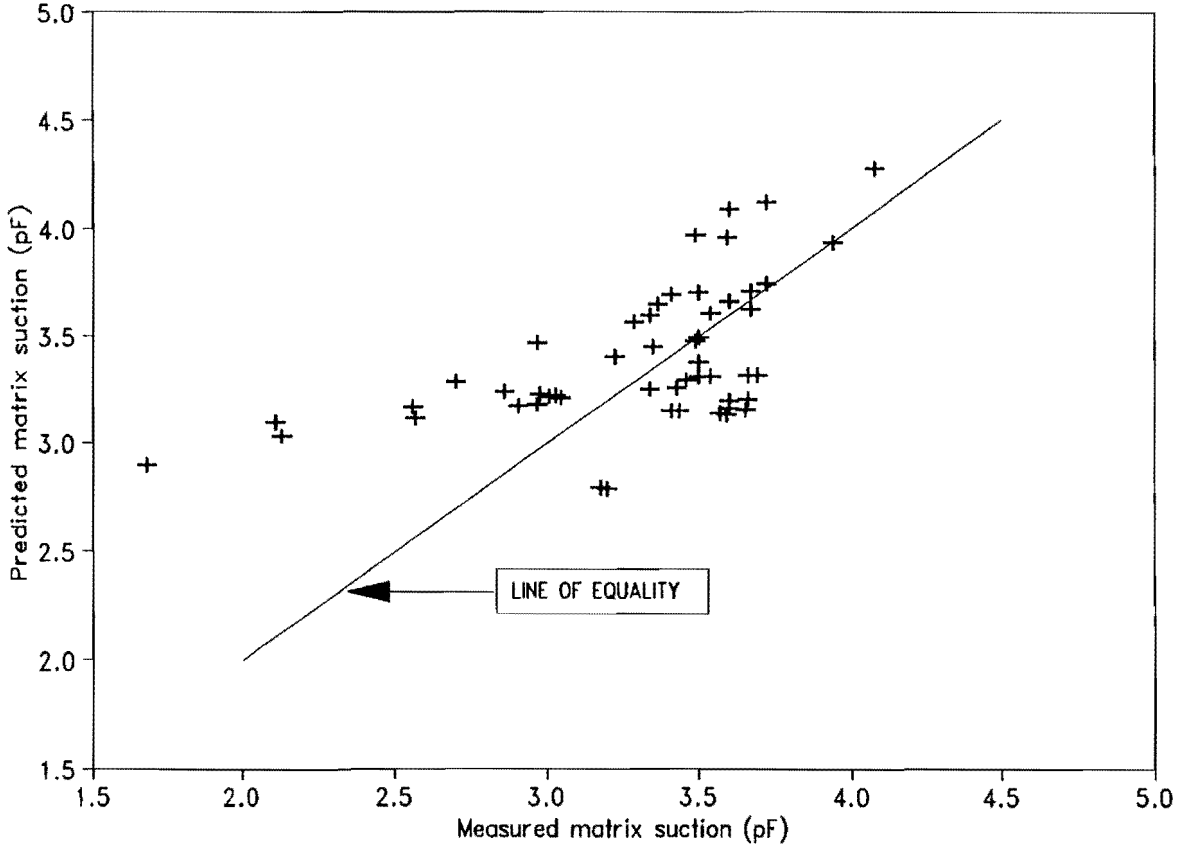

Figure 42. Measured Soil Suction vs. Predicted Soil Suction at Seguin

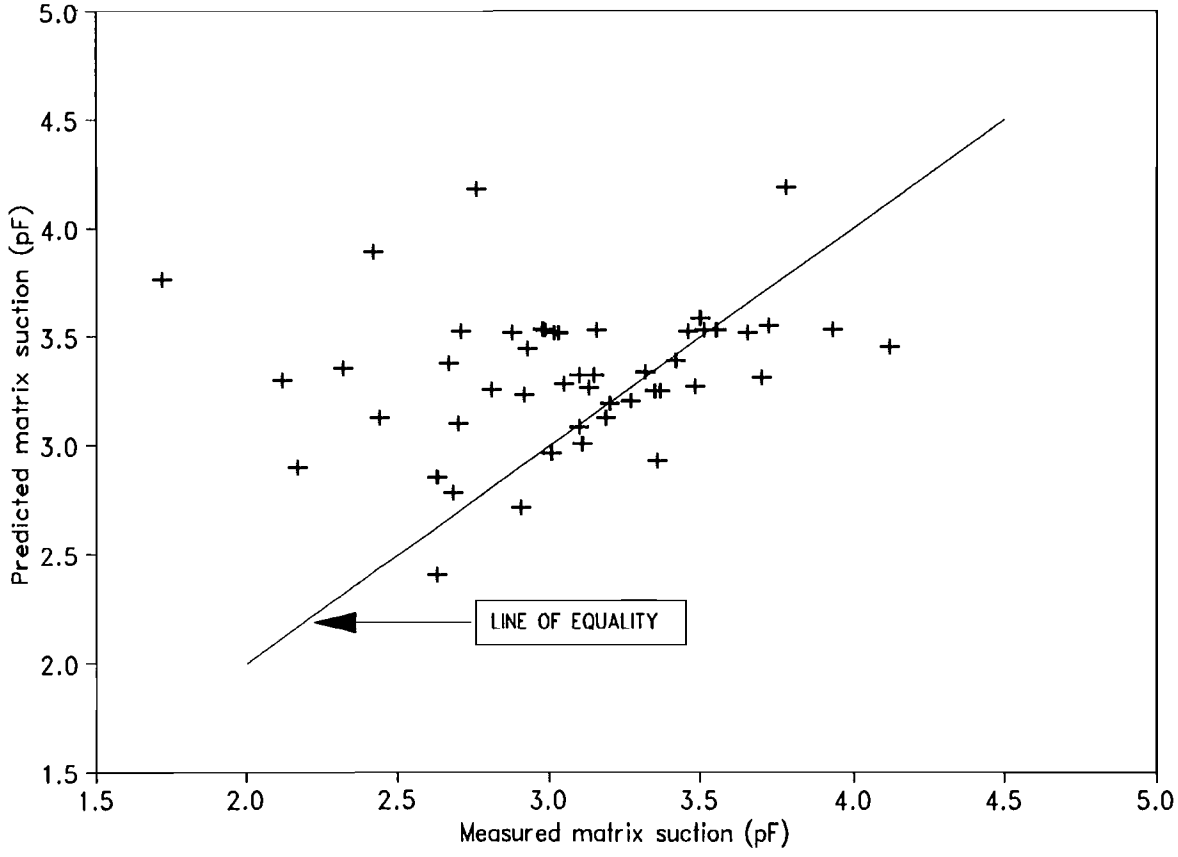

Figure 43. Measured Soil Suction vs. Predicted Soil Suction at Converse

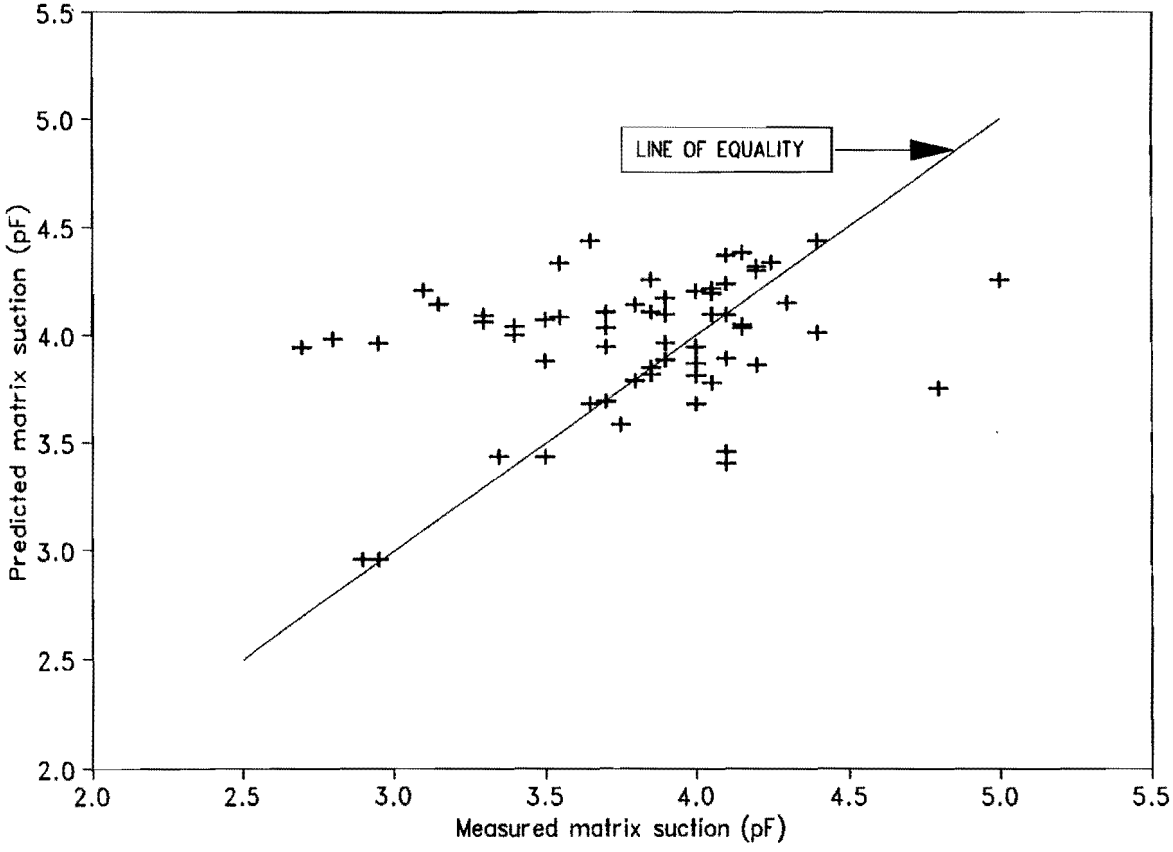

Figure 44. Measured Soil Suction vs. Predicted Soil Suction at Snyder 1

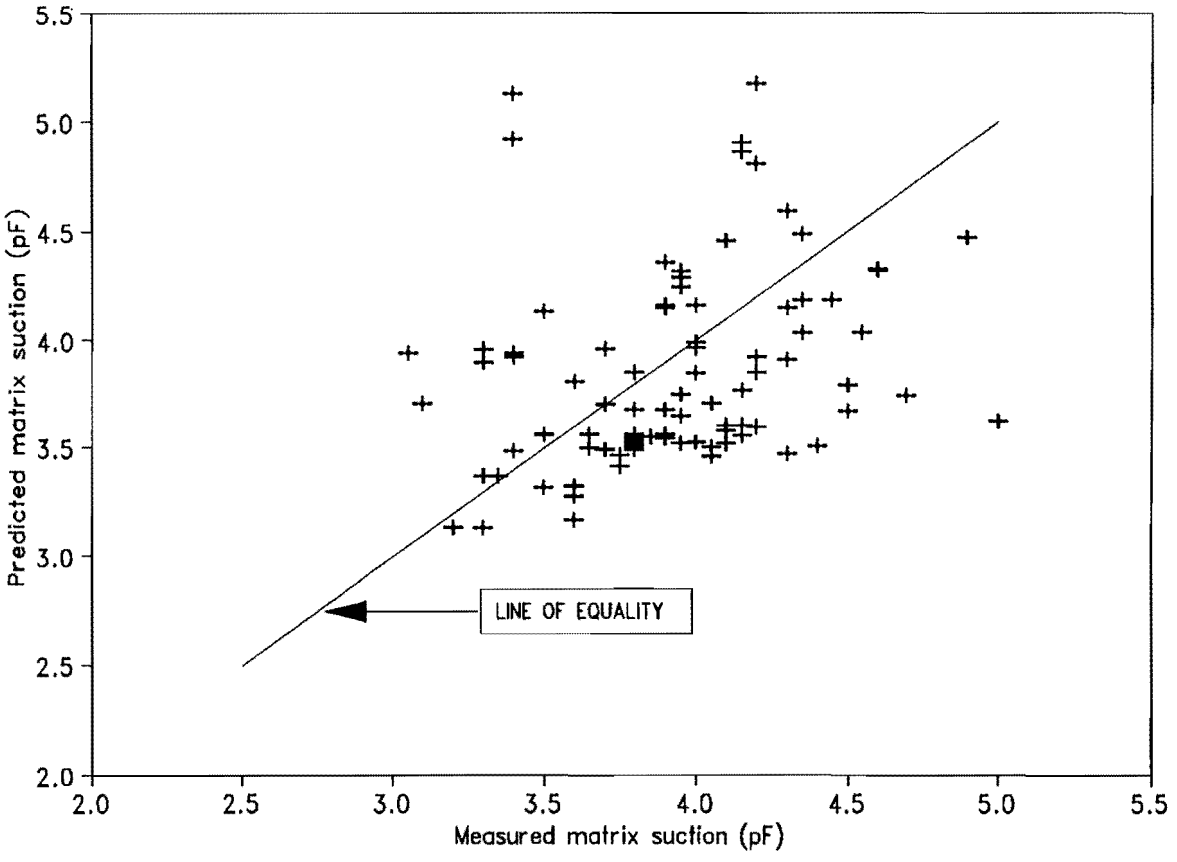

Figure 45. Measured Soil Suction vs. Predicted Soil Suction at Wichita Falls 2

Table 15. Regression Results of Soil Suction vs. Water Content

Site	Boring No.	Sample Depth (ft)	Slope of Straight Line	Intercept	Coefficient of Correlation, R^2	No. of Points
Dallas	BH1	0-3	-8.01	5.92	0.9787	10
		4-7	-8.15	5.94	0.9792	10
		7-10	-7.98	5.93	0.9708	10
Ennis 1	BH4	0-4	-7.25	5.67	0.9775	10
		5-7	-6.95	5.60	0.9771	10
Ennis 2	BH5	0-3	-7.16	5.78	0.9687	10
		4-6	-7.41	5.61	0.9768	10
		6-10	-9.59	5.60	0.9610	10
Seguin	BH8	2-3	-10.16	5.83	0.9910	10
		4-6	-8.22	5.84	0.9664	10
		6-9	-7.84	5.92	0.9933	10
Converse	BH11	0-3	-10.55	5.74	0.9858	10
		3-7	-7.76	6.02	0.9278	10
		7-10	-5.84	5.87	0.9776	10
Snyder	--	0-3	-14.19	5.92	0.9837	9
	--	4-5	-16.19	5.75	0.9816	9
Wichita Falls	--	0-3	-13.84	5.85	0.9827	9

By studying suction measurements at six expansive clay sites, McKeen (44) developed the following equation to estimate the diffusion coefficient.

$$\alpha = b_0+b_1(TMI)+b_2(dh/dw)+b_3(SCI) \quad (17)$$

Where

α = diffusion coefficient

b_0 = 0.010134

b_1 = 0.000002

b_2 = 0.05468

b_3 = -0.03509

TMI = Thornthwaite moisture index

dh/dw = suction-water-content slope

SCI = suction compression index

Using this equation the diffusion coefficients were calculated for the sites at Dallas, Ennis, Converse, and Seguin for which the necessary data were available. These are compared in Table 16 with the diffusion coefficients, unsaturated permeabilities, and saturated permeabilities which were determined in this study. The results show that the values of diffusion coefficients obtained from the comparison of measured and predicted suction compare well with the values obtained from Equation 17. The values of saturated permeability obtained for different sites range between 1.8×10^{-6} and 3.5×10^{-6} with an average value of 2.8×10^{-6}.

Table 16. Estimated Flow Properties of Soil

Site	TMI	Boring No.	Unsaturated Permeability, P (cm^2/sec)	Saturated Permeability, K_o (cm/sec)	Diffusion Coefficient, α (cm^2/sec)	Diffusion Coefficient from Equation 17. (cm^2/sec)
Dallas	-11.3	BH1	0.00069	3.0×10^{-6}	0.0031	0.0022
Ennis 1	-11.3	BH4	0.00081	3.5×10^{-6}	0.0032	0.0032
Ennis 2	-11.3	BH5	0.00083	3.6×10^{-6}	0.0037	0.0037
Seguin	-21.3	BH8	0.00042	1.8×10^{-6}	0.0021	0.0027
Converse	-21.3	BH11	0.00058	2.5×10^{-6}	0.0026	0.0026
Snyder	--	--	0.00059	2.6×10^{-6}	0.0050	--
Wichita Falls	--	--	0.00059	2.6×10^{-6}	0.0045	--

Based on the results of this study, the following conclusions can be made.

1. The FLODEF program is capable of predicting soil suction changes in the field.
2. The suction compression index is a powerful tool in characterizing expansive soils. This can be accurately estimated from the chart method.
3. The diffusion coefficient, unsaturated permeability, and saturated permeability can be accurately estimated from the comparison of measured and predicted soil suction.

CHAPTER V

PREDICTION OF VERTICAL MOVEMENT AND ROUGHNESS DEVELOPMENT

INTRODUCTION

In this chapter, a method of predicting vertical movement and roughness development in highway pavements in different climatic regions is presented and the vertical movement and roughness measures such as Serviceability Index, International Roughness Index, and Maximum Expected Bump Height are estimated for different conditions that are expected in highway pavements. The different conditions considered for this study are:

1. Soil type (cracked or highly permeable, tightly closed cracks or minimally permeable, and medium cracked or moderately permeable)
2. Drainage type (normal, ponded, and slope)
3. Root depth (four feet or shallow root zone, and eight feet or deep root zone)
4. Sodded and paved medians
5. Roadways with and without vertical moisture barriers.

The three different drainage conditions considered for this study cover almost all of the drainage conditions that can be expected in a highway pavement. The "normal," "slope," and "ponded" drainage conditions occur in pavements built on a flat terrain, on a sloping terrain, and in a valley area, respectively. These different drainage conditions are shown in Figure 46. The locations considered for this study were El Paso, San Antonio, Dallas, Houston, and Port Arthur. The study was carried out in the following steps:

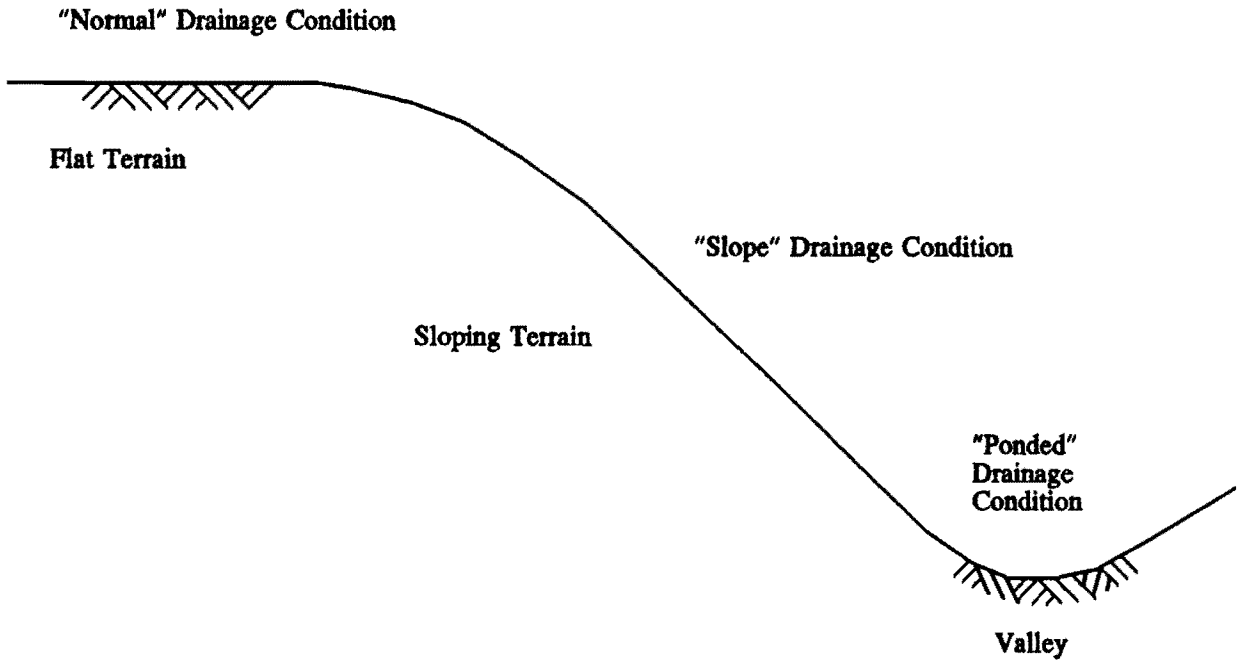

Figure 46. Types of Drainage Conditions

1. Estimation of mean, dry, and wet moisture depths for the five different locations
2. Selection of a function describing surface suction variation with time for the exposed soil area on the side slopes of the pavement
3. Estimation of equilibrium, dry, and wet suction profiles
4. Estimation of maximum vertical movement that is expected in a pavement
5. Estimation of roughness measures
6. Comparison of measured and predicted roughness measures.

ESTIMATION OF MOISTURE DEPTH

The amount of moisture stored in the profile of a given type of soil depends on the climate since this controls the balance between rainfall and evapotranspiration. The "moisture depth" may be defined as the volume of water stored in a volume of the soil profile having a unit cross-sectional area and a depth equal to the depth of the rooting zone of the vegetation at a particular location. The moisture depth varies in response to rainfall and evapotranspiration. Rainfall and evapotranspiration at a particular location are stochastic in nature, and therefore the moisture depth should also be stochastic. A design which relates to the moisture condition of soil should be based on the extreme moisture profiles that have the desired probability of not being exceeded.

The Thornthwaite Moisture Index

The Thornthwaite moisture index (TMI) is a number that indicates the moisture condition at a particular location. The TMI is calculated

on an annual basis by a procedure which involves (a) determination of the potential evapotranspiration, (b) allocation of available water to storage, deficit, and runoff, and (c) computation of the annual summation. The parameters involved in this procedure are the precipitation, potential evapotranspiration, and depth of available moisture (17). The depth of available moisture is the maximum depth of moisture that may be stored within the rooting depth of the soil profile.

In the moisture balance procedure, an initial value of moisture depth is specified which is dependent upon the previous moisture condition and the computation is done on a monthly basis by calculating the difference between precipitation and evapotranspiration. If the precipitation exceeds the evapotranspiration, the difference is added to the soil storage up to a maximum value of the depth of available moisture. If the soil profile reaches its moisture condition to the depth of available moisture, the additional water runs off. When the evapotranspiration exceeds the precipitation, a loss of soil moisture occurs until it reaches zero moisture storage. After reaching zero moisture storage, the additional difference between evapotranspiration and precipitation causes a moisture deficit. The total runoff, deficit, and evapotranspiration for a year are obtained by summing the monthly values. Then the Thornthwaite moisture index is given by:

$$TMI = \frac{100R - 60DEF}{E_p} \tag{18}$$

Where

R = runoff moisture depth

DEF = deficit moisture depth

E_p = the total potential evapotranspiration for the year

The statistical parameters such as the mean and the standard deviation of TMI can be computed from historical records of weather data at a particular location. Gay (17) developed a procedure to estimate the parameters required for the evaluation of the moisture condition at a particular location. A description of this procedure is presented in the next section of this chapter.

The Variability of TMI

The distribution of TMI at a particular location follows the normal probability distribution, the standard deviation of which is given by:

$$\sigma_{TMI} = 0.2833\mu_{TMI} + 17.73 \tag{19}$$

Where

σ_{TMI} = standard deviation

μ_{TMI} = mean Thornthwaite moisture index at that location

Relationship between Mean Annual Moisture Depth and TMI

The mean annual moisture depth for a particular location is given by:

$$S_m = \frac{\sum_{i-1}^{N} d_{mi}}{N} \tag{20}$$

Where

S_m = mean annual moisture depth

d_{mi} = mean moisture depth for the i^{th} year

N = number of years over which the moisture balance is carried out

The mean moisture depth for a particular year is defined as the average monthly moisture storage in the soil profile over the year and is given by:

$$d_m = \frac{\sum_{i-1}^{12} s_i}{12} \tag{21}$$

Where

d_m = mean moisture depth for a particular year

s_i = moisture storage in the soil profile for month i

The mean annual moisture depth can be expressed as functions of TMI and the depth of available moisture and is given by (17):

$$d = \frac{d_{am}}{\left[1 + \frac{d_{am} - d_1}{d_1 \left[\frac{T}{T_1}\right]^{\gamma}}\right]} \tag{22}$$

Where

T = TMI + 60

d = mean annual moisture depth

d_{am} = available moisture depth

γ = 0.039337 d_{am} + 1.357033

d_1 = 0.449079 d_{am} + 0.304560

T_1 = 0.062651 d_{am} + 59.53593

Relationship between mean pF and TMI at a site

A relationship between volumetric moisture content and matrix suction of a given soil exists through the desorption curve of that soil. The desorption relationship can be expressed mathematically as:

$$| h | = \left[A \left[\frac{\theta_s - \theta_r}{\theta - \theta_r} - 1 \right] \right]^{\frac{1}{B}} \qquad (23)$$

Where

h = soil suction in cm

θ_s = saturation volumetric moisture content

θ_r = residual volumetric moisture content

θ = volumetric moisture content

A, B = constants obtained by fitting this expression to measured data

Substituting mean volumetric moisture content for θ in the above expression, the mean matrix suction for a site can be obtained, given the desorption relationship for that site. Mean volumetric moisture content is expressed as functions of TMI and d_{am} as:

$$\theta_m = \frac{d_{am}/Z_c}{\left[1 + \frac{d_{am} - d_1}{d_1 \left[\frac{T}{T_1} \right]^{\gamma}} \right]} + \theta_{dry} \qquad (24)$$

Where

Z_c = characteristic soil depth. This depth of soil is the minimum depth of soil over which the available moisture depth d_{am} may be stored.

θ_m = volumetric moisture content at field capacity

θ_{dry} = volumetric moisture content at the driest soil state

Z_c is given by:

$$Z_c = \frac{d_{am}}{\theta_{fc} - \theta_{dry}} \tag{25}$$

Where

θ_{fc} = volumetric moisture content at field capacity

θ_{fc} is given by:

$$\theta_{fc} = 0.88\ \theta_s \tag{26}$$

Amplitude of Moisture Depth

The amplitude of moisture depth describes the variability of moisture depth over a year at a specific site. This relationship is expressed as:

$$a_{dm} = a_1 \exp\left[-\left[\frac{\mu_{TMI} - a_2}{a_3}\right]^2\right] + a_4 \tag{27}$$

Where

a_{dm} = amplitude of moisture depth

μ_{TMI} = mean TMI at site analyzed

a_1, a_2, a_3, a_4 = regression coefficients

a_1, a_2, a_3, a_4 are given by:

$$a_i = \beta_{i,4} + \beta_{i,1}\ d_{am} - \beta_{i,2} \exp\left(-\left(\beta_{i,3}\ d_{am}\right)\right) \tag{28}$$

Where

$\beta_{i,j}$ = regression coefficients for parameter a_i, i,j=1,4

These parameters are given in Table 17.

Table 17. Coefficients for the Estimation of Parameters for Amplitude of Moisture Depths

a_i	$\beta_{1,j}$	$\beta_{2,j}$	$\beta_{3,j}$	$\beta_{4,j}$
a_1	0.007327	17.601	0.057207	16.10400
a_2	-0.000100	-19.000	0.010000	-7.00000
a_3	-0.236260	-52.811	0.130077	39.55800
a_4	0.034308	0.000	0.000000	1.54771

Calculation Procedure

The mean, dry, and wet moisture depths for a particular climatic environment can be estimated using the concepts presented in the previous section and this procedure is described in the following steps.

1. The frequency distribution of the TMI at a desired location is obtained by using a historical mean of TMI (T_{mean}) at the site and obtaining the standard deviation of TMI from Equation 19. The extreme values of the mean TMI for a dry year and wet year (T_{wet} and T_{dry}) for a specific return period are then estimated. For this study, a 25 year return period is used. T_{mean}, T_{wet}, and T_{dry} are graphically shown in Figure 47.
2. Mean annual moisture depths (d_{mean}, d_{dry} and d_{wet}) corresponding to T_{mean}, T_{wet} and T_{dry} are estimated from Equation 22 by substituting T_{mean}, T_{wet} and T_{dry} in place of TMI in the equation. The depth of available moisture d_{am} is required for this computation. This depth varies from place

to place depending on the site conditions. Typical values for d_{am} found in the literature lie between 5-27 cm (17). For this analysis, a depth of 30 cm is used.

3. The amplitude of moisture depth for a site (a_{dm}) is calculated from Equation 27. Then the extreme moisture depths are estimated as follows.

$$d_{max} = d_{wet} + a_{dm}$$

$$d_{min} = d_{dry} - a_{dm}$$

If the estimated value of d_{max} exceeds d_{am}, the value of d_{am} is used for d_{max}, and if estimated d_{min} goes below zero, zero is used for d_{min}.

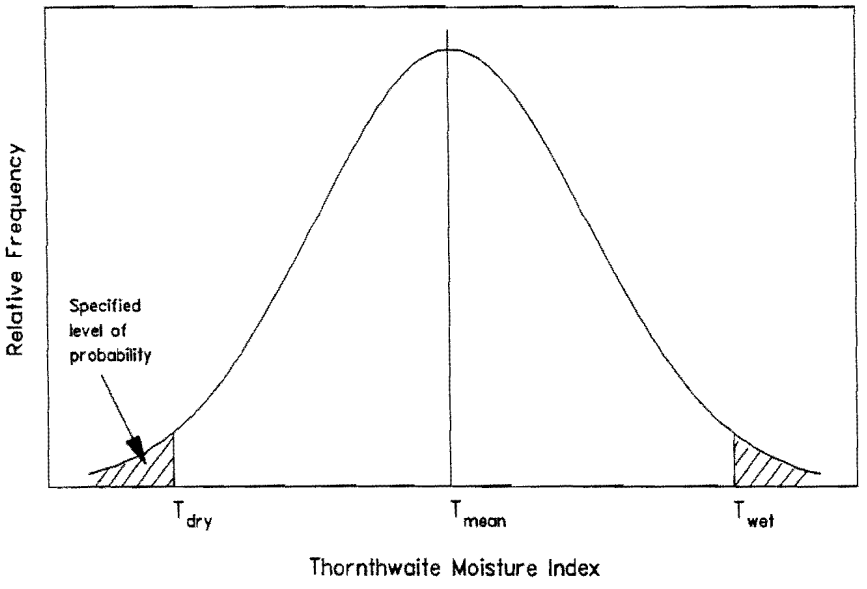

Figure 47. Frequency Distribution of TMI at a Site

SURFACE SUCTION VARIATION WITH TIME

Surface Suction Variation for "Normal" Drainage Condition

The suction at the soil surface varies with time in response to rainfall and evapotranspiration at a particular site. The evapotranspiration, in turn, depends on the atmospheric temperature distribution over time. Furthermore, if a pavement is built on soil which is initially in an equilibrium moisture state, the surface displacements should fluctuate around zero under average weather conditions. Considering these facts, a tentative surface suction distribution over time is developed for each site under study based on the historical means of monthly rainfall and temperature distribution over time. The final surface suction distribution over time is obtained by modifying the surface suction distribution derived from the rainfall and temperature criteria so that the displacement of a pavement surface fluctuates around zero under the equilibrium initial moisture condition as shown in Figure 48. The initial moisture profiles, which are derived later in this chapter, are used to obtain the displacement variation of the pavement over time. The surface suction distributions derived in this manner are used for the "normal" drainage condition. These surface suction distributions along with the average monthly rainfall and temperature patterns for the sites under study are shown in Figures 49 through 58.

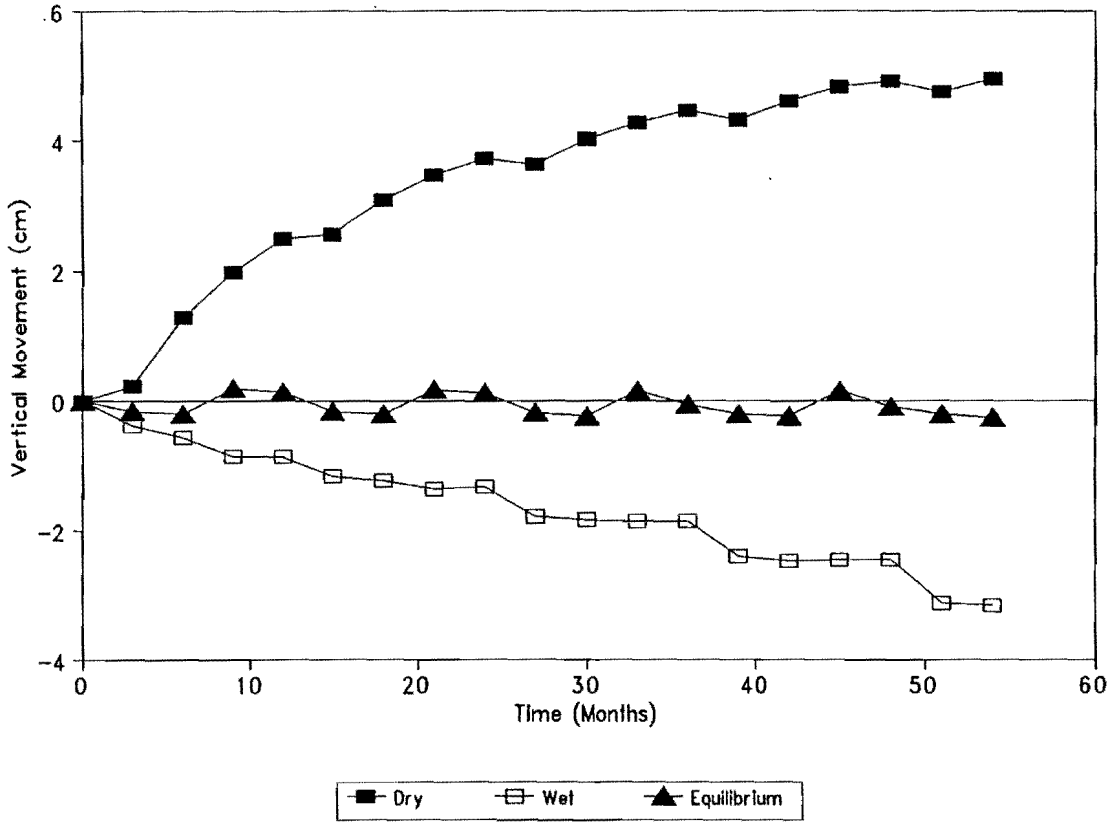

Figure 48. A typical Pattern of Vertical Movement Variation with Time for Different Initial Moisture Conditions

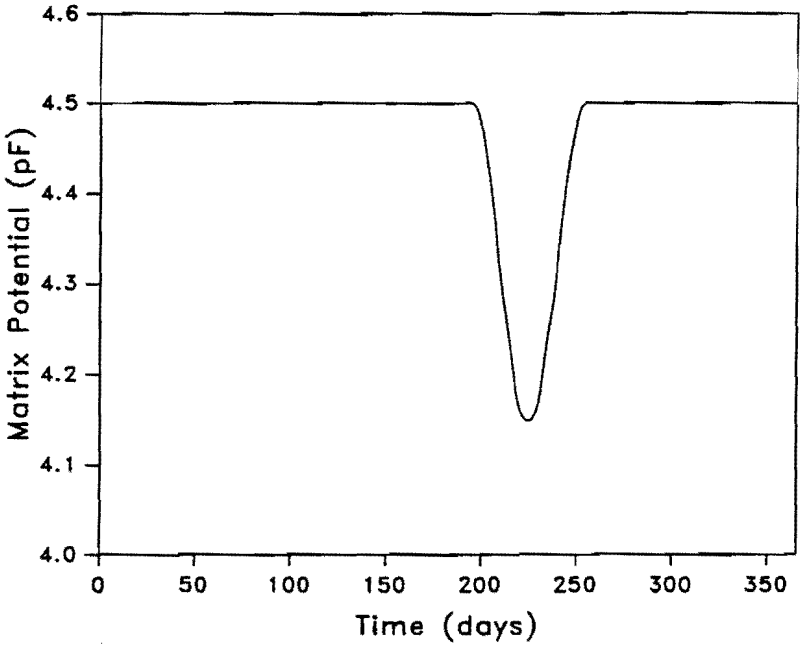

Figure 49. Surface Suction Distribution over Time for the "Normal" Drainage Condition in El Paso

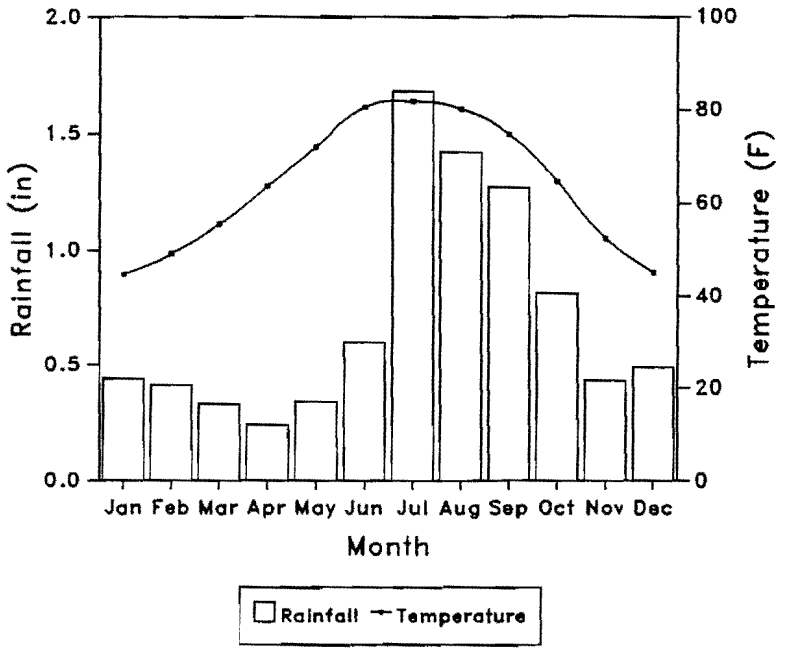

Figure 50. Mean Monthly Rainfall and Temperature Distribution over Time in El Paso

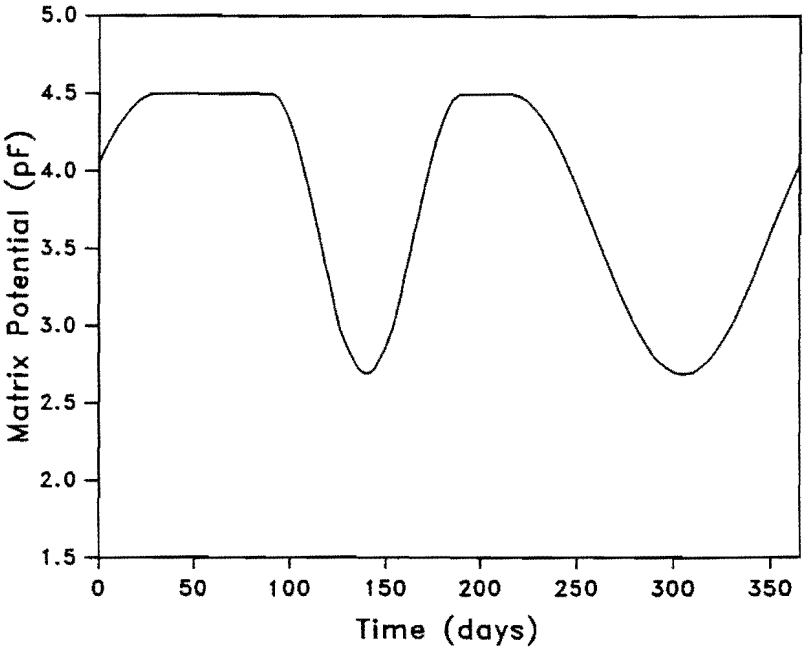

Figure 51. Surface Suction Distribution over Time for the "Normal" Drainage Condition in San Antonio

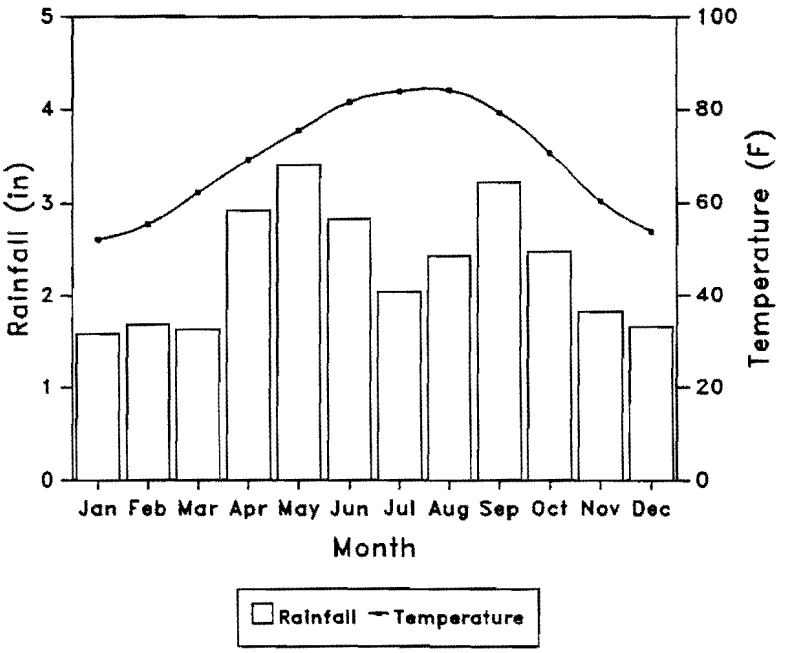

Figure 52. Mean Monthly Rainfall and Temperature Distribution over Time in San Antonio

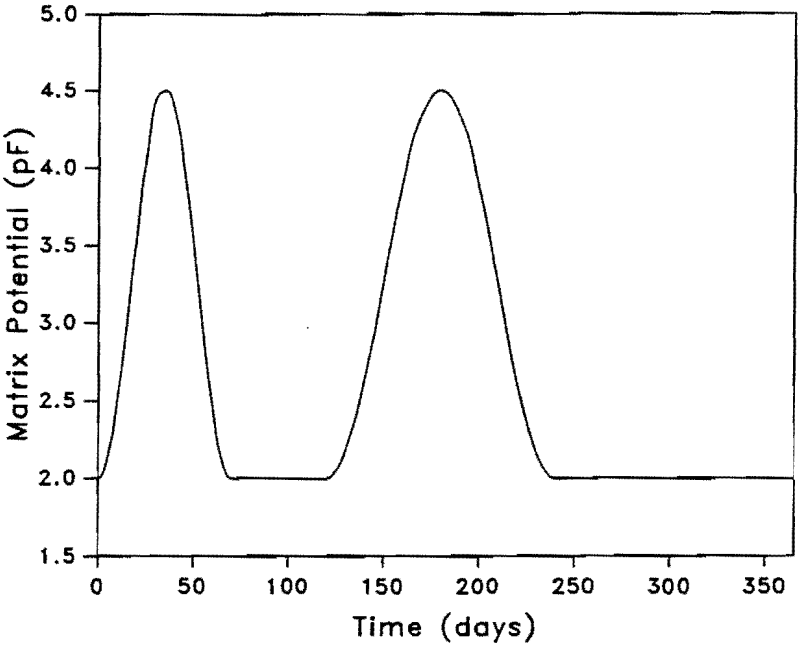

Figure 53. Surface Suction Distribution over Time for the "Normal" Drainage Condition in Dallas

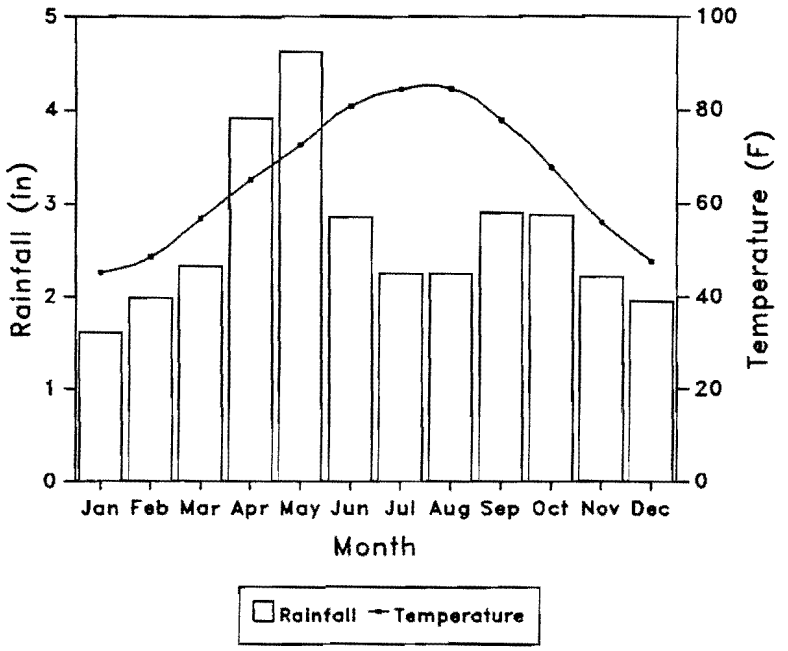

Figure 54. Mean Monthly Rainfall and Temperature Distribution over Time in Dallas

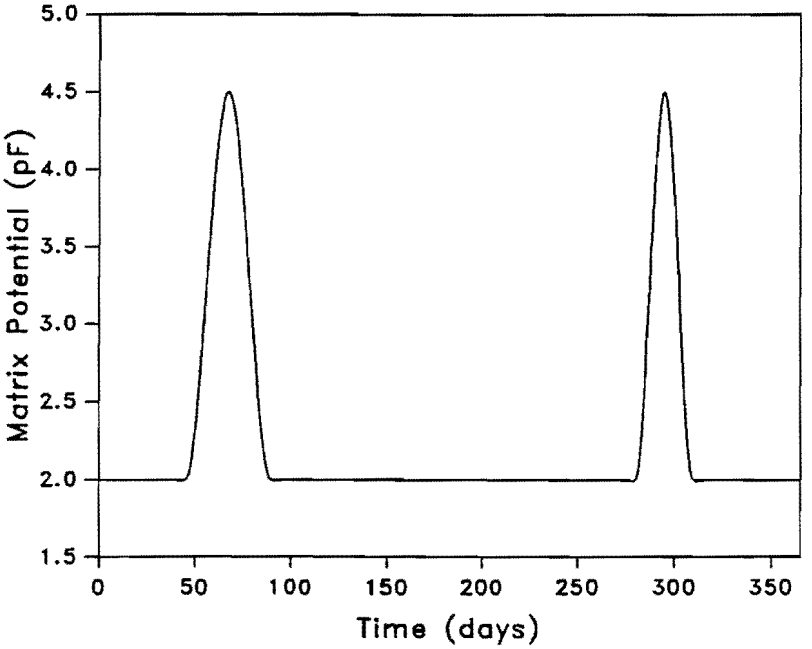

Figure 55. Surface Suction Distribution over Time for the "Normal" Drainage Condition in Houston

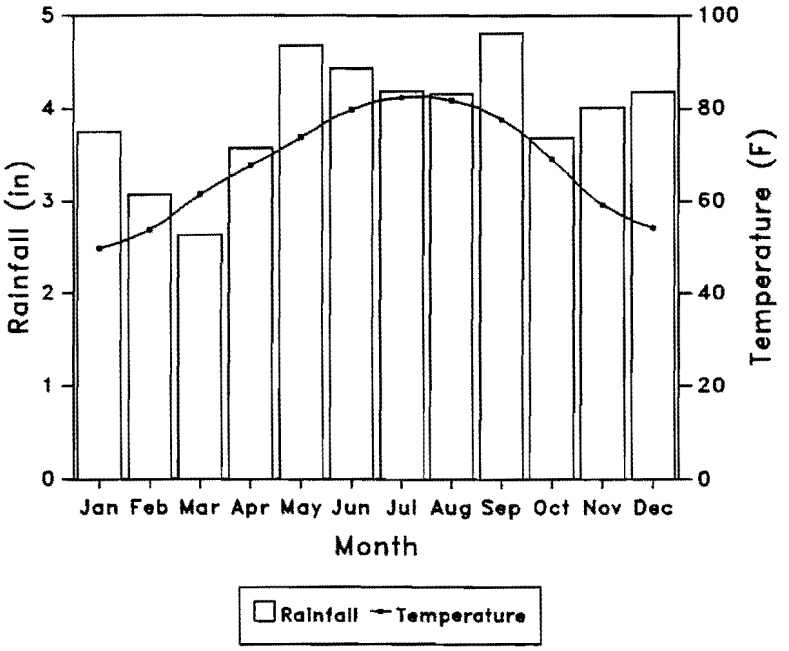

Figure 56. Mean Monthly Rainfall and Temperature Distribution over Time in Houston

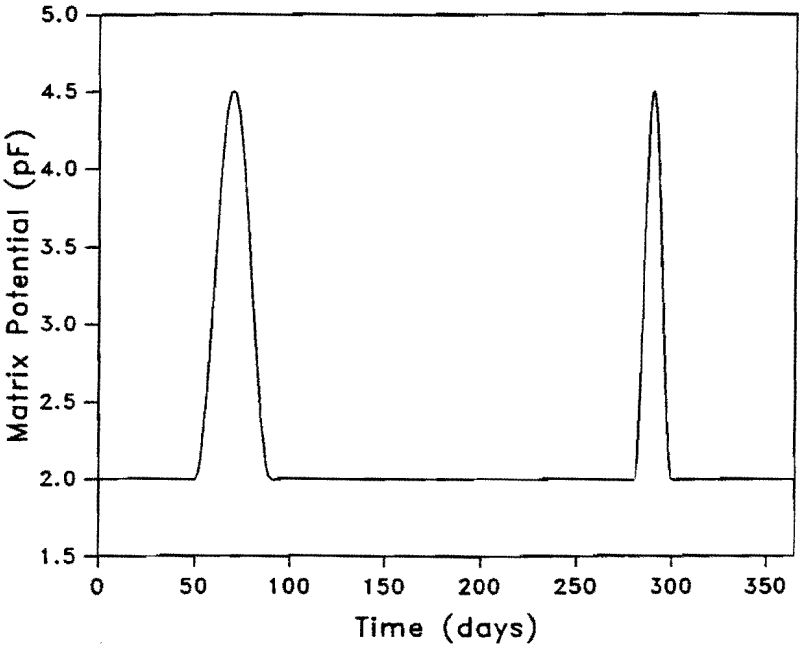

Figure 57. Surface Suction Distribution over Time for the "Normal" Drainage Condition in Port Arthur

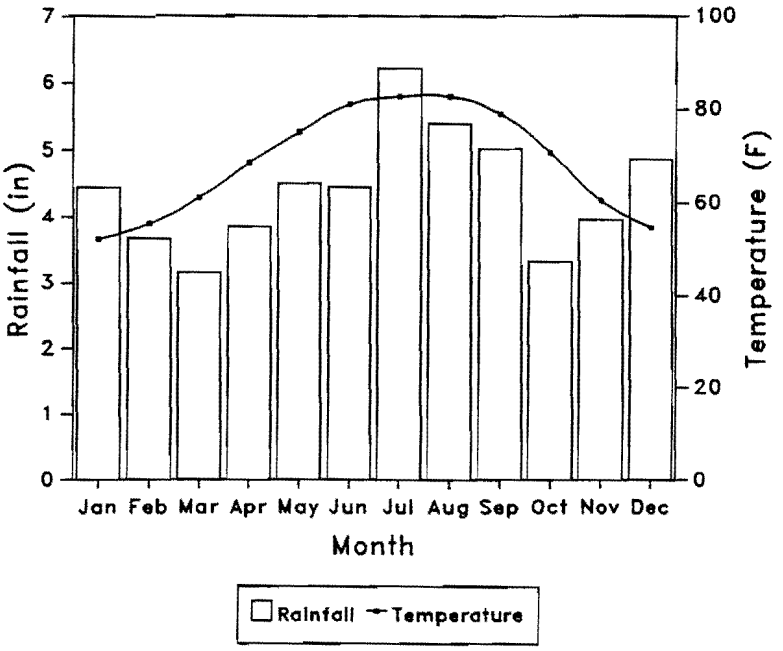

Figure 58. Mean Monthly Rainfall and Temperature Distribution over Time in Port Arthur

Surface Suction Variation for "Slope" and "Ponded" Drainage Conditions

The surface suction distribution over time evaluated in the previous section is valid for the "normal" drainage condition in which runoff is normal. The availability of moisture to the soil beneath a pavement on sloping terrain is less than the availability of moisture beneath a pavement on normal terrain because water runs off which under "normal" drainage conditions would infiltrate. Therefore, it can be assumed that the surface suction distribution over time for the "slope" drainage condition is drier than that of the "normal" drainage condition. Considering this factor, the surface suction distributions for the "slope" drainage condition are developed and are shown in Figures 59 through 63.

The "ponded" drainage condition occurs when there is water standing in the drainage ditch of a roadway for a long period of time. This condition can be modelled by assigning a constant surface suction of 2.00 pF throughout the year in the ditch of the roadway, and a variable suction with time, equal to the "normal" drainage condition, on the side slope of the roadway.

ESTIMATION OF SUCTION PROFILES

The initial moisture condition is given to the FLODEF program in the form of Equation 14. Therefore, a suction profile given in the form of this equation which corresponds to the moisture depth may be used to represent the initial moisture condition of the soil. The relationship between moisture content and soil suction exists through a desorption curve. For this study, the desorption curve obtained for a site at Greenville, Texas (24) is used. This desorption relationship may be

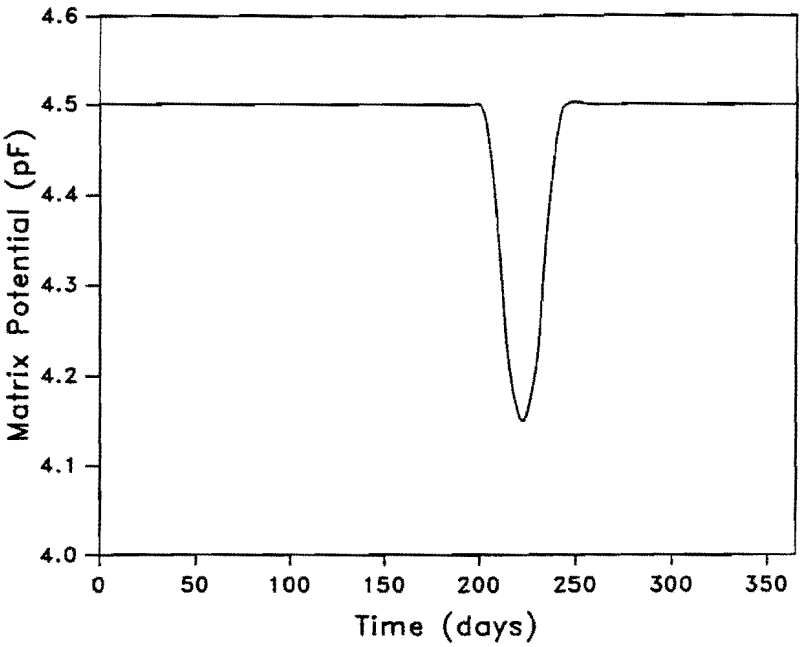

Figure 59. Surface Suction Distribution over Time for the "Slope" Drainage Condition in El Paso

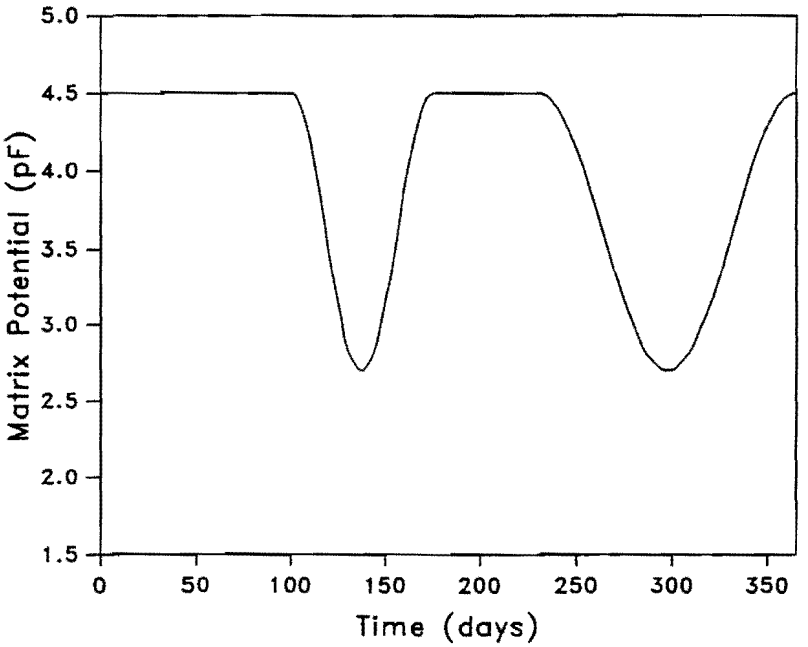

Figure 60. Surface Suction Distribution over Time for the "Slope" Drainage Condition in San Antonio

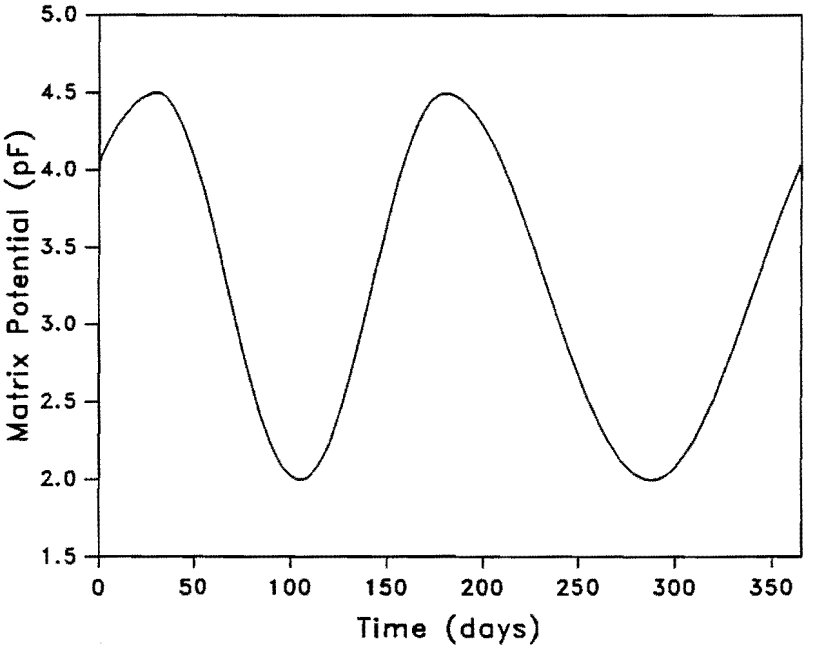

Figure 61. Surface Suction Distribution over Time for the "Slope" Drainage Condition in Dallas

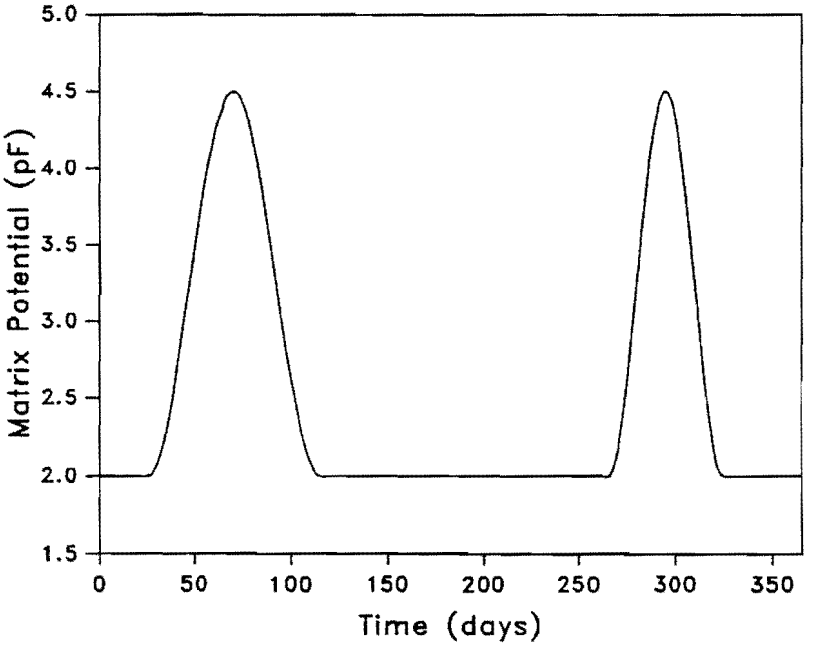

Figure 62. Surface Suction Distribution over Time for the "Slope" Drainage Condition in Houston

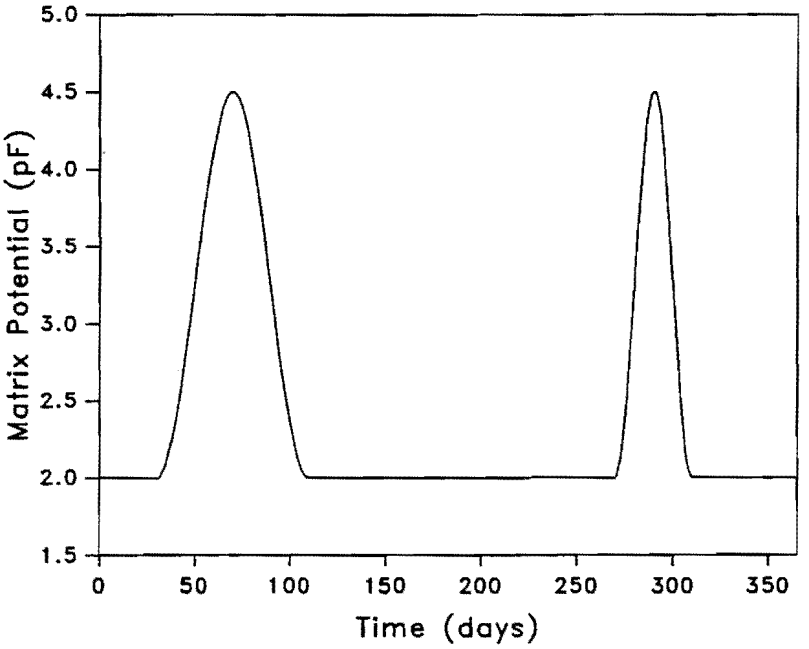

Figure 63. Surface Suction Distribution over Time for the "Slope" Drainage Condition in Port Arthur

expressed in the form of Equation 23, and the corresponding coefficients which satisfy this equation are as follows (17):

θ_s = 0.50

θ_r = 0.04

A = 150

B = 0.50

For this purpose, the following equation can also be used instead of Equation 23.

$$h = a - c\left[\frac{\gamma_w}{\gamma_d}\right]\theta \qquad (29)$$

Where

h = soil suction in pF

a = the intercept in Table 15

c = the slope of straight line in Table 15

γ_w = density of water

γd = dry density of soil

θ = volumetric moisture content

Calculation Procedure

The procedure of estimating mean, dry, and wet suction profiles at a particular location is described in the following steps:

1. The volumetric moisture content at field capacity is estimated from Equation 26 by substituting the value of θ_s in the equation. Numerically, θ_s is equal to the porosity of soil which is given by:

$$n = \frac{\gamma_s - \gamma_d}{\gamma_s} \qquad (30)$$

Where

n = porosity of soil

γ_s = density of soil particles

γ_d = dry density of soil

2. Assuming the matrix potential at the driest state of soil to be 4.5 pF, which corresponds to the wilting point of vegetation, the volumetric moisture content at the driest state of soil, θ_{dry}, is estimated from Equation 23 or Equation 29.

3. The characteristic soil depth (Z_c) is calculated from Equation 25, and the mean volumetric moisture content is estimated from Equation 24. Substituting the estimated mean volumetric moisture content in place of θ in Equation 23 or Equation 29, the mean matrix potential is estimated.

4. Assuming trial values for frequency (n), amplitude (U_0), and equilibrium matrix potential (U_e) which describe the suction profile of soil through Equation 14, a numerical integration is carried out to estimate the soil moisture depth in the zone of characteristic soil depth. For this study, the frequency was assumed as 1 for El Paso and 2 for other locations. The diffusion coefficients (α) used for cracked soil, medium cracked soil, and tight soil are 0.006, 0.0025, and 0.0002 cm^2/sec, respectively. The values of amplitude and equilibrium matrix potential that satisfy the corresponding estimated minimum and maximum moisture depths (d_{min}, d_{max}) are selected to represent the dry and wet

suction profiles, respectively. For this computation, it is assumed that the matrix potential varies in the range of 2.0-4.5 pF. The equilibrium suction profile is obtained by using the mean matrix potential estimated in Step 3, assuming trial values for the amplitude of matrix suction and following the same procedure as for the dry and wet suction profiles.

5. The estimated suction profiles in Step 4 are valid for the "normal" drainage condition. However, the extreme dry and wet profiles that can be expected in a sloping terrain do not vary much from those in the normal terrain. Therefore, the same dry and wet suction profiles are used for the "normal" and "slope" drainage conditions. Also, for the "ponded" drainage condition, the same dry suction profile may be used. However, in a ponded situation, the extreme wet profile is wetter than that in a normal situation. Therefore, a constant suction of 2.00 pF for the entire section is used for the "ponded" drainage condition.

The estimated moisture depths for soils under the "normal" drainage condition are presented in Table 18, and the suction profile constants for cracked soil, medium cracked soil, and tight soil under the "normal" drainage condition are presented in Tables 19 through 21.

Table 18. Moisture Depths for Soils under "Normal" Drainage Conditions

Location	TMI	d_{mean} (cm)	d_{min} (cm)	d_{max} (cm)
El Paso	-46.5	0.5358	0.00	5.28
San Antonio	-21.3	6.2493	0.00	22.10
Dallas	-11.3	9.6114	0.00	29.66
Houston	14.8	17.5022	0.00	30.00
Port Arthur	26.8	20.1403	0.00	30.00

Table 19. Suction Profile Constants for Cracked Soil under "Normal" Drainage Conditions

Location	Equilibrium (pF)		Dry (pF)		Wet (pF)	
	U_e	U_0	U_e	U_0	U_e	U_0
El Paso	4.48	0.01	4.50	0.00	4.47	0.32
San Antonio	4.20	-0.01	4.50	0.00	4.18	1.48
Dallas	4.04	0.00	4.50	0.00	3.65	1.65
Houston	3.62	-0.03	4.50	0.00	3.58	1.58
Port Arthur	3.47	0.00	4.50	0.00	3.58	1.58

Table 20. Suction Profile Constants for Tight Soil under "Normal" Drainage Conditions

Location	Equilibrium (pF)		Dry (pF)		Wet (pF)	
	U_e	U_0	U_e	U_0	U_e	U_0
El Paso	4.48	0.01	4.50	0.00	4.26	0.11
San Antonio	4.20	-0.04	4.50	0.00	3.40	0.70
Dallas	4.04	0.00	4.50	0.00	2.80	0.80
Houston	3.62	-0.07	4.50	0.00	2.76	0.76
Port Arthur	3.47	-0.02	4.50	0.00	2.76	0.76

Table 21. Suction Profile Constants for Medium Cracked Soil under "Normal" Drainage Conditions

Location	Equilibrium (pF)		Dry (pF)		Wet (pF)	
	U_e	U_0	U_e	U_0	U_e	U_0
El Paso	4.48	0.01	4.50	0.00	4.37	0.22
San Antonio	4.20	-0.01	4.50	0.00	3.77	1.07
Dallas	4.04	0.00	4.50	0.00	3.20	1.20
Houston	3.62	-0.02	4.50	0.00	3.14	1.14
Port Arthur	3.47	0.00	4.50	0.00	3.14	1.14

MAXIMUM EXPECTED VERTICAL MOVEMENT

The extreme dry and wet suction profiles and surface suction distribution over time, which were developed in the previous sections of this chapter, are used in the FLODEF program to estimate the maximum expected vertical movement in a highway pavement. For this analysis, a two lane roadway with two 12 ft wide travelway lanes and 2 ft wide paved shoulders on either side of the roadway was considered. The analysis was carried forward for a period of four and half years. The expected vertical movements in the outside wheel path of the roadway for both dry and wet initial conditions were estimated separately and added together to obtain the maximum vertical movement that should be expected during the life time of the pavement. The outside wheel path was considered to be at a distance of 10 ft from the center line of the pavement.

The maximum expected vertical movement was estimated for roadways with and without vertical moisture barriers. The different barrier depths considered were 3 ft, 5 ft, and 8 ft. The different conditions considered for this study were:

1. Soil type (cracked or high permeable, tight or low permeable, and medium cracked)
2. Drainage type (normal, ponded, and slope)
3. Root depth (four feet or shallow root zone, and eight feet or deep root zone)
4. Median type (sodded, and paved)

The pavement section considered for this study consisted of a 45 cm deep combined subbase and surface layer and one 450 cm deep subgrade soil layer. The vertical moisture barrier consisted of a 10 cm wide

fabric and a 30 cm wide backfill adjacent to the fabric. The finite element mesh used for the analysis is shown in Figure 64. The same material properties given in Table 13 were used for this study. The combined subbase and surface layer was assumed to have the unsaturated permeability (P) of 0.001 cm^2/sec and diffusion coefficient (α) of 0.001 cm^2/sec. The values of unsaturated permeability used for the cracked soil, medium cracked soil, and tight soil were 0.0025, 0.0005, and 0.000025 cm^2/sec, respectively.

The estimated vertical movements were plotted against the Thornthwaite moisture index and are shown in Figures 65 through 82. A listing of these values is given in Appendix D.

These results show that the maximum vertical movements occur in sites where the mean TMI is approximately -10 and the vertical movements decrease for values of TMI greater or lesser than -10. Also, the vertical movements in "slope" drainage conditions are lower than those in the "normal" drainage conditions in sites where there is a mean TMI of approximately -20 or higher. For the cracked soils with deep roots and tight soils with shallow roots, the vertical movements in "ponded" drainage conditions are higher than those in the "normal drainage conditions in sites below the mean TMI of +10 and are lower in sites above that level of mean TMI. The same trend is observed for the medium cracked soils with deep roots; however, the breaking point, in this case, is at the TMI of approximately +24.

Moreover, the results show that the vertical movements increase with the increase of unsaturated permeability. Generally, the increase in moisture barrier depth decreases the vertical movement; however, in some cases of tight soil with shallow roots, this trend has been

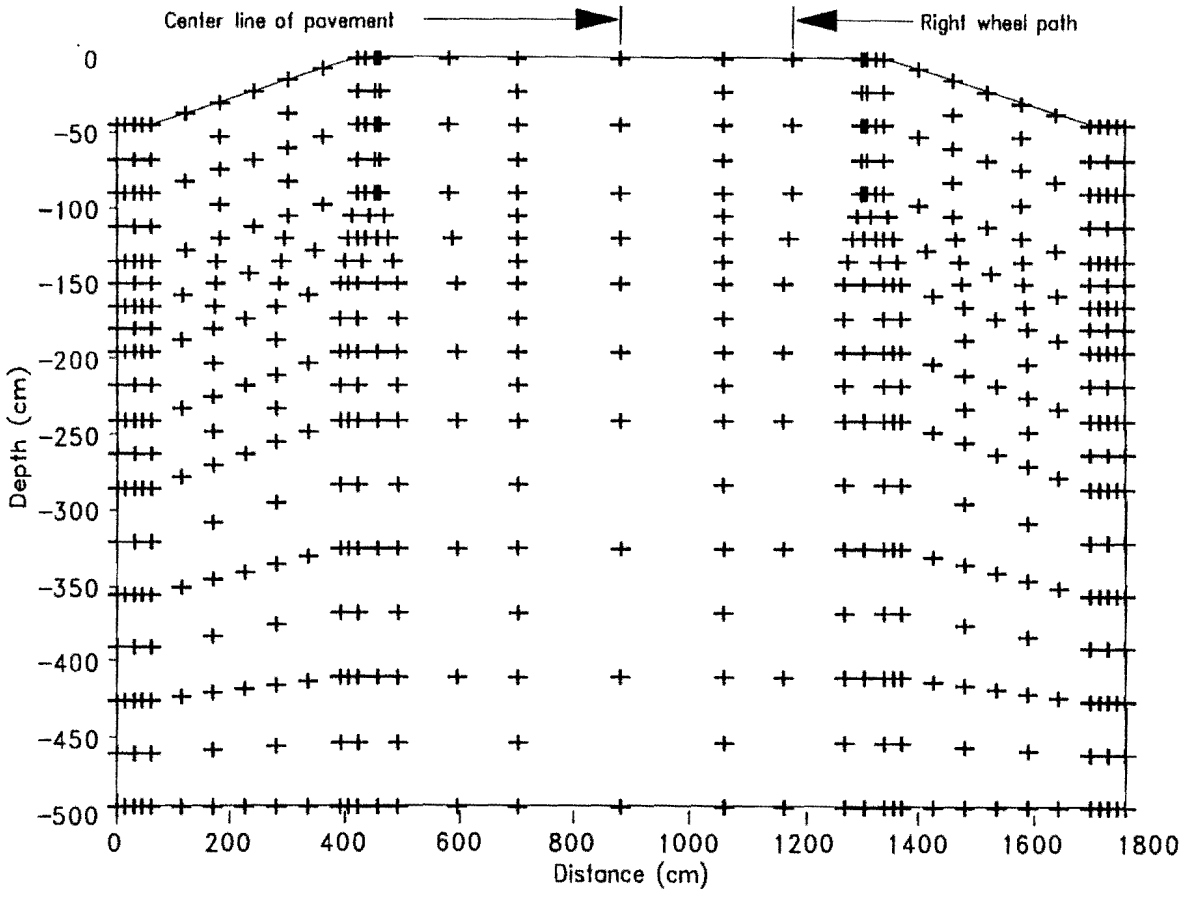

Figure 64. Finite Element Mesh used for the Estimation of Vertical Movement

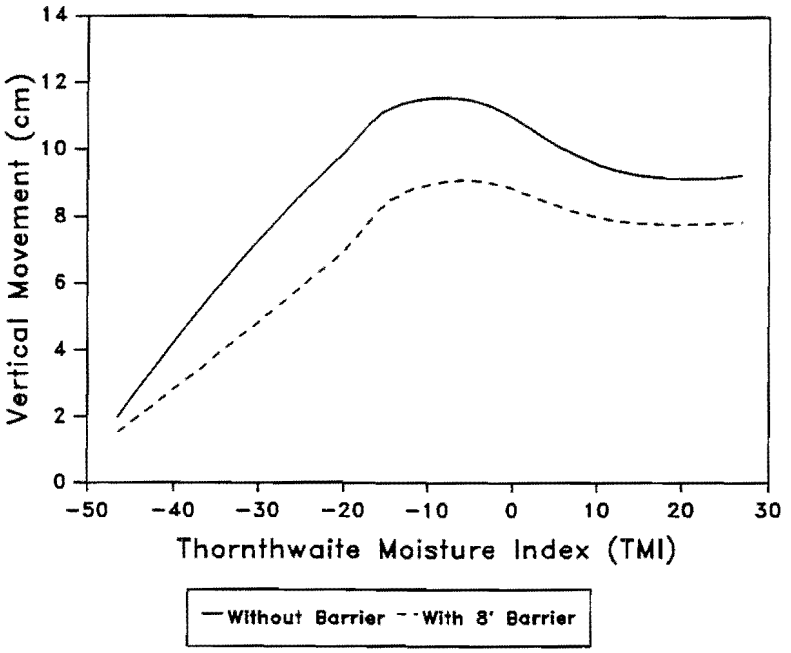

Figure 65. Vertical Movement vs. TMI for Paved Median with Cracked Soil and Deep Roots under "Normal" Drainage

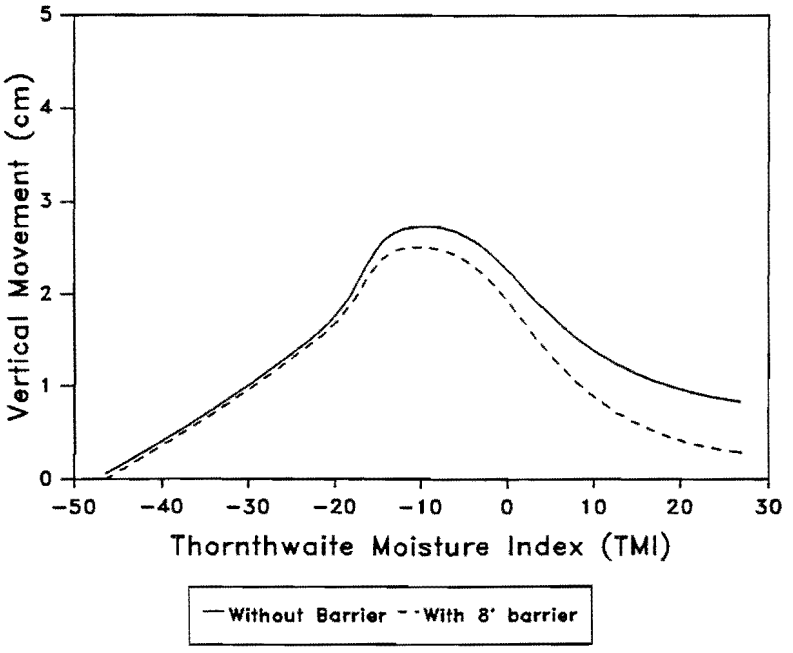

Figure 66. Vertical Movement vs. TMI for paved Median with Tight Soil and Shallow Roots under "Normal" Drainage

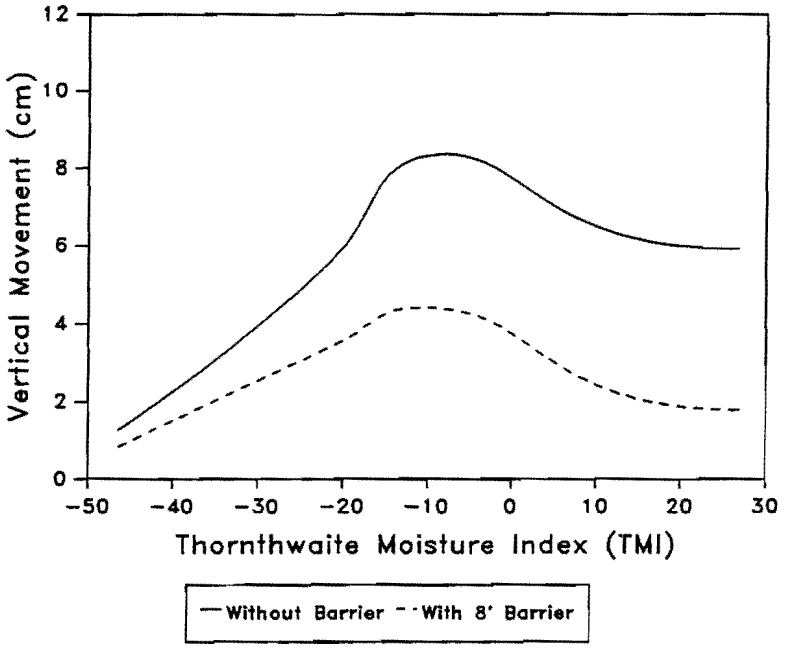

Figure 67. Vertical Movement vs. TMI for Paved Median with Medium Cracked Soil and Deep Roots under "Normal" Drainage

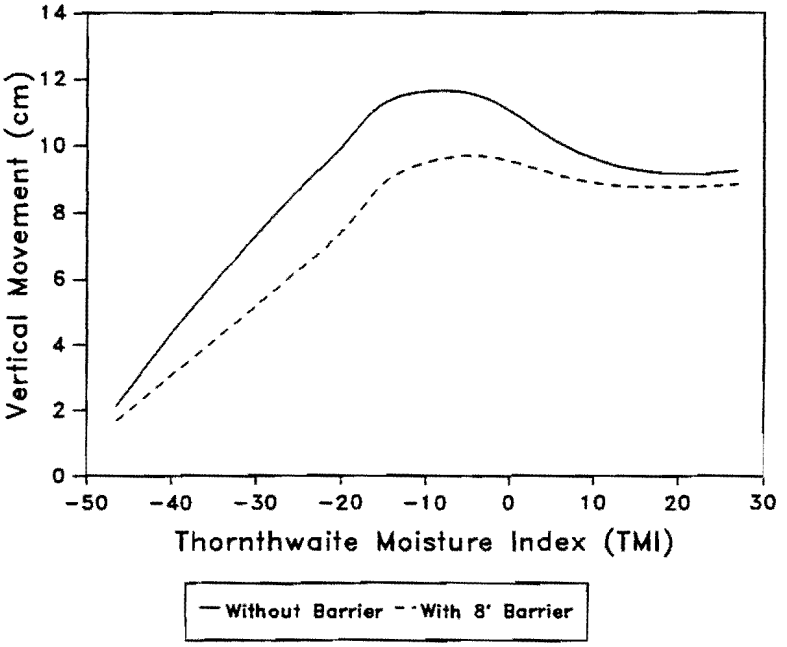

Figure 68. Vertical Movement vs. TMI for Sodded Median with Cracked Soil and Deep Roots under "Normal" Drainage

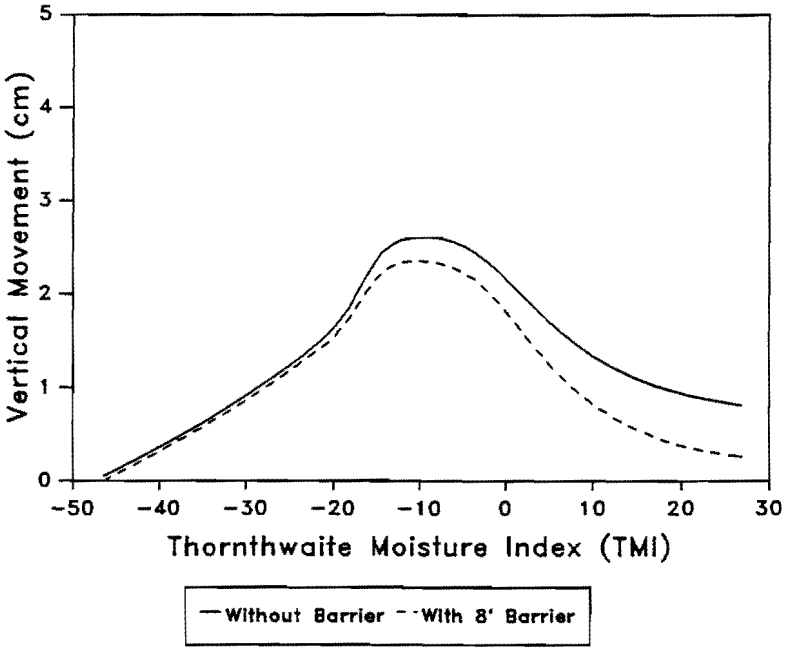

Figure 69. Vertical Movement vs. TMI for Sodded Median with Tight Soil and Shallow Roots under "Normal" Drainage

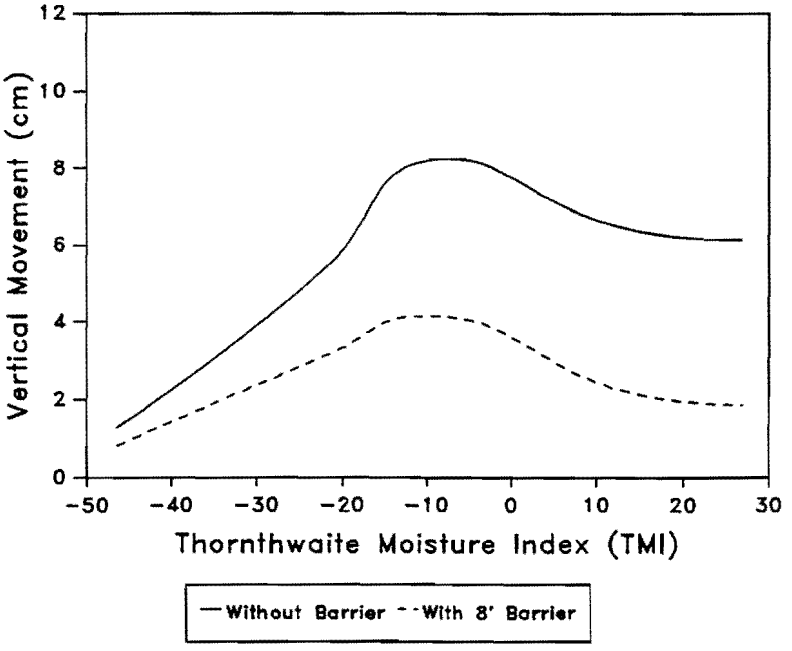

Figure 70. Vertical Movement vs. TMI for Sodded Median with Medium Cracked Soil and Deep Roots under "Normal" Drainage

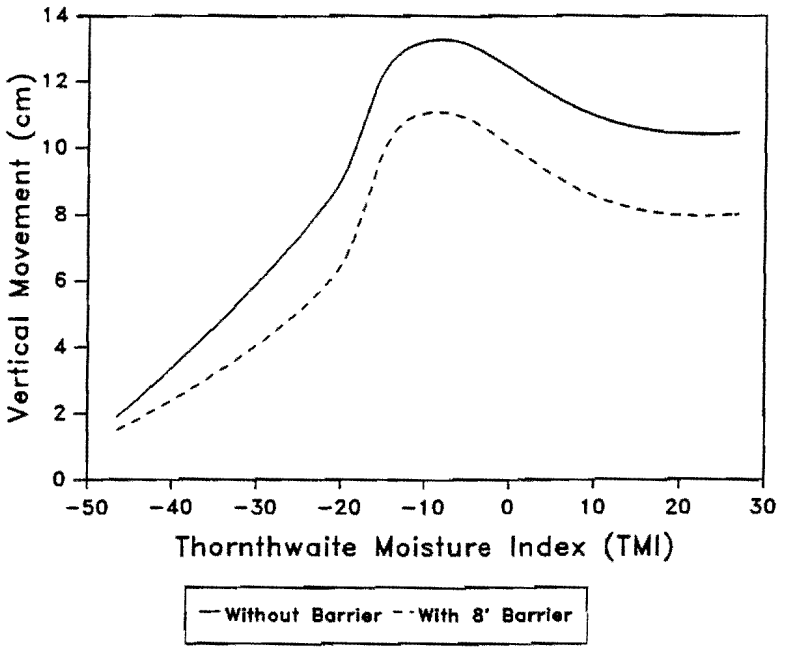

Figure 71. Vertical Movement vs. TMI for Paved Median with Cracked Soil and Deep Roots under "Slope" Drainage

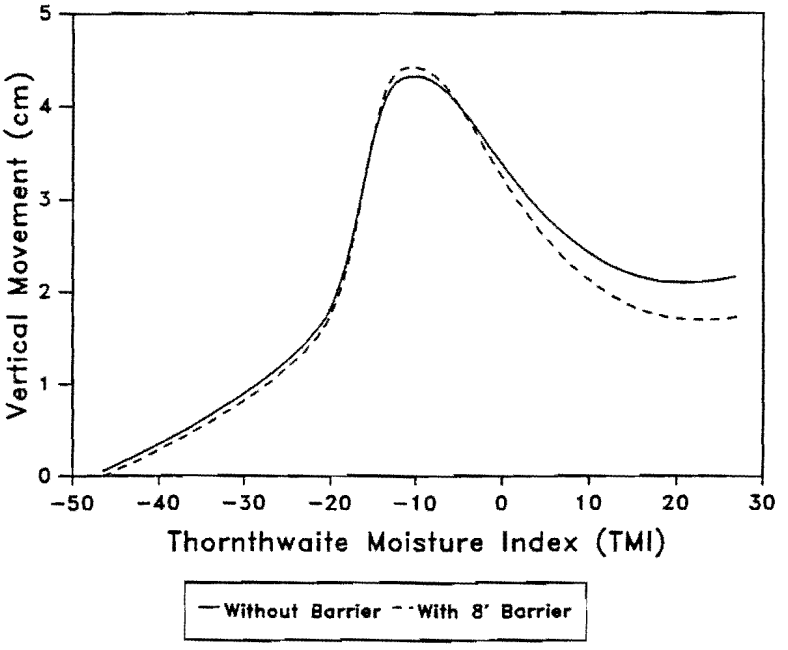

Figure 72. Vertical Movement vs. TMI for Paved Median with Tight Soil and Shallow Roots under "Slope" Drainage

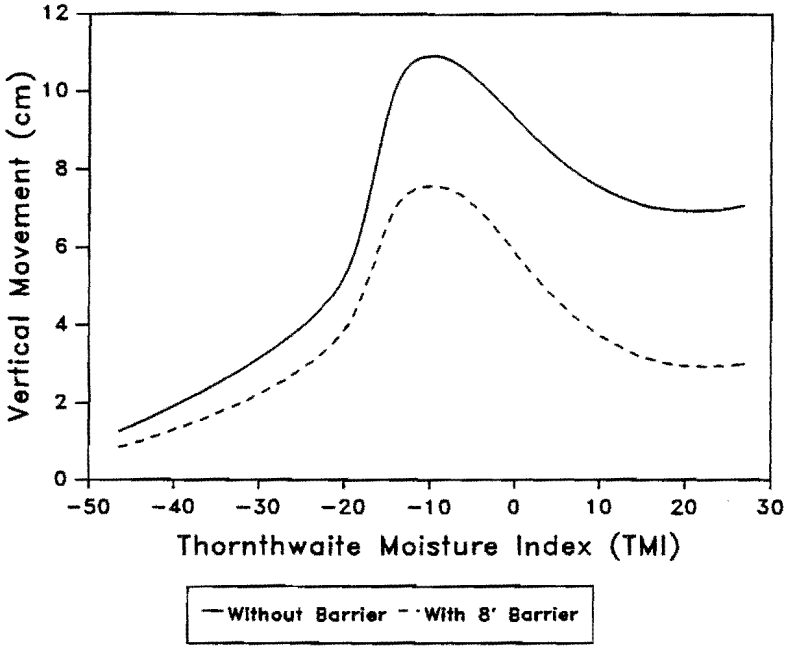

Figure 73. Vertical Movement vs. TMI for Paved Median with Medium Cracked Soil and Deep Roots under "Slope" Drainage

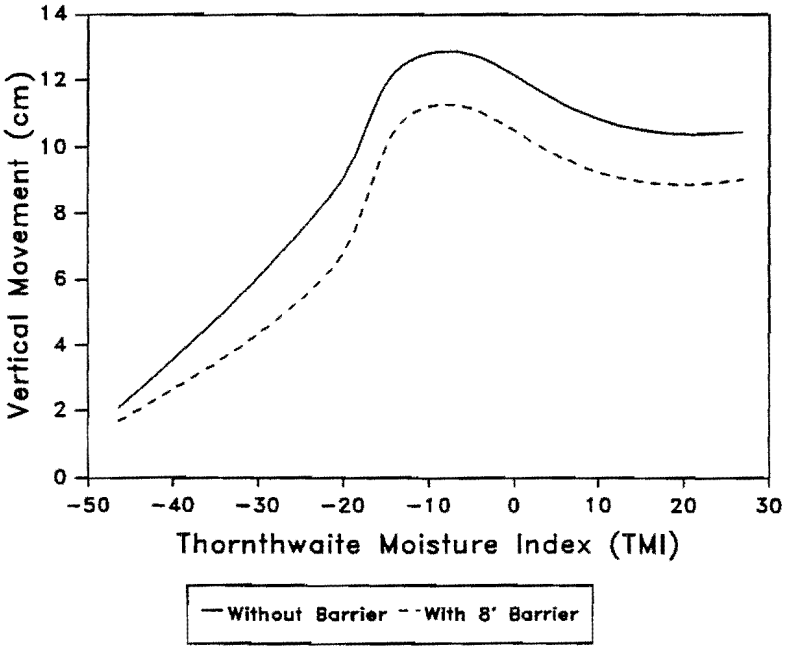

Figure 74. Vertical Movement vs. TMI for Sodded Median with Cracked Soil and Deep Roots under "Slope" Drainage

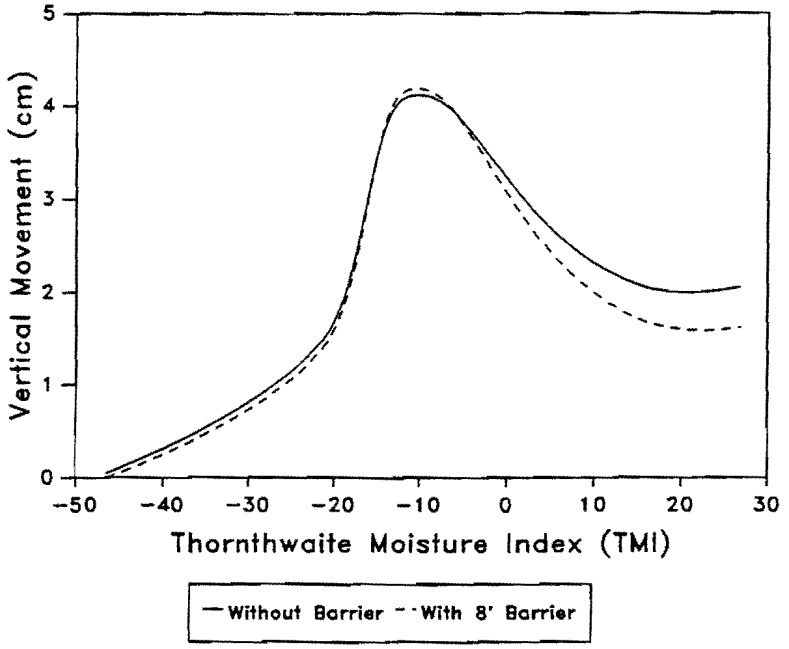

Figure 75. Vertical Movement vs. TMI for Sodded Median with Tight Soil and Shallow Roots under "Slope" Drainage

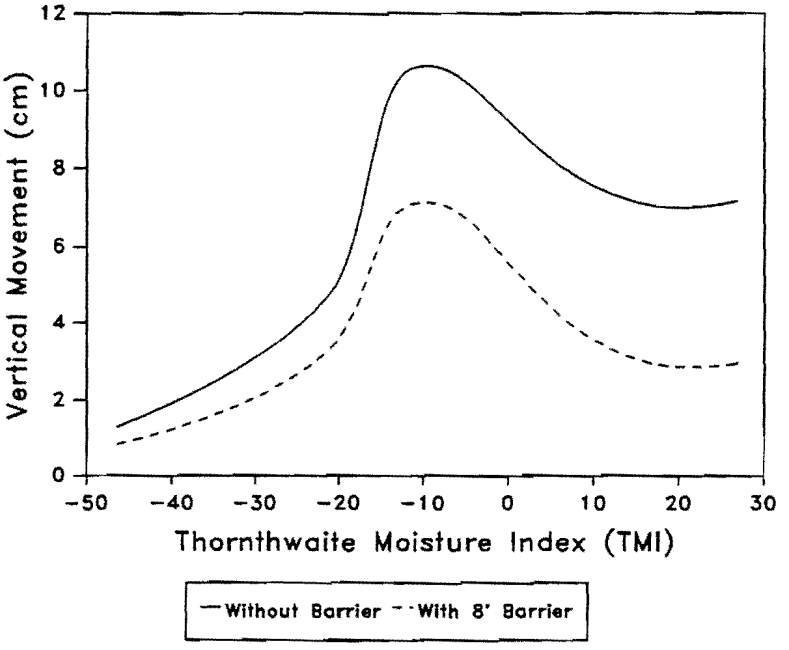

Figure 76. Vertical Movement vs. TMI for Sodded Median with Medium Cracked Soil and Deep Roots under "Slope" Drainage

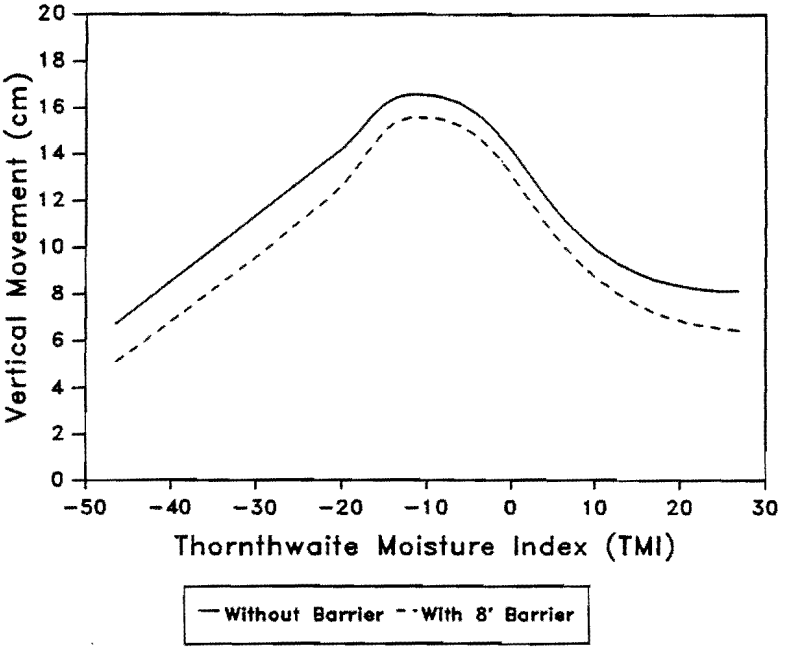

Figure 77. Vertical Movement vs. TMI for Paved Median with Cracked Soil and Deep Roots under "Ponded" Drainage

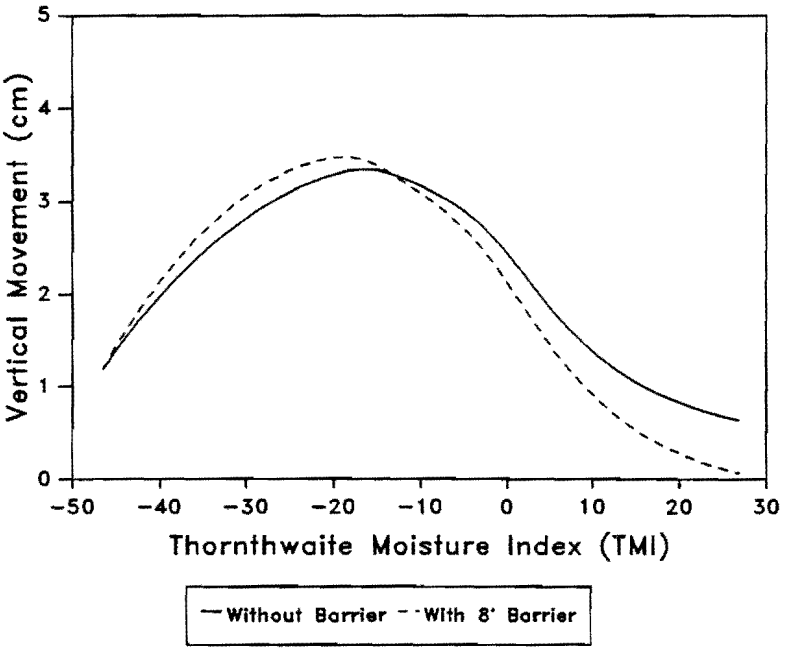

Figure 78. Vertical Movement vs. TMI for Paved Median with Tight Soil and Shallow Roots under "Ponded" Drainage

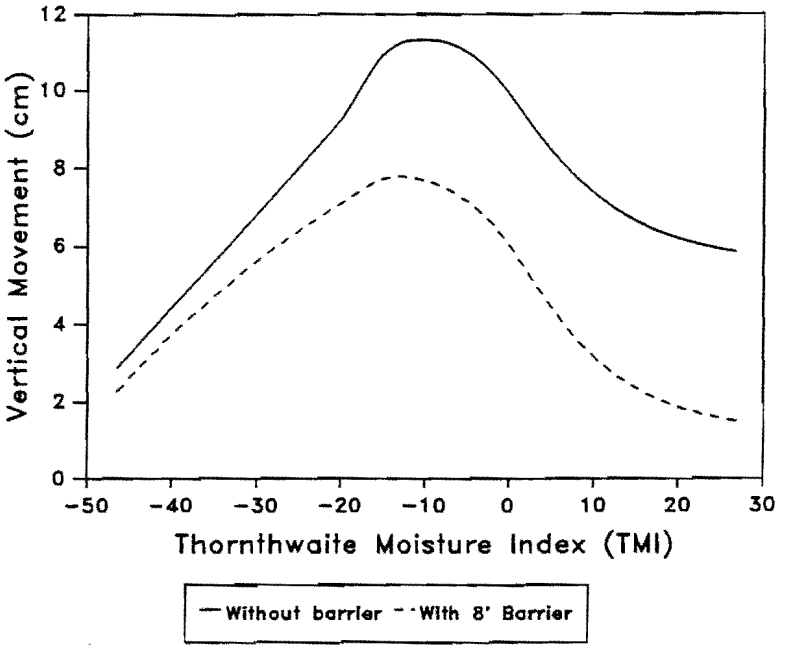

Figure 79. Vertical Movement vs. TMI for Paved Median with Medium Cracked Soil and Deep Roots under "Ponded" Drainage

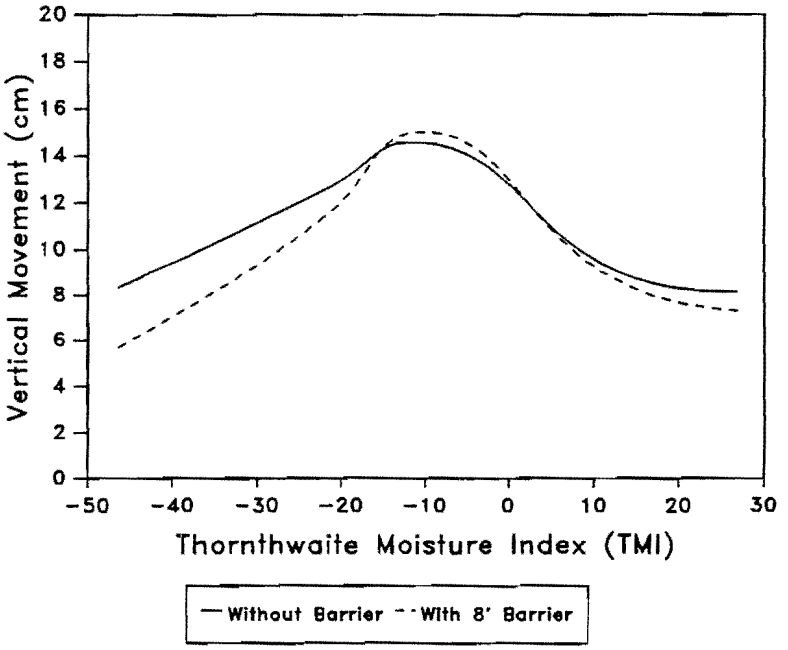

Figure 80. Vertical Movement vs. TMI for Sodded Median with Cracked Soil and Deep Roots under "Ponded" Drainage

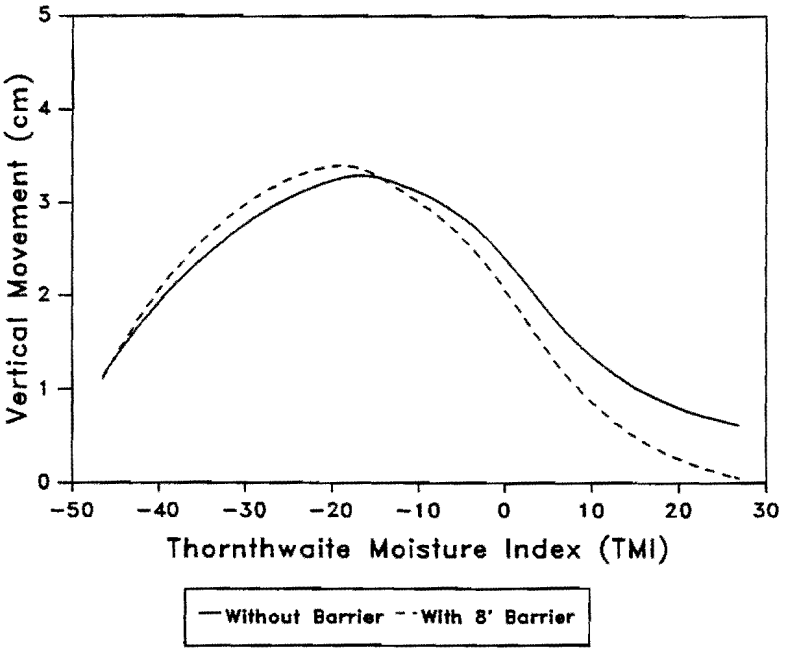

Figure 81. Vertical Movement vs. TMI for Sodded Median with Tight Soil and Shallow Roots under "Ponded" Drainage

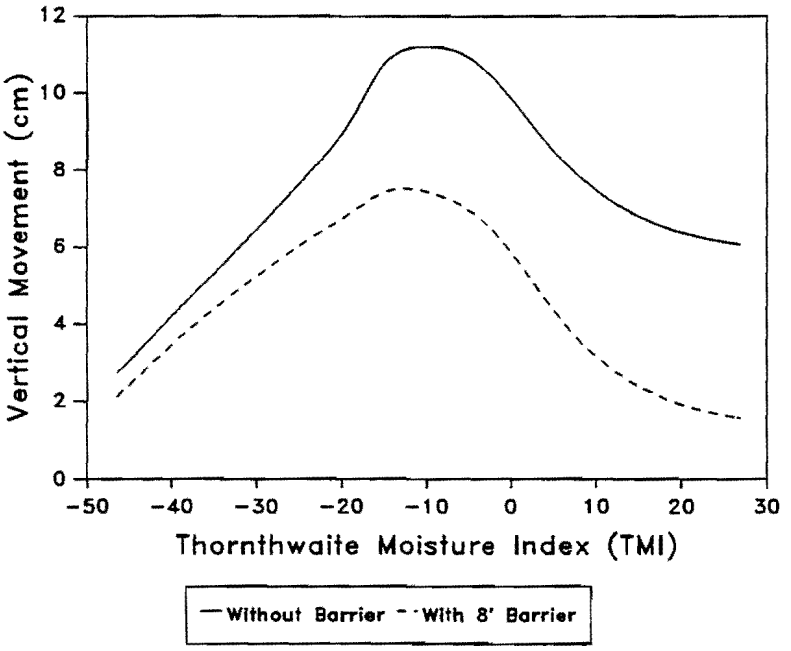

Figure 82. Vertical Movement vs. TMI for Sodded Median with Medium Cracked Soil and Deep Roots under "Ponded" Drainage

reversed. Of the three soil types, the highest decrease in vertical movement with an introduction of a vertical moisture barrier is observed in the medium cracked soils. The decrease in vertical movement is negligible in tight soils. The decrease in vertical movement is not significant in dry climates such as El Paso (mean TMI = -46.5) under the "normal" and "slope" drainage condition; however, this is significant in the "ponded" drainage condition. There is not an appreciable difference in vertical movements in the outside wheel path between the pavements with paved and sodded medians. However, the paving of a median may reduce the vertical movement in the inside wheel path or in inside lanes.

PREDICTION OF ROUGHNESS DEVELOPMENT

The following roughness prediction models developed through the regression analysis of the rates of roughness development (dR/dt) and the expected value of vertical movement (ΔH) are used for the prediction of roughness measures for the different cases studied in the previous sections of this chapter.

Serviceability Index (SI)

The change in SI/year, dR/dt is given by:

$$\frac{dR}{dt} = \beta_1(\Delta H) + \beta_2 \qquad (31)$$

Where for category

A Moisture barriers with paved medians

$\beta_1 = 0.02176$ $\beta_2 = 0.03226$

B Moisture barriers with sodded medians

$\beta_1 = 0.03430$ $\beta_2 = 0.07269$

C Control sections with and without medians

$\beta_1 = 0.04418$ $\beta_2 = 0.12461$

International Roughness Index (IRI)

The mean rate of change of IRI (in/mile/yr), dR/dt is given by:

$$\frac{dR}{dt} = \beta_1(\Delta H) + \beta_2 \quad (32)$$

Where for category

A Moisture barriers with paved medians

$\beta_1 = 0.61939$ $\beta_2 = 1.2954$

B Moisture barriers with sodded medians

$\beta_1 = 1.5825$ $\beta_2 = 2.0105$

C Control sections with and without medians

$\beta_1 = 2.7014$ $\beta_2 = 4.0146$

Maximum Expected Bump Height (BH)

The mean rate of change of Bump Height (in/yr), dR/dt is given by:

$$\frac{dR}{dt} = \beta_1 + \beta_2 \exp[\beta_3(\Delta H)] \quad (33)$$

Where for category

A Moisture barriers with paved medians

$\beta_1 = 0.011$ $\beta_2 = 0.012$ $\beta_3 = 0.216$

B Moisture barriers with sodded medians

$\beta_1 = 0.010$ $\beta_2 = 0.011$ $\beta_3 = 0.305$

C Control sections with and without medians

$\beta_1 = 0.000$ $\beta_2 = 0.018$ $\beta_3 = 0.302$

In the development of these models, the expected vertical movement was estimated by integrating over depth the changes in vertical movement as a function of the change in matrix suction between the expected wet and dry suction profiles. In this study, in order to remain consistent with the development of these equations 31, 32,and 33 the ΔH that was used was that obtained for pavements with a sodded median and without vertical moisture barriers. The results were plotted against the Thornthwaite Moisture Index and are shown in Figures 83 through 109.

These results indicate that the presence of a vertical moisture barrier significantly reduces the development of roughness in pavements on expansive soils. However, the development of roughness in pavements on tight subgrade soils is generally low even without a moisture barrier. Therefore, a vertical moisture barrier may not be useful in pavements on tight soils.

COMPARISON OF MEASURED AND PREDICTED ROUGHNESS MEASURES

In the following section, the measured roughness values at sites in Seguin, Converse, and Dallas which are given in Appendix C are compared with the values predicted in the previous section of this chapter. The estimated values of unsaturated permeability for these sites which are given in Table 14 falls around 0.0005 cm^2/sec. The pavement sections in Seguin and Dallas consist of sodded medians while the section at Converse is a two lane roadway without a median. According to the topography of the sites, the drainage condition of these sites can be considered as "Normal". Therefore, the roughness values predicted for pavement sections with sodded medians and medium

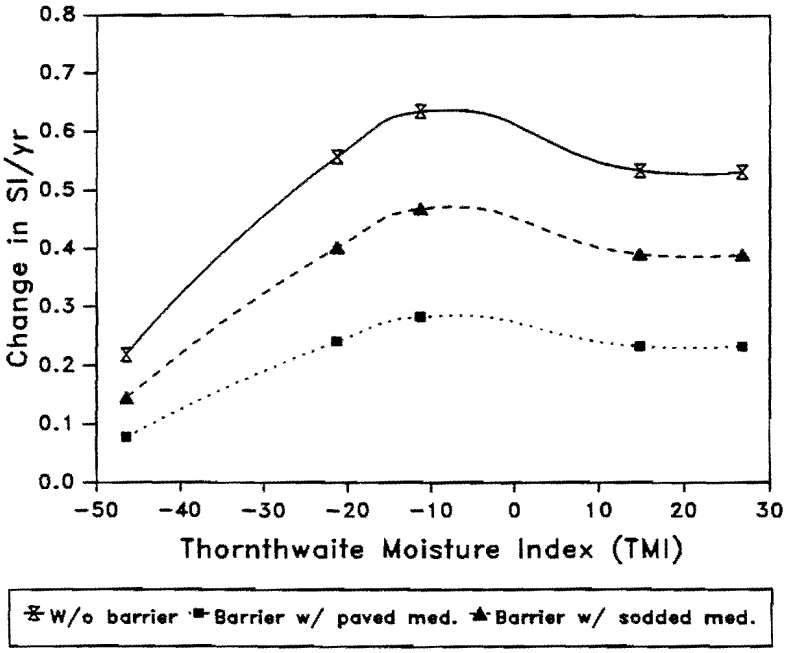

Figure 83. Change in SI/yr vs. TMI for Cracked Soil with Deep Roots in "Normal" Drainage

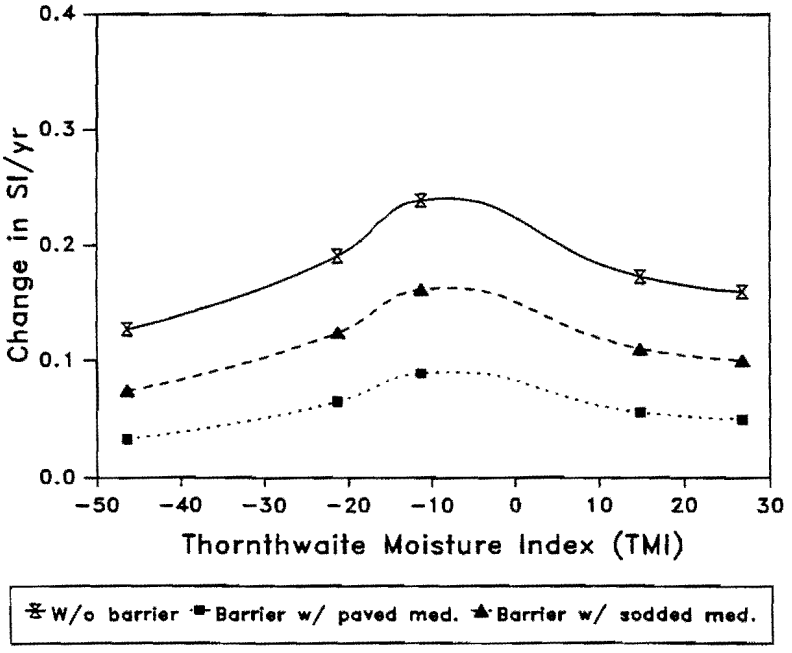

Figure 84. Change in SI/yr vs. TMI for Tight Soil with Shallow Roots in "Normal" Drainage

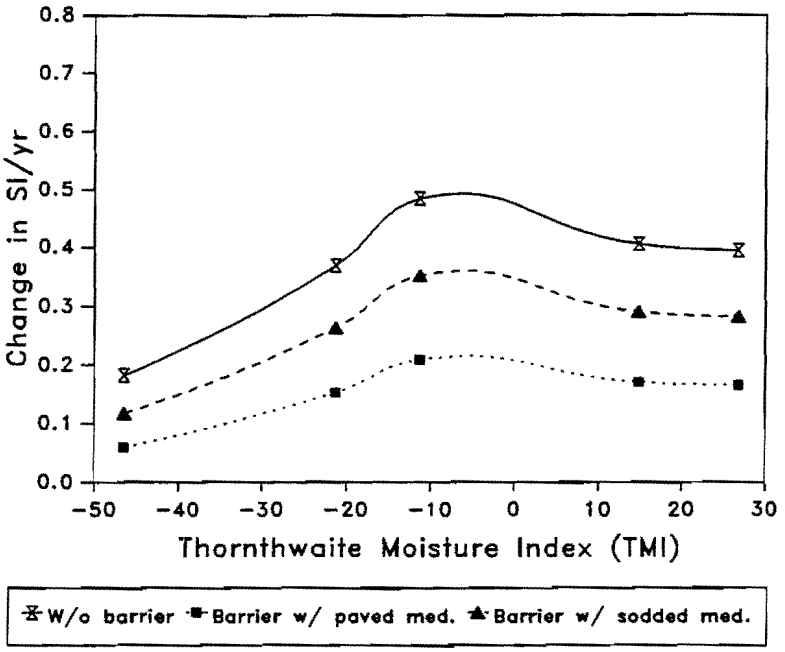

Figure 85. Change in SI/yr vs. TMI for Medium Cracked Soil with Deep Roots in "Normal" Drainage

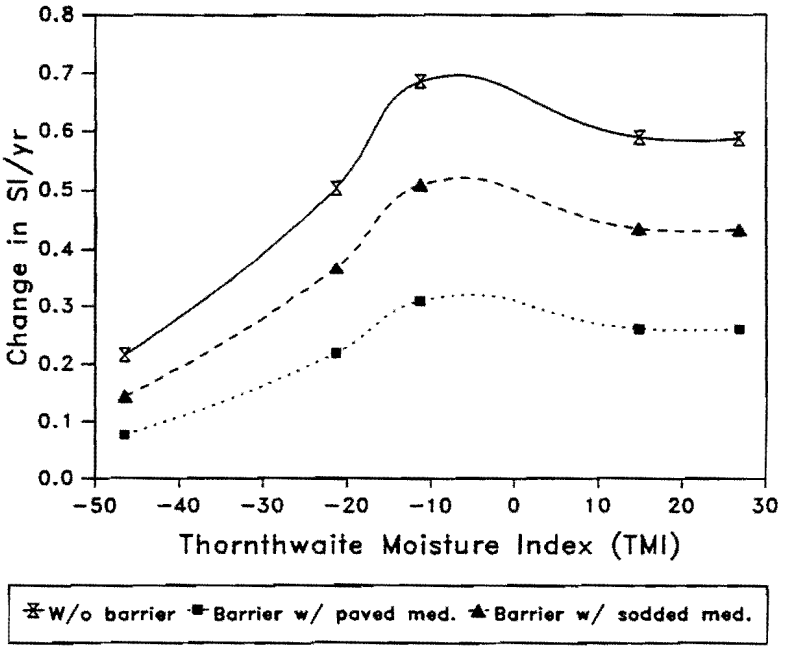

Figure 86. Change in SI/yr vs. TMI for Cracked Soil with Deep Roots in "Slope" Drainage

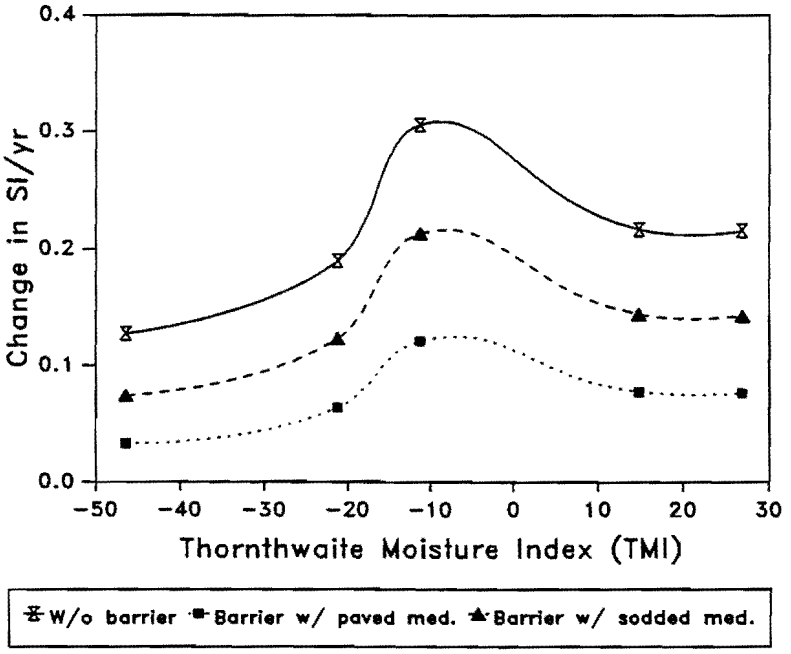

Figure 87. Change in SI/yr vs. TMI for Tight Soil with Shallow Roots in "Slope" Drainage

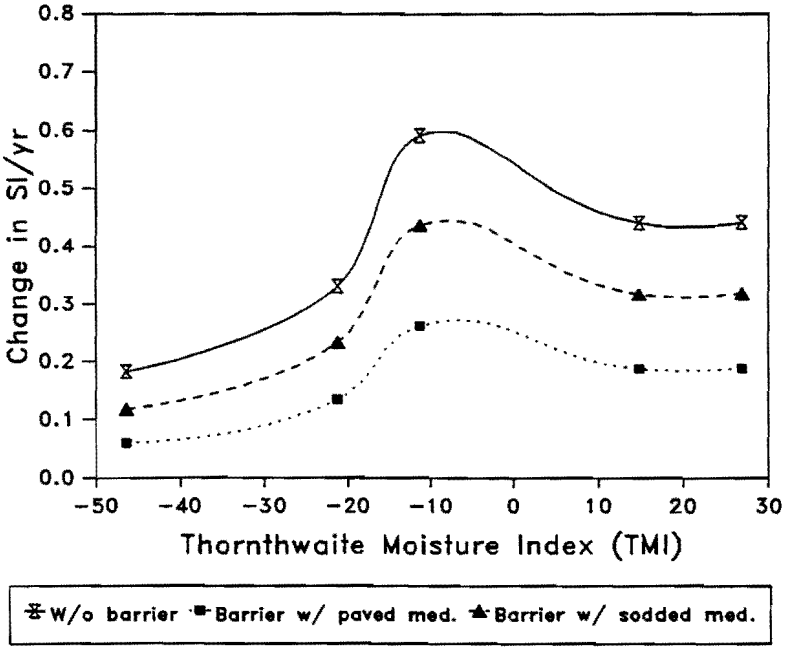

Figure 88. Change in SI/yr vs. TMI for Medium Cracked Soil with Deep Roots in "Slope" Drainage

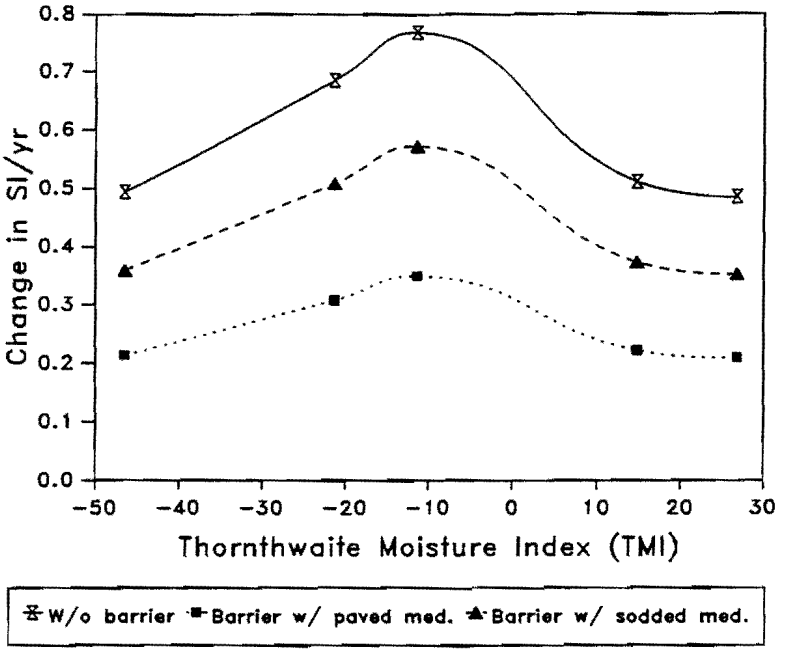

Figure 89. Change in SI/yr vs. TMI for Cracked Soil with Deep Roots in "Ponded" Drainage

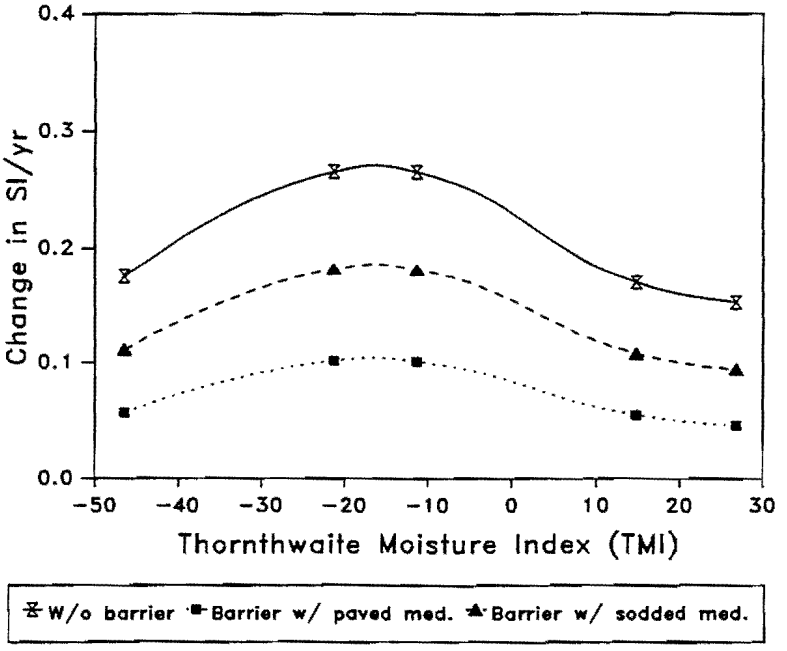

Figure 90. Change in SI/yr vs. TMI for Tight Soil with Shallow Roots in "Ponded" Drainage

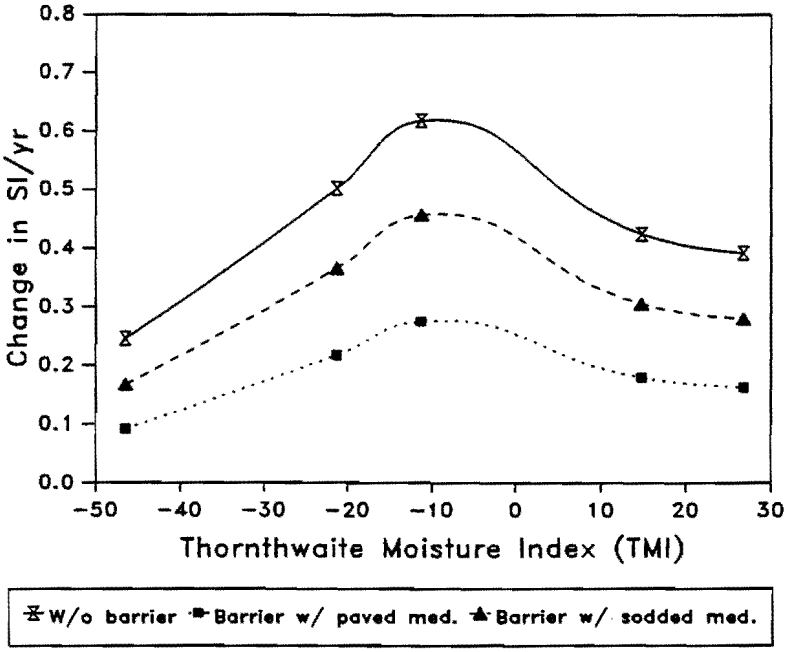

Figure 91. Change in SI/yr vs. TMI for Medium Cracked Soil with Deep Roots in "Ponded" Drainage

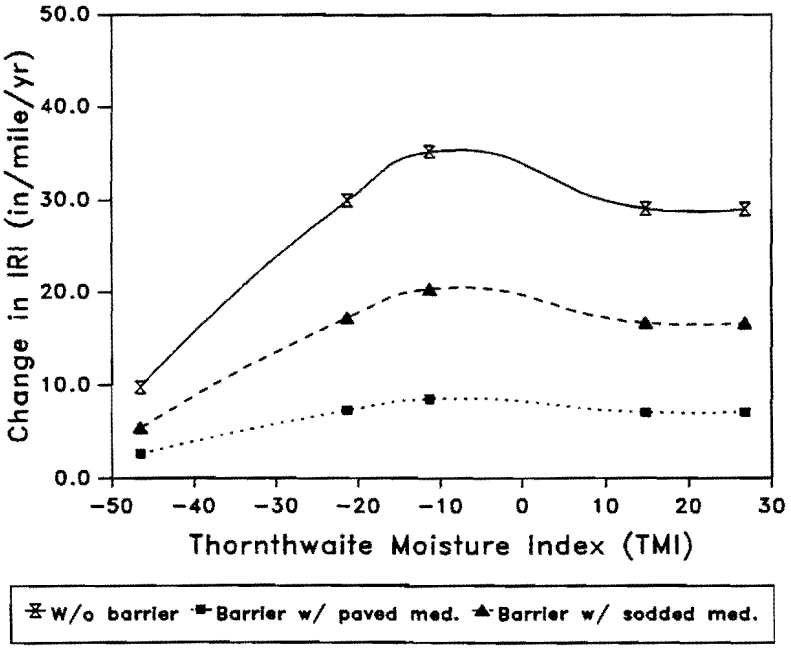

Figure 92. Change in IRI vs. TMI for Cracked Soil with Deep Roots in "Normal" Drainage

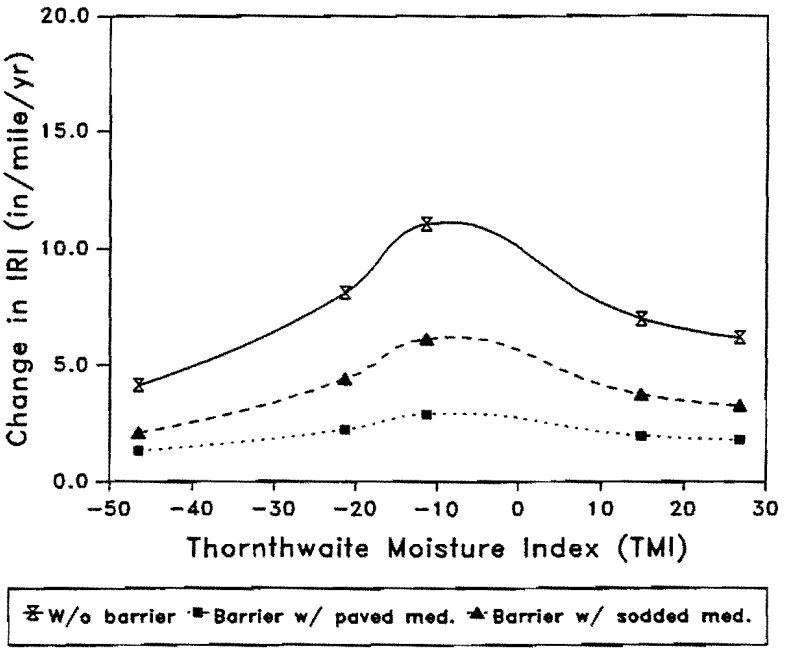

Figure 93. Change in IRI vs. TMI for Tight Soil with Shallow Roots in "Normal" Drainage

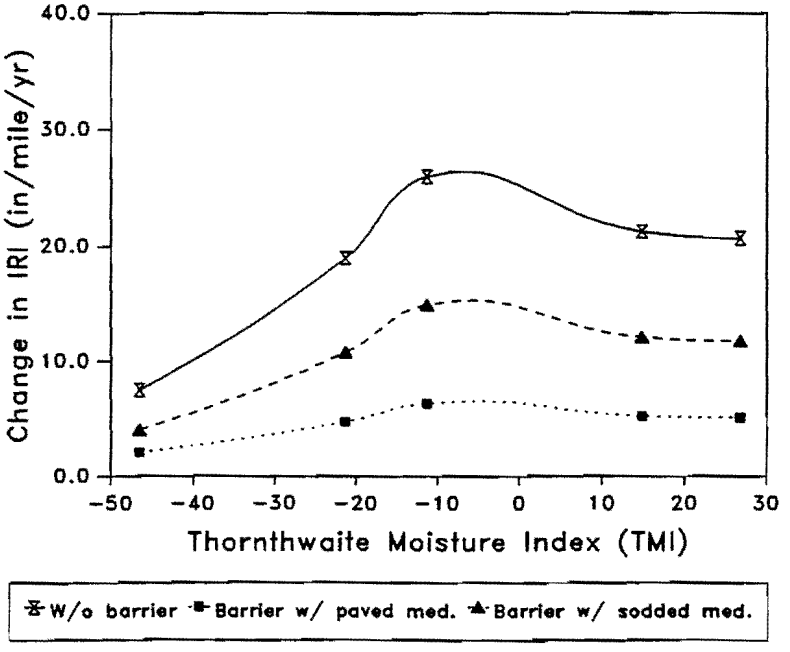

Figure 94. Change in IRI vs. TMI for Medium Cracked Soil with Deep Roots in "Normal" Drainage

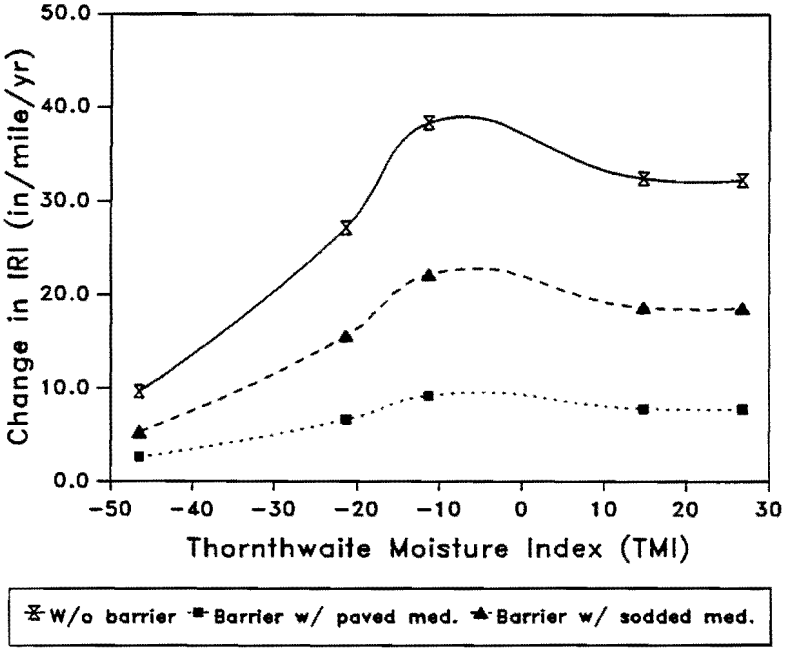

Figure 95. Change in IRI vs. TMI for Cracked Soil with Deep Roots in "Slope" Drainage

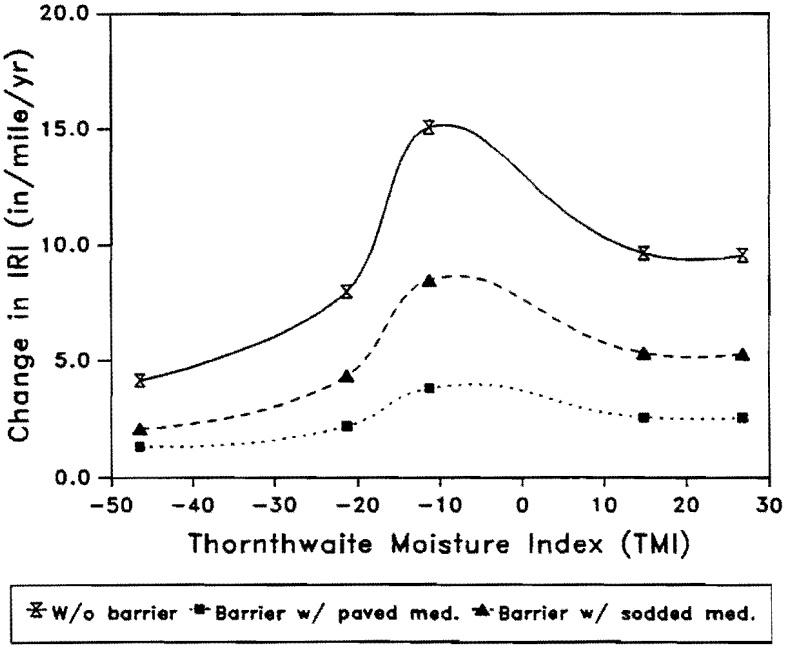

Figure 96. Change in IRI vs. TMI for Tight Soil with Shallow Roots in "Slope" Drainage

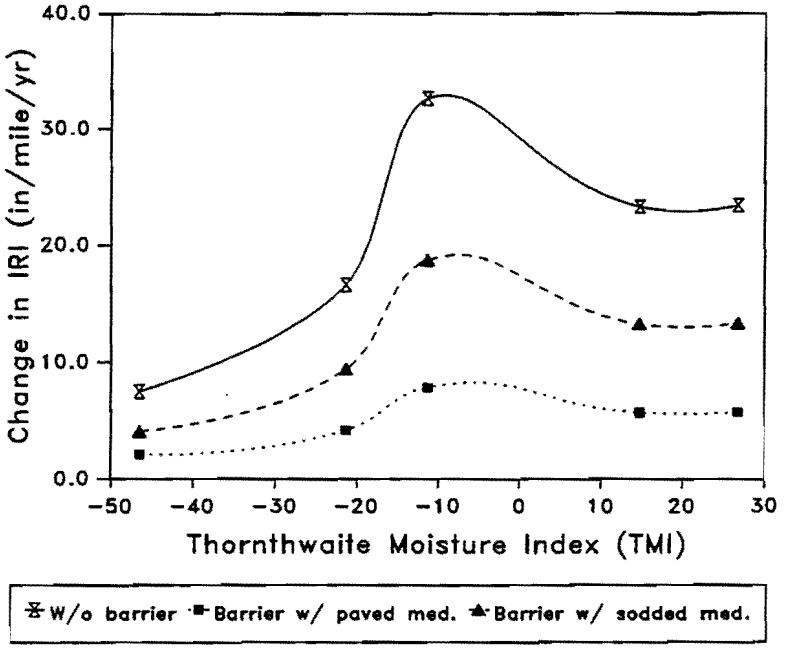

Figure 97. Change in IRI vs. TMI for Medium Cracked Soil with Deep Roots in "Slope" Drainage

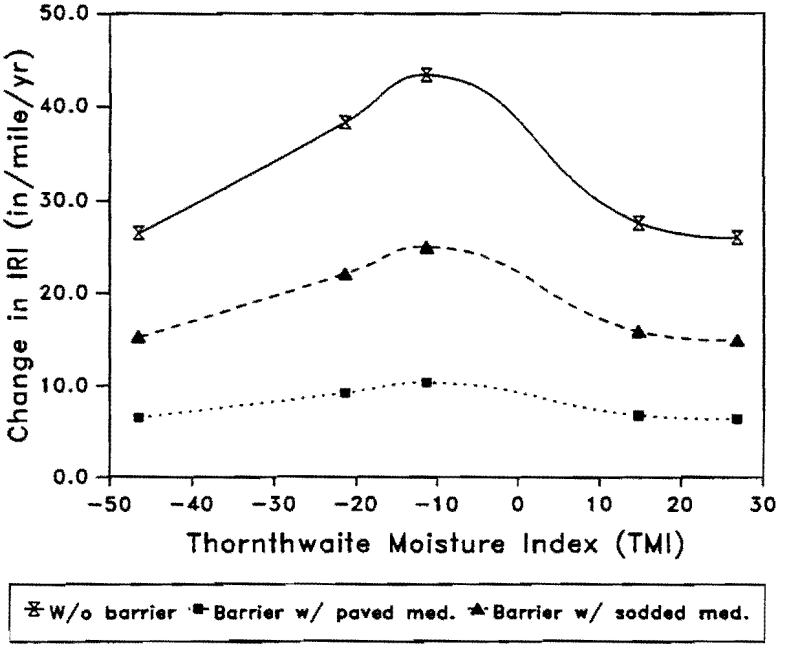

Figure 98. Change in IRI vs. TMI for Cracked Soil with Deep Roots in "Ponded" Drainage

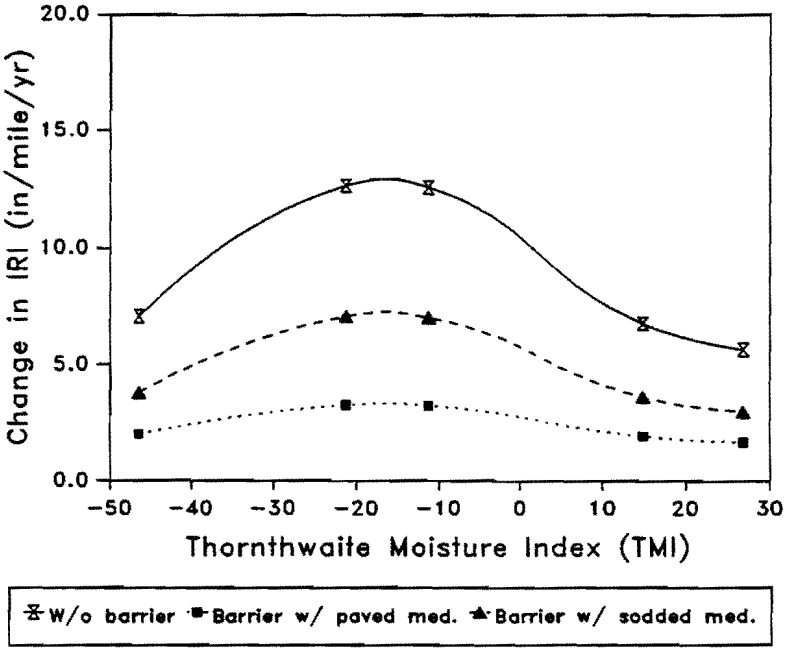

Figure 99. Change in IRI vs. TMI for Tight Soil with Shallow Roots in "Ponded" Drainage

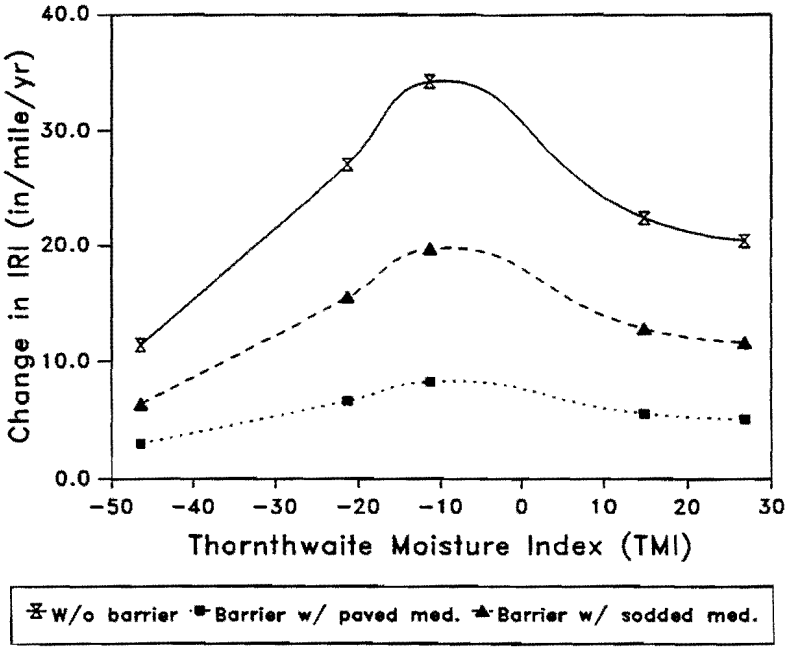

Figure 100. Change in IRI vs. TMI for Medium Cracked Soil with Deep Roots in "Ponded" Drainage

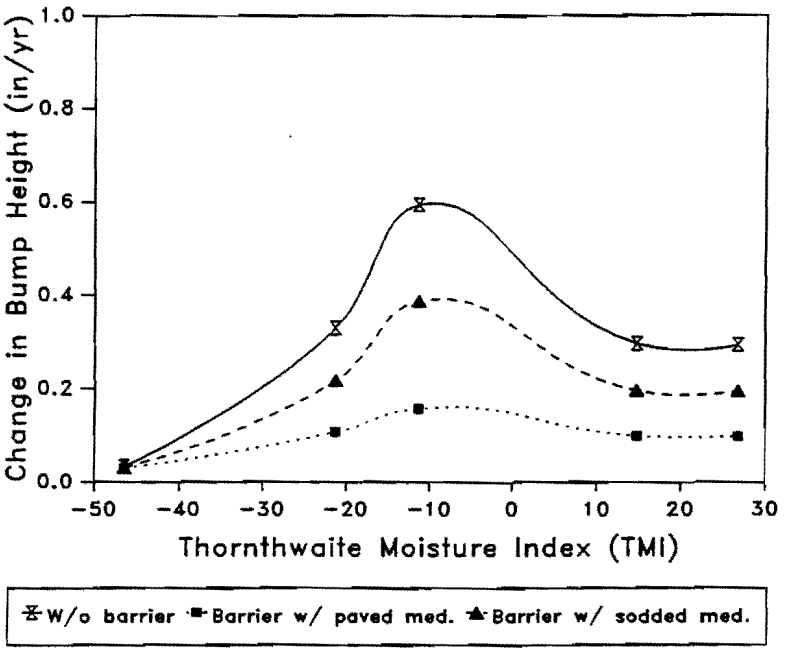

Figure 101. Change in Bump Height vs. TMI for Cracked Soil with Deep Roots in "Normal" Drainage

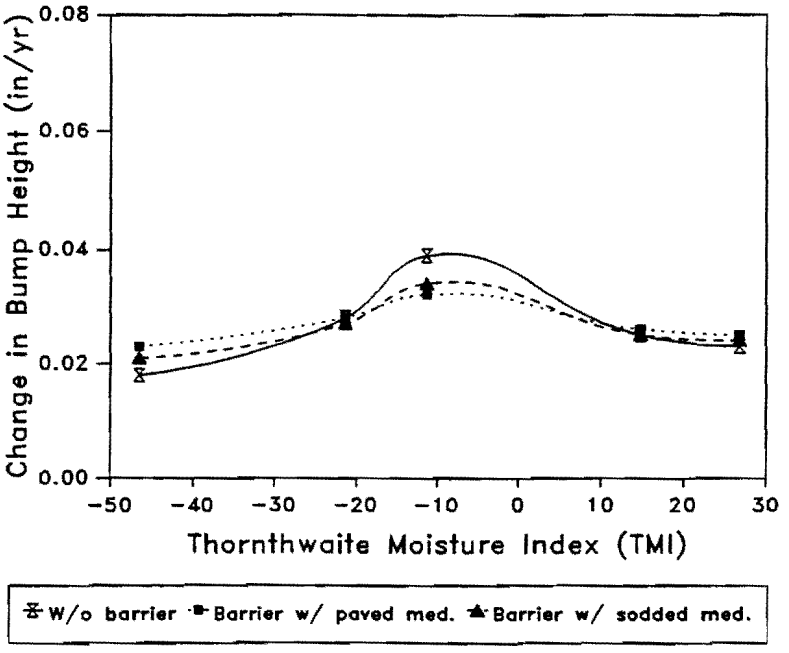

Figure 102. Change in Bump Height vs. TMI for Tight Soil with Shallow Roots in "Normal" Drainage

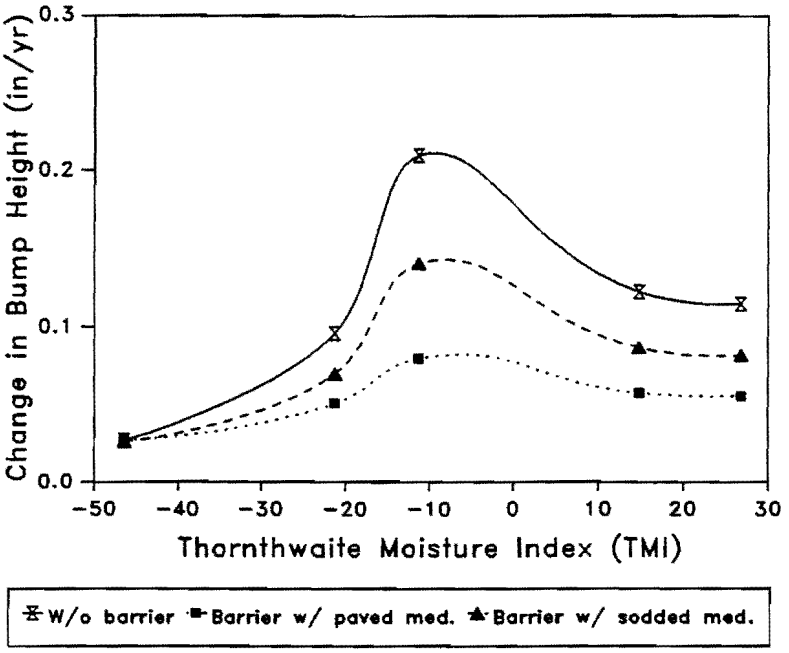

Figure 103. Change in Bump Height vs. TMI for Medium Cracked Soil with Deep Roots in "Normal" Drainage

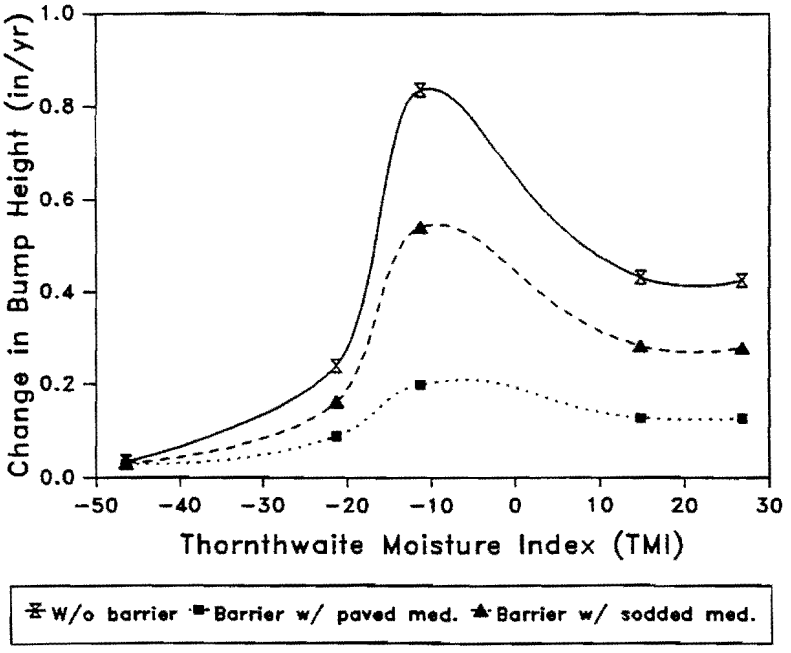

Figure 104. Change in Bump Height vs. TMI for Cracked Soil with Deep Roots in "Slope" Drainage

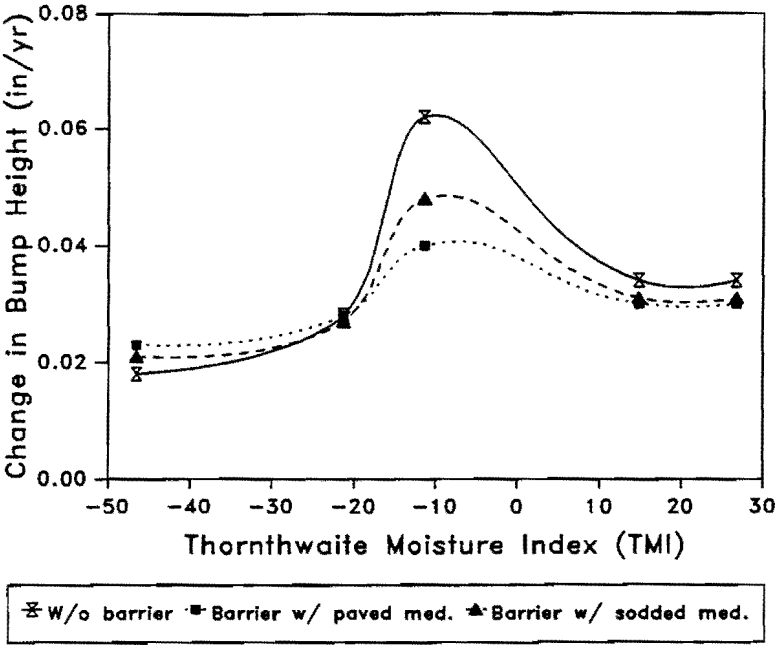

Figure 105. Change in Bump Height vs. TMI for Tight Soil with Shallow Roots in "Slope" Drainage

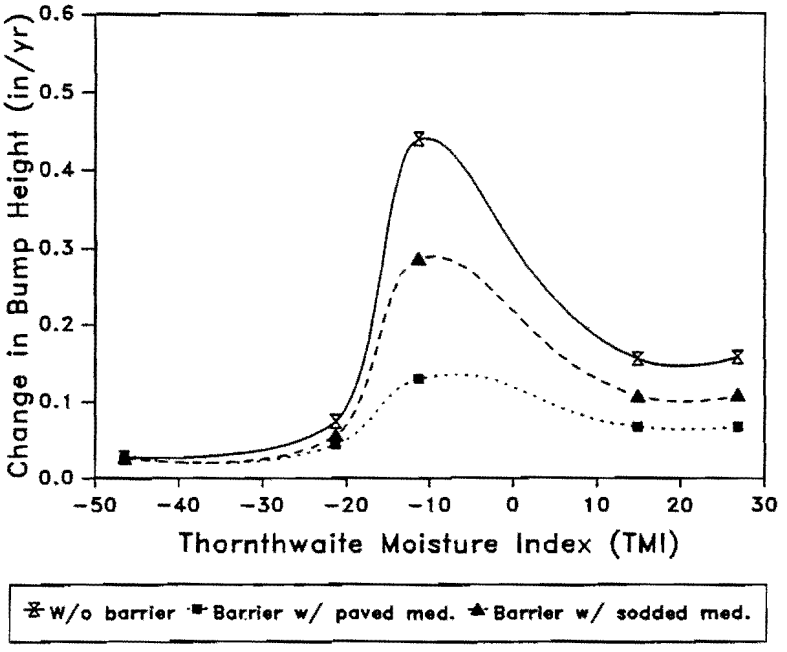

Figure 106. Change in Bump Height vs. TMI for Medium Cracked Soil with Deep Roots in "Slope" Drainage

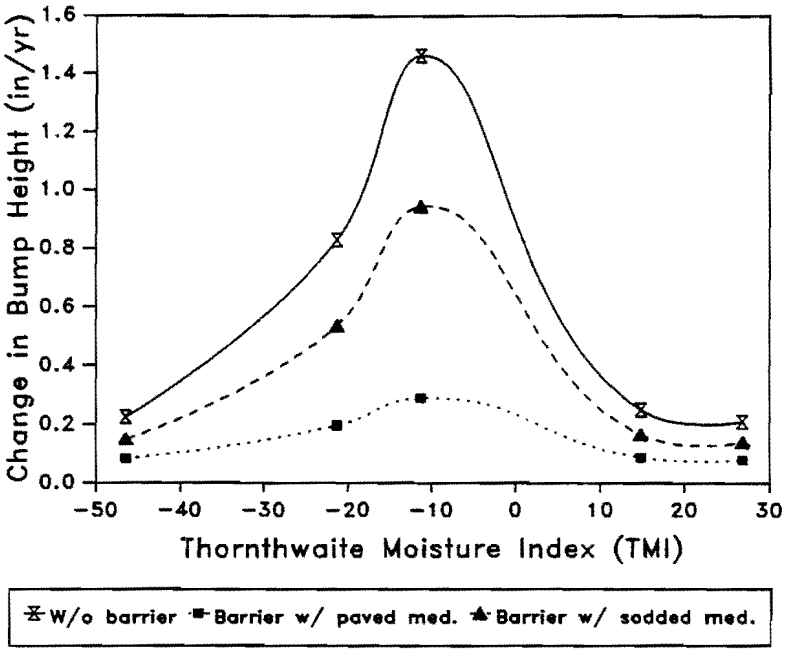

Figure 107. Change in Bump Height vs. TMI for Cracked Soil with Deep Roots in "Ponded" Drainage

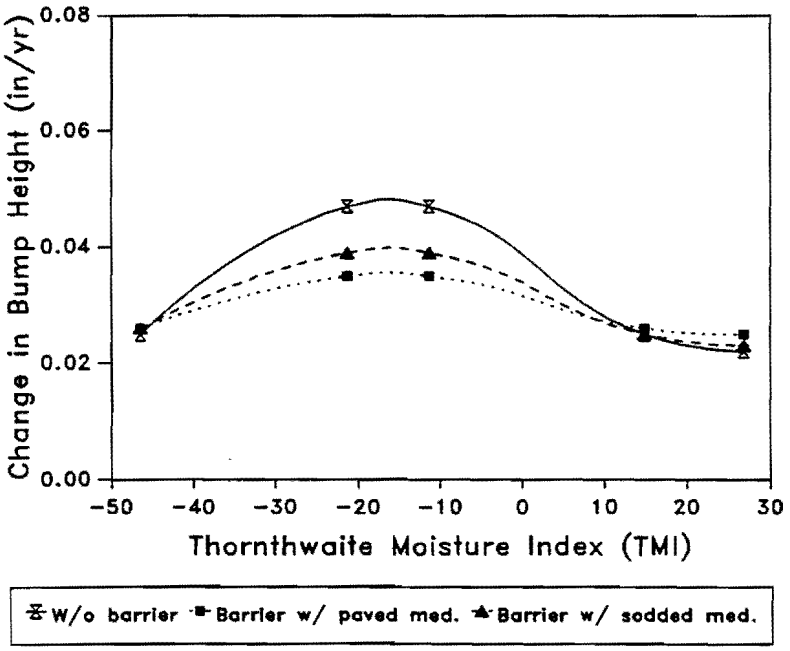

Figure 108. Change in Bump Height vs. TMI for Tight Soil with Shallow Roots in "Ponded" Drainage

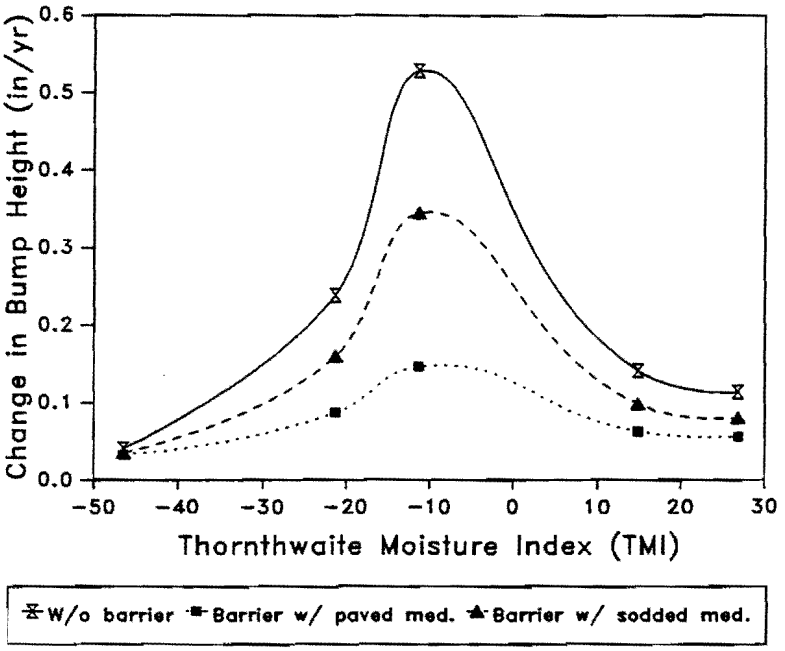

Figure 109. Change in Bump Height vs. TMI for Medium Cracked Soil with Deep Roots in "Ponded" Drainage

cracked soils under "Normal" drainage conditions are used to compare the measured values. For Seguin and Converse, the values predicted for San Antonio are used, while the values predicted for Dallas are used for sites in Dallas. These predicted roughness measures are given in Table 22.

Table 22. Predicted Rates of Change of Roughness Measures used for the Comparison

Location	SI/yr	IRI (in/mile/yr)	BH (in/yr)
San Antonio, without Barrier	0.369	18.980	0.096
San Antonio, with Barrier	0.263	10.778	0.070
Dallas, without barrier	0.484	25.977	0.210
Dallas, with Barrier	0.352	14.876	0.141

The comparisons are illustrated in Figures 110 through 127. In these plots, the values of Serviceability Index measured at each lane (inside, outside, and center or northbound, and southbound) of roadways and the International Roughness Index and Maximum Expected Bump Height values obtained for the right and left wheel path of each lane are shown. These plots show that the predicted values of roughness measures compare well with the measured values in the majority of the cases studied.

Based on the results of this study, the following conclusions can be made.

1. The vertical moisture barriers are effective in reducing the development of roughness in pavements on expansive soils under certain circumstances. They are not effective

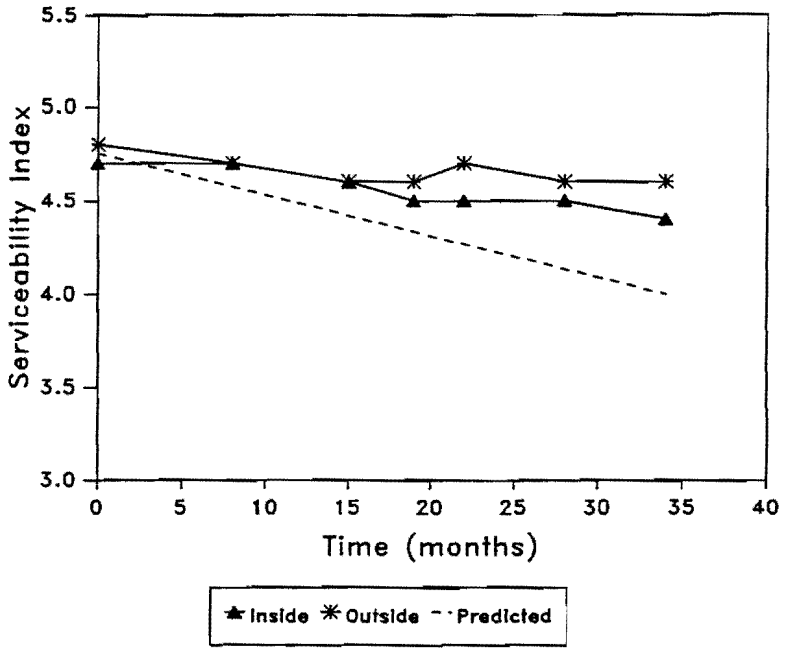

Figure 110. Comparison of Predicted and Measured Results of Serviceability Index in Moisture Barrier Section at Seguin, IH 10

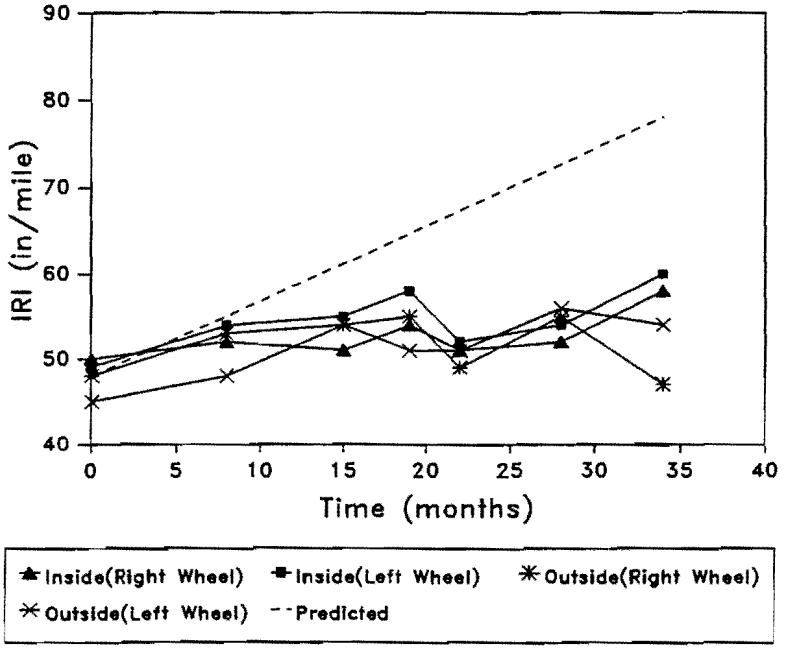

Figure 111. Comparison of Predicted and Measured Results of International Roughness Index in Moisture Barrier Section at Seguin, IH 10

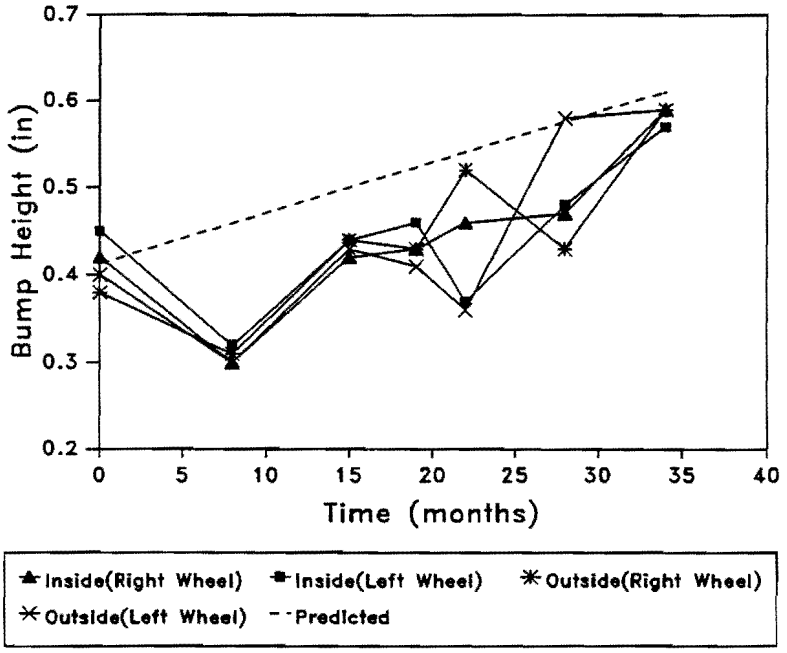

Figure 112. Comparison of Predicted and Measured Results of Maximum Expected Bump Height in Moisture Barrier Section at Seguin, IH 10

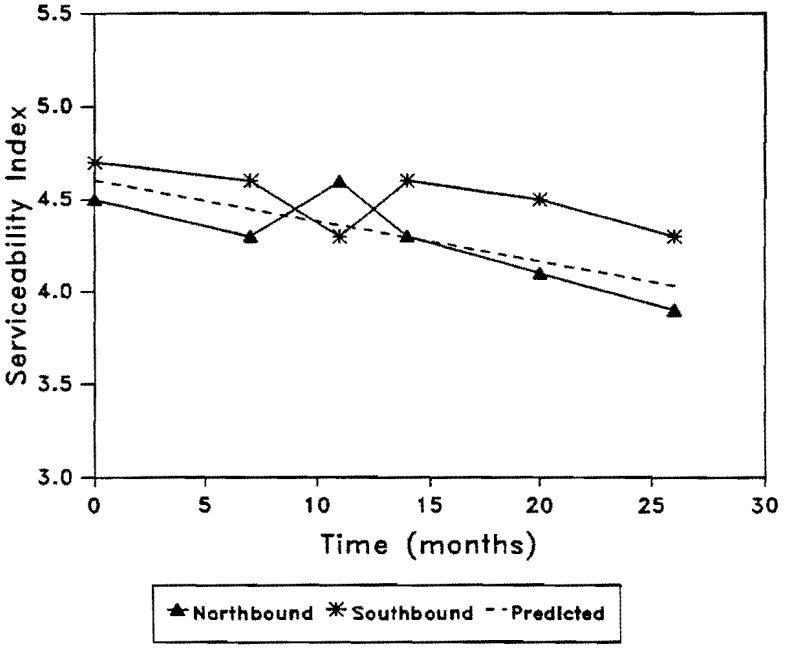

Figure 113. Comparison of Predicted and Measured Results of Serviceability Index in Moisture Barrier Section at Converse, FM 1516

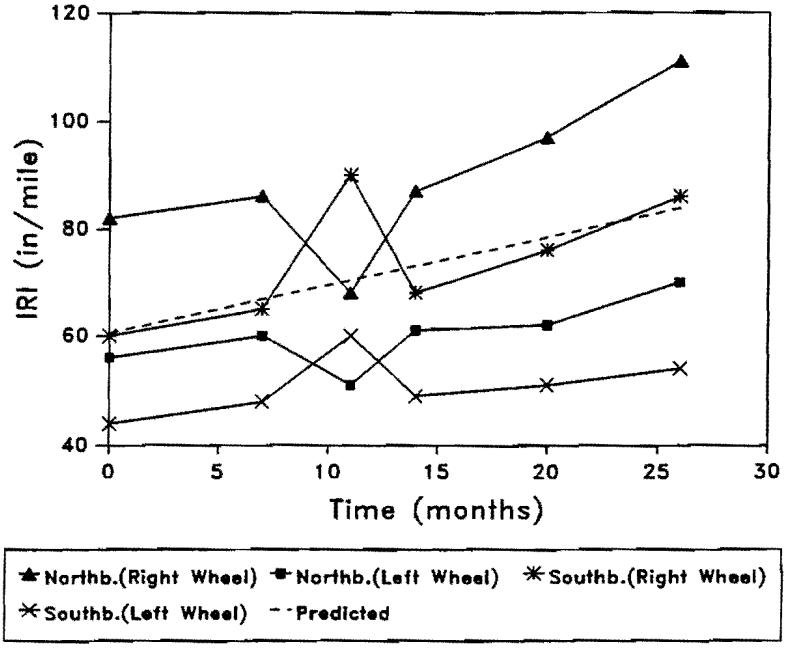

Figure 114. Comparison of Predicted and Measured Results of International Roughness Index in Moisture Barrier Section at Converse, FM 1516

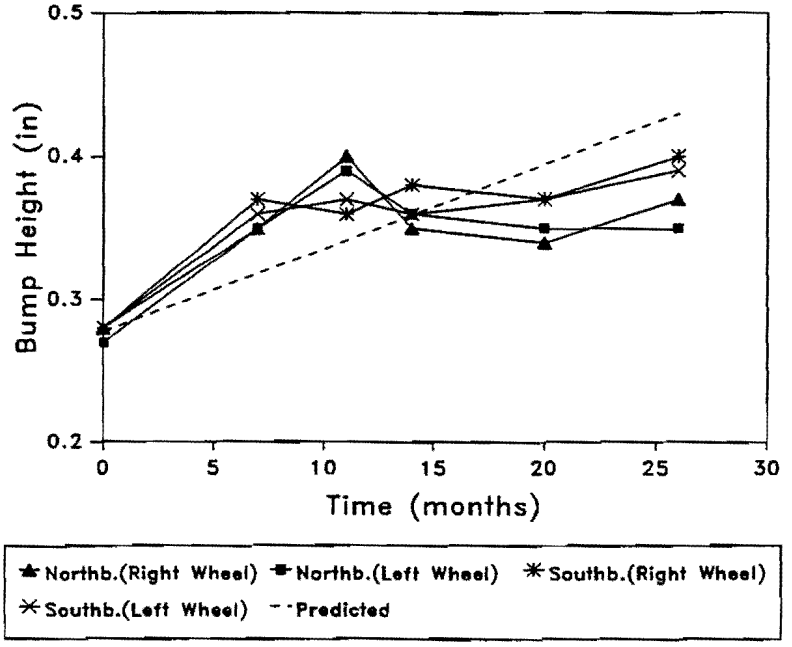

Figure 115. Comparison of Predicted and Measured Results of Maximum Expected Bump Height in Moisture Barrier Section at Converse, FM 1516

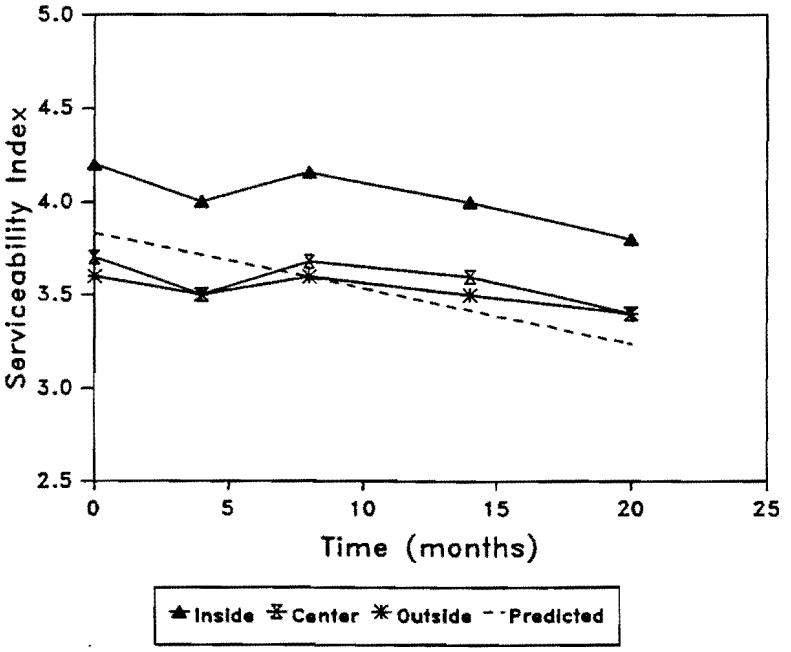

Figure 116. Comparison of Predicted and Measured Results of Serviceability Index in Moisture Barrier Section at Dallas, IH 635 Westbound

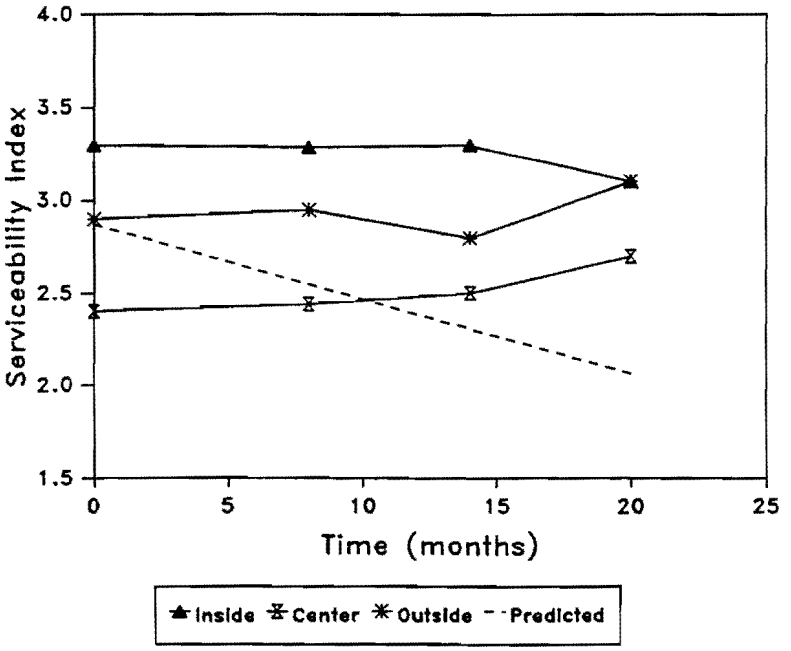

Figure 117. Comparison of Predicted and Measured Results of Serviceability Index in Control Section at Dallas, IH 635 Westbound

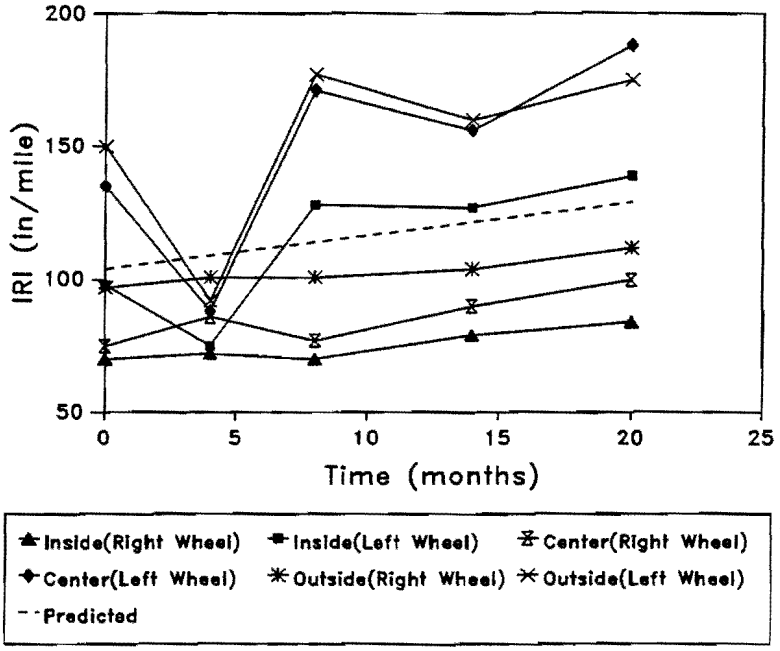

Figure 118. Comparison of Predicted and Measured Results of International Roughness Index in Moisture Barrier Section at Dallas, IH 635 Westbound

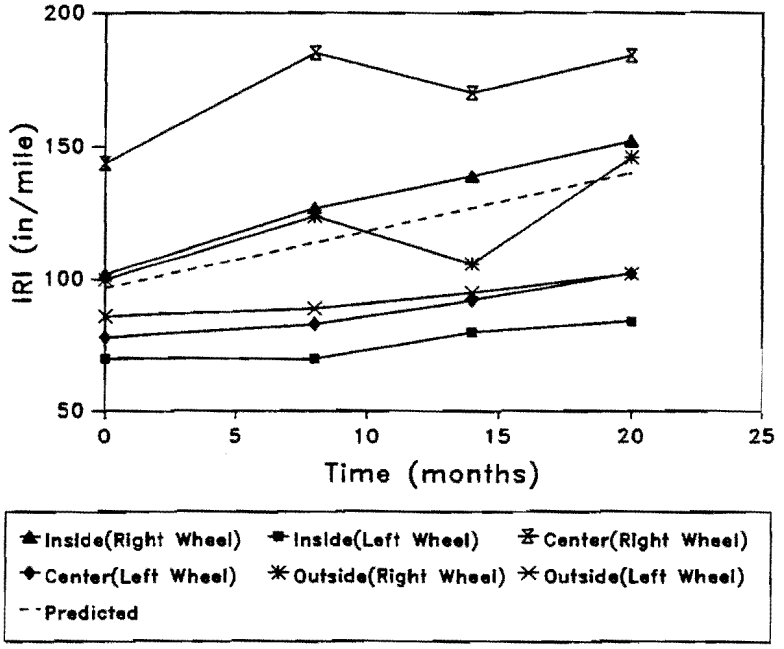

Figure 119. Comparison of Predicted and Measured Results of International Roughness Index in Control Section at Dallas, IH 635 Westbound

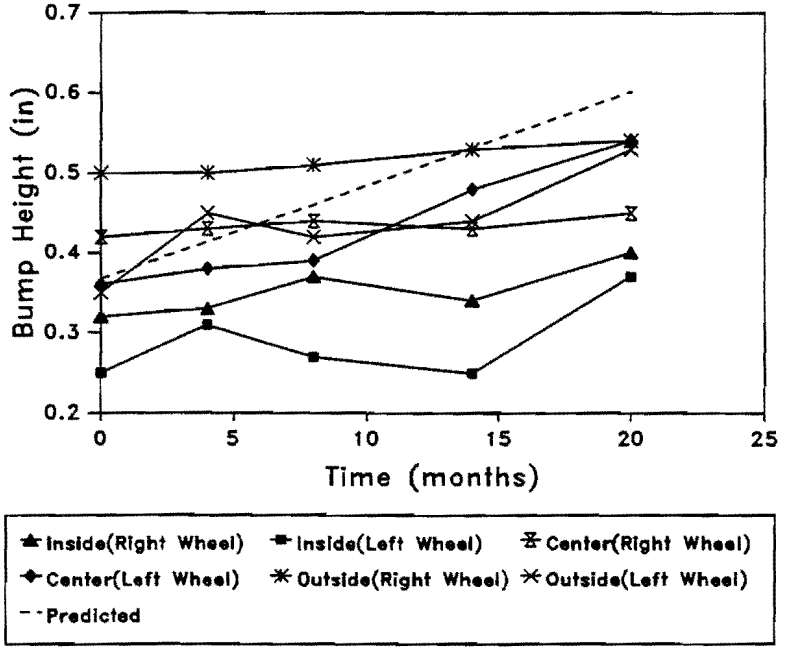

Figure 120. Comparison of Predicted and Measured Results of Maximum Expected Bump Height in Moisture Barrier Section at Dallas, IH 635 Westbound

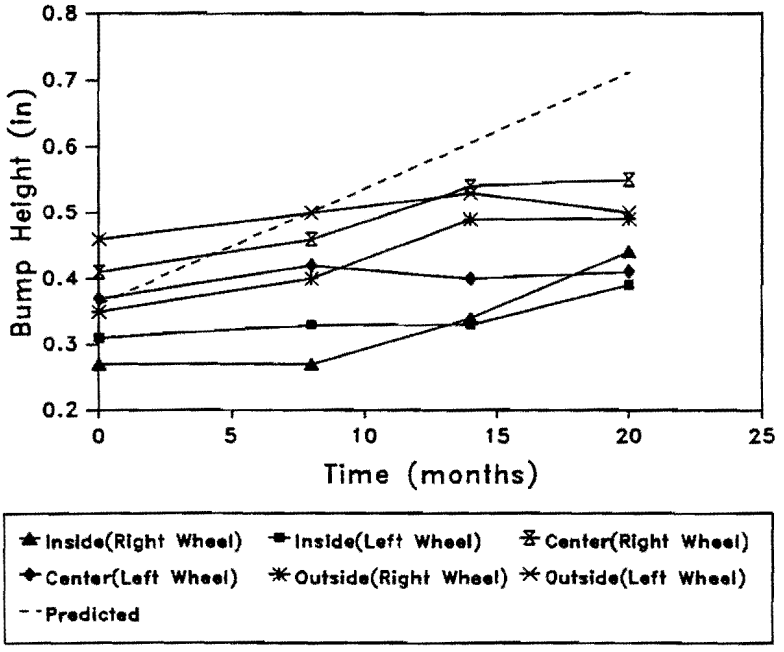

Figure 121. Comparison of Predicted and Measured Results of Maximum Expected Bump Height in Control Section at Dallas, IH 635 Westbound

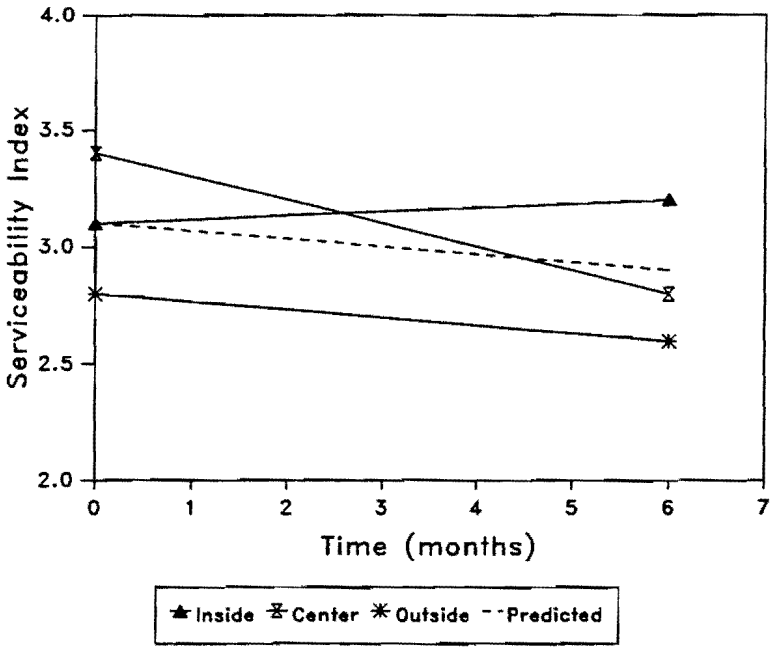

Figure 122. Comparison of Predicted and Measured Results of Serviceability Index in Moisture Barrier Section at Dallas, IH 635 Eastbound

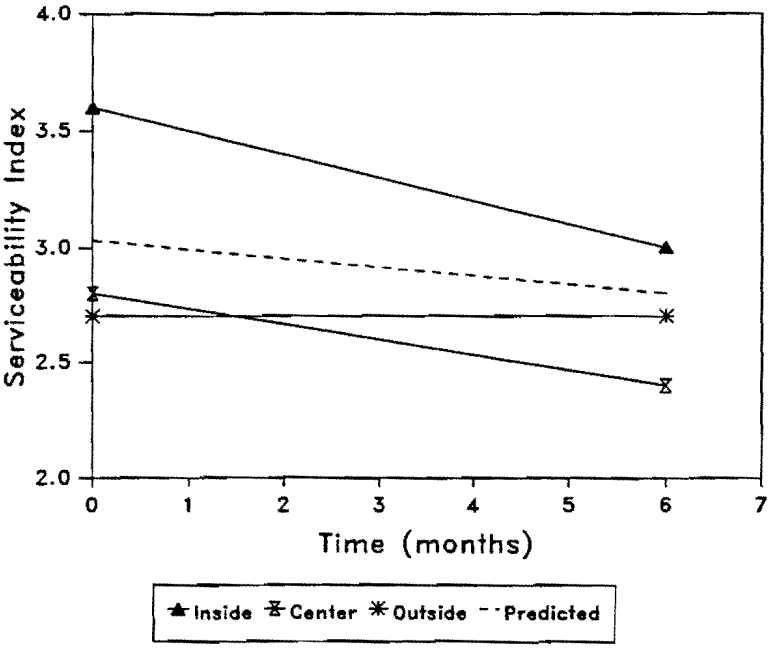

Figure 123. Comparison of Predicted and Measured Results of Serviceability Index in Control Section at Dallas, IH 635 Eastbound

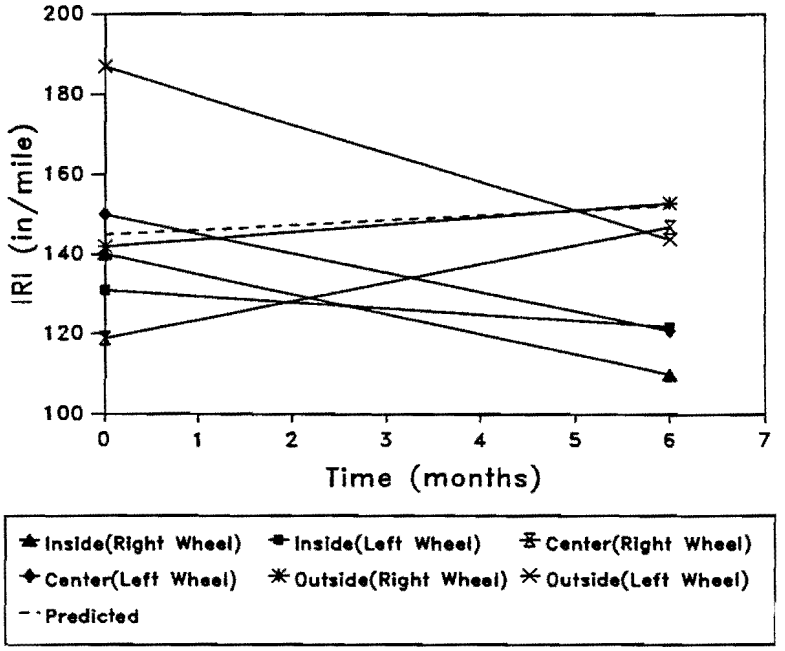

Figure 124. Comparison of Predicted and Measured Results of International Roughness Index in Moisture Barrier Section at Dallas, IH 635 Eastbound

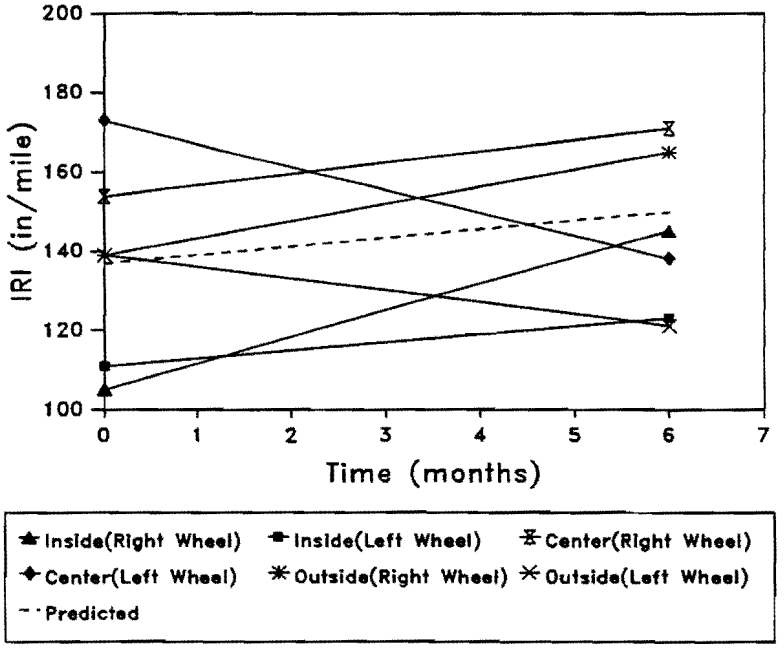

Figure 125. Comparison of Predicted and Measured Results of International Roughness Index in Control Section at Dallas, IH 635 Eastbound

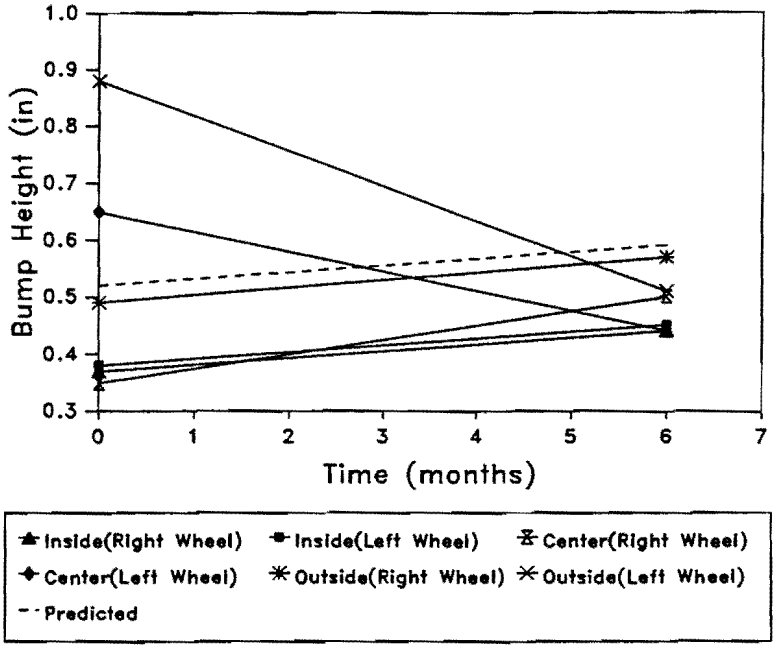

Figure 126. Comparison of Predicted and Measured Results of Maximum Expected Bump Height in Moisture Barrier Section at Dallas, IH 635 Eastbound

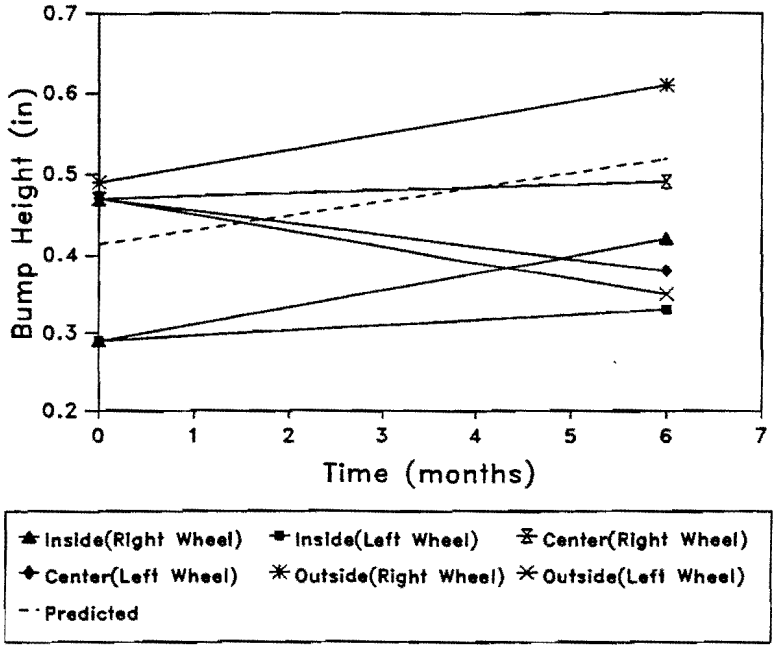

Figure 127. Comparison of Predicted and Measured Results of Maximum Expected Bump Height in Control Section at Dallas, IH 635 Eastbound

in extremely dry climates such as in El Paso when the pavement is subjected to "normal" and "slope" drainage conditions. Also, they are not effective in tight subgrade soils.

2. In extremely dry climates, the vertical moisture barriers are effective in "ponded" drainage conditions.
3. In cracked or medium cracked soils, the vertical moisture barriers are effective in reducing the development of roughness in all climates except for the extremely dry climates and under all drainage conditions.
4. Depth of barrier should be greater than or at least equal to the depth of the root zone.

CHAPTER VI

CONCLUSIONS AND RECOMMENDATIONS

CONCLUSIONS

Criteria were established for the effectiveness of vertical moisture barriers as follows.

1. If the vertical movement in the outside wheel path without a barrier is 2.5 cm or more, the barrier reduces it by 25% or more.
2. If the vertical movement in the outside wheel path without a barrier is less than 2.5 cm, the barrier reduces it by 1 cm or more.

Using this criteria, the following conclusions can be made from the results of this study.

1. The vertical moisture barriers are effective in reducing the development of roughness in pavements on expansive soils only when medium cracked soil is present on the site.
2. In cracked soil, vertical moisture barriers are not effective in any of the drainage conditions.
3. In medium cracked soils, the vertical moisture barriers are effective in reducing the development of roughness in all climates except for the extremely dry climates under nearly all drainage conditions. The barriers are ineffective in the semi-arid climates under "ponded" drainage conditions.
4. In tight subgrade soils, the vertical moisture barriers are not effective in any of the drainage conditions.

5. Depth of barrier should be greater than or at least equal to the depth of the root zone.
6. Site investigation is essential before installing vertical moisture barriers in pavements. The site investigation should include the soil tests such as the Atterberg limits, grain size distribution, specific gravity of soil particles, dry density of soil, natural moisture content of soil, and the filter paper suction. Also, an estimation of the crack pattern of subgrade soils, and the rooting depth of vegetation should be obtained.
7. The suction compression index is a powerful tool in characterizing expansive soils.
8. The suction compression index can reliably be estimated from the chart method. This procedure requires only the conventional soil tests such as the Atterberg limits and grain size distribution of soils, and the cation exchange capacity.
9. The FLODEF program is capable of predicting soil suction changes in the field and estimating vertical movement in pavements on expansive soils.
10. The measurement of in situ suction and the measurement of laboratory suction using the pressure plate apparatus can be used in evaluating flow properties of expansive soils.

11. The roughness prediction models which were described in Chapter V are reliable in predicting the changes in roughness measures such as Serviceability Index, International Roughness Index, and Maximum Expected Bump Height with time in pavements on expansive soils.

RECOMMENDATIONS

The recommendations that result from this study are presented herein:

1. All of the currently available methods of measuring soil suction have certain limitations. Thermal moisture sensors are not reliable when soils are too dry. Thermocouple psychrometers are not accurate in measuring soil suction in extremely wet soils. Further research is needed in improving the currently available methods of measuring soil suction and devising new equipment that can be used in both dry and wet soil moisture conditions.
2. The roughness prediction models used in this study are based on limited data collected from several expansive clay sites in Texas. A wide database involving subgrade soil properties, drainage conditions, crack patterns of soils, geometries of road profiles, moisture barrier depths, and roughness measures such as Serviceability Index, International Roughness Index, and Maximum Expected Bump Height must be formed in order to further refine the study of roughness development behavior in pavements. This database can be used in improving the currently available models for predicting the development of roughness in pavements on expansive soils.

REFERENCES

1. S. Oloo, H.D. Schreiner, J.B. Burland. Identification and Classification of Expansive Soils. Proc., Sixth International Conference on Expansive Soils, New Delhi, India, Dec. 1987.

2. J.E. Holland and C.E. Lawrence. Seasonal Heave of Australian Clay Soils. Proc., Fourth International Conference on Expansive Soils, Denver, Colo., ASCE, 1980, pp.302-321.

3. D.R. Snethen. An Evaluation of Methodology for Prediction and Minimization of Detrimental Volume Change of Expansive Soils in Highway Subgrades. Report FHWA-RD-79-49, Federal Highway Administration, U.S.Department of Transportation, Washington, D.C., March 1979.

4. I. Ravina. The Influence of Vegetation on Moisture and Volume Changes. Geotechnique, Vol.XXXIII, No.2, 1983, pp.151-157.

5. J.P. Krohn and J.E. Slosson. Assessment of Expansive Soils in the United States. Proc., Fourth International Conference on Expansive Soils, Denver, Colo., ASCE, 1980, pp.596-608.

6. D.E. Jones and W.G. Holtz. Expansive Soils - The Hidden Disaster. Journal of Civil Engineering, ASCE Vol.43, No.8, Aug. 1973, pp.49-51.

7. M. Picornell and R.L. Lytton. Field Measurement of Shrinkage Crack Depth in Expansive Soils. Transportation Research Record 1219, TRB, National Research Council, Washington, D.C., 1989, pp.121-130.

8. R.L. Lytton, R.L. Boggess, and J.W. Spotts. Characteristics of Expansive Clay Roughness of Pavements. Transportation Research Record 568, TRB, National Research Council, Washington, D.C., 1976, pp.9-23.

9. G.E. Hammitt and R.G. Ahlvin. Membranes and Encapsulation of Soils for Control of Swelling. Proc., Workshop on Expansive Clays and Shales in Highway Design and Construction, Vol.2, Federal Highway Administration, U.S.Department of Transportation, Washington, D.C., May 1973, pp.80-95.

10. J.R. Sallberg and P.C. Smith. Pavement Design over Expansive Clays: Current Practices and Research in the United States. Proc.,International Research and Engineering Conference on Expansive Clay Soils, Texas A& M University, College Station, Texas, 1965, pp.208-230.

11. Federal Highway Administration, Expansive Soils in Highway Subgrades: Summary, Report FHWA-TS-80-236, U.S.Department of Transportation, Washington, D.C., April 1980.

12. M.L. Steinberg. Ponding an Expansive Clay Cut: Evaluations and Zones of Activity. In Transportation Research Record 641, TRB, National Research Council, Washington, D.C., 1977, pp.61-66.

13. D. Forstie, H. Walsh, and G. Way. Membrane Technique for Control of Expansive Clays. Transportation Research Record 705, TRB, National Research Council, Washington, D.C., 1979, pp.49-53.

14. R.G. Mckeen. Validation of Procedures for Pavement Design on Expansive Soils. Report DOT/FAA/PM-85/15, Federal Aviation Administration, Washington, D.C., July 1985.

15. R.G. Mckeen and D.J. Hamberg. Characterization of Expansive Soils. Transportation Research Record 790, TRB, National Research Council, Washington, D.C., 1981, pp.73-78.

16. R.G. Mckeen. Field Studies of Airport Pavements on Expansive Clay. Proc., Fourth International Conference on Expansive Soils, Denver, Colo., ASCE, pp.242-261, 1980.

17. D.A. Gay. Development of a Predictive Model for Pavement Roughness on Expansive Clay. Ph.D. dissertation, Texas A & M University, College Station, Texas, Aug. 1991.

18. C.W. Thornthwaite. An Approach Toward a Rational Classification of Climate. Geographical Review, 1948, pp.54-94.

19. M.Picornell, R.L.Lytton, and M.L.Steinberg. Matrix Suction Instrumentation of a Vertical Moisture Barrier. Transportation Research Record 945, TRB, National Research Council, Washington, D.C., 1987, pp.16-21.

20. M.L.Steinberg. Deep Vertical Fabric Moisture Seals. Proc., Fourth International Conference on Expansive Soils, Denver, Colo., ASCE, 1980, pp.383-400.

21. M.L.Steinberg. Deep-Vertical-Fabric Moisture Barriers in Swelling Soils. Transportation Research Record 790, TRB, National Research Council, Washington, D.C., 1981, pp.87-94.

22. M.L.Steinberg. Controlling Expansive Soil Destructiveness by Deep Vertical Geomembranes on Four Highways. Transportation Research Record 1032, TRB, National Research Council, Washington, D.C., 1985, pp.48-53.

23. K.Russam and J.D.Coleman. The Effect of Climatic Factors on Subgrade Moisture Conditions. Geotechnique, Vol.II, No.1, 1961, pp.22-28.

24. M.Picornell. The Development of Design Criteria to Select the Depths of a Vertical Moisture Barrier. Ph.D. dissertation, Texas A & M University, College Station, Texas, Dec. 1985.

25. M.Picornell and R.L.Lytton. Behavior and Design of Vertical Moisture Barriers. Transportation Research Record 1137, TRB, National Research Council, Washington, D.C., 1987, pp.71-81.

26. D.R. Snethen. A Review of Engineering Experiences with Expansive Soils in Highway Subgrades. Report FHWA-RD-75-48, Federal Highway Administration, U.S.Department of Transportation, Washington, D.C., June 1975.

27. D.R. Snethen. Characterization of Expansive Soils using Soil Suction Data. Proc., Fourth International Conference on Expansive Soils, Denver, Colo., ASCE, 1980, pp.54-75.

28. J. Krahn and D.G. Fredlund. On Total, Matrix and Osmotic Suction. Soil Science, Vol. 114, No.5, 1972, pp.339-348.

29. D.G Fredlund and H. Rahardjo. State-of-Development in the Measurement of Soil Suction. International Conference on Engineering Problems on Regional Soils. Beijing, China, August 11-15, 1988

30. M.E. Bloodworth and J.B. Page. Use of Thermistors for the Measurement of Soil Moisture and Temperature. Soil Science Society of American Proceedings, Vol. 21, 1957, pp.11-15.

31. B. Shaw and L.D. Baver. An Electrothermal Method for Following Moisture Changes of the Soil In Situ. Soil Science Society of American Proceedings, Vol. 4, 1939, pp.78-83.

32. C.J. Phene, G.J. Hoffman, and S.L. Rawlins. Measuring Soil Matrix Potential In Situ by Sensing Heat Dissipation within a Porous Body: I. Theory and Sensor Construction. Soil Science Society of American Proceedings, Vol. 35, 1971, pp.27-33.

33. C.J. Phene, S.L. Rawlins, and G.J. Hoffman. Measuring Soil Matrix Potential In Situ by Sensing Heat Dissipation within a Porous Body: II. Experimental Results. Soil Science Society of American Proceedings, Vol. 35, 1971, pp.225-229.

34. S. Al-Khafaf and R.J. Hanks. Evaluation of the Filter Paper Method for Estimating Soil Water Potential. Soil Science, Vol. 117, pp.194-199.

35. T.B. Edil and S.E. Motan. Laboratory Evaluation of Soil Suction Components. Geotechnical Testing Journal, Vol. 7, Dec. 1984.

36. I.S. McQueen and R.F. Miller. Calibration and Evaluation of a Wide-range Gravimetric Method for Measuring Moisture Stress. Soil Science, Vol. 106, pp.225-231.

37. A.R.G. Lang. Osmotic Coefficients and Water Potentials of Sodium Chloride Solutions from 0 to 40°C. Australian Journal of Chemistry, Vol. 20, pp.2017-2023.

38. R.L. Lytton. The Characterization of Expansive Soils in Engineering. Presented at the December 1977, American Geophysical Union Symposium on Water Movement and Equilibrium in Swelling Soils, held at San Francisco, California.

39. M. Sayers. Development Implementation and Application of the Reference Quarter-car Simulation. Measuring Road Roughness and Its Effects on User Cost and Comfort, ASTM STP 884. T.D. Gillesple and M. Sayers editors. American Society for Testing and Materials, Philadelphia, PA, 1985.

40. M.O. Velasco and R.L. Lytton. Pavement Roughness on Expansive Clays. Research Report 284-2, Texas Transportation Institute, Texas A & M University, College Station, Texas, 1981.

41. D.A. Gay and R.L. Lytton. Moisture Effects on Pavement Roughness. Measured Performance of Shallow Foundations, Geotechnical Special Publication No. 15, American Society of Civil Engineers, 1988.

42. P.W. Mitchell. The Concepts Defining the Rate of Swell of Expansive Soils. Proc., Fourth International Conference on Expansive Soils, Denver, Colo., ASCE, 1980, pp.106-116.

43. E.C. Mojekwu. A Simplified Method for Identifying the Predominant Clay Mineral. M.S. Thesis, Texas Tech. University, Lubbock, Texas, Aug. 1979.

44. R.G. McKeen and L.D. Johnson. Climate-Controlled Soil Design Parameters for Mat Foundations. Journal of Geotechnical Engineering, ASCE Vol.116, No.7, July 1990, pp.1073-1094.

APPENDIX A

METHOD OF MEASURING SOIL SUCTION WITH FILTER PAPERS

METHOD OF MEASURING SOIL SUCTION WITH FILTER PAPERS

SCOPE

This method covers the procedure for determining total soil suction using filter papers.

MATERIALS AND EQUIPMENT

1. Filter paper (5.5 cm diameter)
2. Analytical balance accurate to 0.0001 gm
3. Sodium chloride reagent grade
4. Self sealing plastic container (500 ml capacity, and diameter greater than that of the filter paper)
5. Rubber stoppers
6. Constant temperature chamber (20°C)
7. Oven, 110°C
8. Heavy aluminum plate
9. Small lightweight weighing boxes such as Soiltext Catalog No. LT-15
10. Pentachlorophenol "Dowcide-7" reagent grade
11. Ethanol reagent grade solvent
12. Rubber rings (diameter less than that of the glass jar)
13. Plastic insulating tape

CALIBRATION PROCEDURE

1. Prepare 200 ml of five different sodium chloride (NaCl) solutions. It is recommended that these solutions have molalities of 0.05, 0.1, 0.5, 1.0, and 2.0. These solutions may be prepared from first principles using the relationship that a 1 M solution of NaCl

contains 1 molecular weight of NaCl in 1 liter of water.

2. Measure 20 ml of each of the NaCl solutions prepared and put this volume into separate labeled self sealing plastic containers. Place a rubber stopper at the center of the container. The rubber stopper will act as a pedestal for the filter paper during moisture equilibrium phase.
3. Place a single sheet of filter paper on the rubber stopper in each of the containers and close the lid. Care should be taken at this point to ensure that at no time must the filter paper come into contact with the NaCl solution in the container.
4. Keep the containers in a temperature controlled (20°C) room for seven days.
5. Remove the filter papers from containers, place in aluminum weighing boxes, and quickly measure the weight of the filter paper + adsorbed water content to an accuracy of 0.0001 gm.
6. Place the weighing boxes in the oven for 24 hours with their lids partly open to permit rapid drying.
7. Close the lids of the weighing boxes while they are in the oven, remove the boxes from oven, place on a heavy aluminum plate for 30 seconds to cool, and measure immediately the weight of each filter paper to an accuracy of 0.0001 gm.
8. Express the moisture content of filter paper in percentage of the weight of the dry filter paper. The percentage shall be calculated as follows:

$$\text{Percentage moisture} = \frac{\text{mass of water}}{\text{mass of oven dried filter paper}} \times 100$$

9. Obtain the suction from Table 23 for the corresponding concentration of NaCl solution and temperature, and plot suction vs. percentage moisture content to obtain the calibration curve. A typical calibration curve is shown in Figure 128.

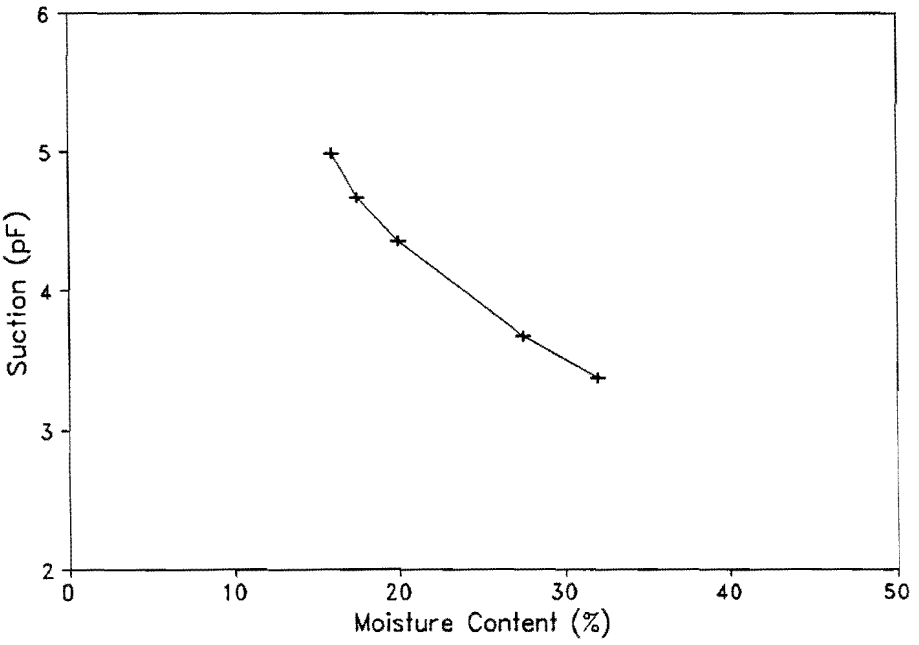

Figure 128. A Typical Calibration Curve for Filter Paper Suction

Table 23. Water Potentials in Bars of NaCl Solutions at Temperatures between 0 and 40°C (37)

Molality	0°C	5°C	10°C	15°C	20°C	25°C	30°C	35°C	40°C
0.05	-2.14	-2.18	-2.22	-2.26	-2.30	-2.34	-2.38	-2.42	-2.45
0.10	-4.23	-4.31	-4.39	-4.47	-4.54	-4.62	-4.70	-4.77	-4.85
0.20	-8.36	-8.52	-8.68	-8.84	-9.00	-9.15	-9.30	-9.46	-9.61
0.30	-12.47	-12.72	-12.97	-13.21	-13.44	-13.68	-13.91	-14.15	-14.37
0.40	-16.58	-16.93	-17.27	-17.59	-17.91	-18.23	-18.55	-18.86	-19.17
0.50	-20.70	-21.15	-21.58	-22.00	-22.41	-22.81	-23.22	-23.62	-24.02
0.60	-24.84	-25.39	-25.93	-26.44	-26.94	-27.44	-27.94	-28.43	-28.91
0.70	-29.01	-29.67	-30.30	-30.91	-31.51	-32.10	-32.10	-32.28	-33.85
0.80	-33.20	-33.98	-34.72	-35.43	-36.12	-36.82	-37.51	-38.18	-38.85
0.90	-37.43	-38.32	-39.17	-39.98	-40.79	-41.58	-43.27	-43.14	-43.90
1.00	-41.69	-42.70	-43.66	-44.59	-45.50	-46.40	-47.29	-48.15	-49.01
1.10	-45.99	-47.13	-48.20	-49.24	-50.26	-51.27	-52.26	-53.22	-54.18
1.20	-50.32	-51.60	-52.78	-53.94	-55.07	-56.20	-57.30	-58.35	-59.41
1.30	-54.70	-56.11	-57.42	-58.69	-59.94	-61.19	-62.39	-63.54	-64.71
1.40	-59.12	-60.68	-62.10	-63.50	-64.87	-66.23	-67.54	-68.80	-70.06
1.50	-63.59	-65.29	-66.84	-68.37	-69.87	-71.34	-72.76	-74.11	-75.48
1.60	-68.11	-69.96	-71.63	-73.30	-74.91	-76.52	-78.05	-79.50	-80.07
1.70	-72.60	-74.60	-76.40	-78.20	-80.00	-81.70	-83.30	-84.90	-86.50
1.80	-77.30	-79.40	-81.30	-83.30	-85.20	-87.00	-88.80	-89.40	-92.10
1.90	-81.90	-84.30	-86.30	-88.40	-90.40	-92.40	-94.30	-96.00	-97.80
2.00	-86.70	-89.20	-91.30	-93.60	-95.70	-97.80	-99.80	-101.60	-103.50

TEST PROCEDURE

1. Treat filter papers to inhibit biological decomposition by dipping them into a solution of pentachlorophenol in 3 percent ethanol and allowing to air dry.
2. Obtain a sample of soil from site in a self sealing plastic container, place a rubber ring on top of the soil, place two or three filter papers on top of the rubber ring, close the lid, and seal with plastic insulating tape. Care must be taken at this point to ensure that no moisture is lost from the sample.
3. Transport the sample to laboratory with care. It is recommended that the sample be placed in an insulated box while transporting. Disturbance of soil sample during transportation should be avoided.
4. Keep the sample in a constant temperature ($20^{o}C$) chamber for seven days for equilibration.
5. Follow the same procedure described in steps 5-8 of calibration procedure, and calculate the moisture content of filter paper in percentage of the weight of the dry filter paper.
6. Use calibration curve to obtain the soil suction for the corresponding percentage moisture content of filter paper.

APPENDIX B

IN SITU SOIL SUCTION MEASUREMENTS

Table 24. In Situ Soil Suction Measurements at Dallas, IH 635 Westbound

Date of Installation: Sept., 1990 Instrument: Thermal Moisture sensor

Date of Measurement	Soil Suction (Bars)							
	Beneath Pavement Depth, ft				Beneath Embankment Depth, ft			
	1.92	4.00	5.83	7.83	1.50	4.00	5.67	8.08
10/26/90	-2.023	--	1.229	-0.631	-21.182	-0.267	-1.742	0.237
11/16/90	0.829	--	4.619	1.718	-10.404	0.505	3.049	1.782
12/19/90	-1.879	-11.701	0.030	-2.758	-13.723	-0.975	-1.875	-20.268
02/04/91	--	-1.850	-0.145	-2.299	-0.893	-1.038	-3.428	-0.082
03/05/91	-6.430	-1.376	-3.609	-3.248	0.214	-2.264	-3.133	-0.305
04/05/91	-0.453	--	--	--	--	--	--	0.444
06/06/91	-2.728	-1.414	-2.498	-7.200	-5.742	-16.603	-3.177	0.237
07/22/91	-3.561	0.048	-2.133	-10.700	-6.823	-3.984	-6.105	0.078
12/05/91	-3.657	-0.773	-5.801	-15.214	-3.305	-0.924	-5.440	-1.594
01/29/92	-11.317	-1.312	-9.207	-4.579	-3.019	-1.683	-7.096	-0.863
03/05/92	-6.157	-0.978	-2.397	-8.986	-3.218	-0.697	-0.160	-0.719
04/28/92	-4.186	--	0.293	-4.992	-5.207	--	0.224	-1.070
06/11/92	-7.022	--	-24.743	--	-16.408	--	-1.387	-16.652
24/08/92	-9.314	--	-19.635	--	-14.145	--	-1.890	-11.652

Table 25. In Situ Soil Suction Measurements at Dallas, IH 635 Eastbound

Date of Installation: Dec., 1991 Instrument: Thermal Moisture sensor

Date of Measurement	Soil Suction (Bars)							
	Beneath Pavement Depth, ft				Beneath Embankment Depth, ft			
	2.00	4.00	6.00	8.00	2.00	4.00	6.00	8.00
01/29/92	-4.947	0.022	-0.219	-2.845	--	-1.635	0.452	-0.090
03/05/92	-3.760	0.022	-0.204	-2.155	-2.865	-2.361	-1.254	-0.063
04/28/92	-3.022	-0.036	-0.188	-2.301	-2.130	-3.233	-5.613	-0.224
06/11/92	-49.997	-4.942	-2.303	-0.987	--	11.683	-8.955	-0.788
24/08/92	-24.487	-3.887	-2.347	-1.431	--	-19.477	-10.436	-0.656

Table 26. In Situ Soil Suction Measurements at Seguin, IH 10 Westbound

Date of Installation: Nov., 1988 Instrument: Thermal Moisture sensor

Date of Measurement	Soil Suction (Bars)							
	Beneath Pavement Depth, ft				Beneath Embankment Depth, ft			
	3.00	4.00	5.50	7.83	2.50	4.17	6.00	7.67
04/06/89	0.175	0.023	0.160	0.118	-1.478	-1.557	-0.047	--
09/26/89	0.662	1.287	-0.132	-0.126	-2.182	-3.044	0.002	--
01/31/90	--	--	--	--	--	--	--	--
03/23/90	3.048	2.569	2.208	-0.357	--	-3.123	-0.916	1.890
05/31/90	1.150	2.221	1.623	-0.794	--	-4.601	-1.668	--
08/02/90	0.505	1.842	1.087	-0.909	--	-5.183	-2.152	--
09/13/90	1.620	1.778	1.656	-1.102	--	-5.198	-3.087	--
10/11/90	1.028	1.430	1.168	-0.999	--	-4.544	-3.889	--
11/30/90	1.602	2.047	1.445	-1.050	--	-3.820	-2.319	--
12/20/90	1.237	1.430	0.925	-0.935	--	-3.919	-2.503	--
01/25/91	1.985	2.205	2.273	-0.704	--	-3.053	--	--
03/08/91	1.811	2.142	28.046	-0.973	--	-3.365	--	-1.906
04/12/91	--	2.174	--	--	--	--	--	--
06/04/91	0.575	1.604	2.143	-2.142	--	-8.564	--	-3.066
07/24/91	0.330	-3.840	1.250	-2.617	--	-11.860	--	--
10/03/91	-0.366	-3.663	0.925	-0.486	--	-21.773	--	22.161
12/03/91	0.627	-2.730	2.127	-2.822	--	--	--	--
01/28/92	0.697	-2.525	1.331	-3.438	--	--	--	--
03/06/92	0.540	-4.407	-3.918	-4.452	--	-16.092	--	--
04/29/92	--	-3.869	-4.487	-4.850	--	-21.347	--	--
06/09/92	--	-12.332	-21.761	-3.104	--	-32.667	--	--
08/26/92	--	-6.854	--	-5.137	--	-18.665	--	--

Table 27. In Situ Soil Suction Measurements at Converse, FM 1516

Date of Installation: June, 1989 Instrument: Thermal Moisture sensor

Date of Measurement	Soil Suction (Bars)					
	Beneath Pavement Depth, ft			Beneath Embankment Depth, ft		
	2.5	5.5	8.0	2.5	5.5	8.0
09/26/89	0.138	-1.020	-3.090	-0.804	-0.459	0.354
03/23/90	--	-1.417	-5.139	-0.465	-0.207	-0.831
05/31/90	--	-0.969	-0.937	-0.418	-0.496	-2.568
08/02/90	--	-3.198	-4.368	-0.144	-1.000	-0.129
09/13/90	--	-8.423	-29.171	-0.015	-1.241	-0.639
10/11/90	--	-3.479	-15.180	0.194	-1.806	-1.314
11/30/90	--	0.337	-17.853	0.221	-1.565	-1.231
12/20/90	--	0.632	-19.754	0.307	-1.517	-1.383
01/25/91	--	1.003	-10.308	0.565	-1.265	-1.093
03/08/91	--	--	--	0.694	--	-0.818
04/12/91	--	--	--	--	--	--
06/04/91	--	0.324	-12.000	0.001	-2.046	-2.279
07/24/91	--	-4.310	-16.190	-0.418	-2.202	-9.997
10/03/91	--	-0.739	0.103	-0.563	-2.960	-4.952
12/03/91	--	0.222	--	-0.257	--	--
01/28/92	--	-1.046	--	-2.270	-2.833	--
03/06/92	--	0.452	-7.888	-5.911	-9.439	--
04/29/92	--	-0.508	-13.843	-0.273	--	2.366
06/09/92	--	0.145	-19.472	18.654	-13.045	--
08/26/92	--	-1.315	--	-0.987	-13.334	--

Table 28. In Situ Soil Suction Measurements at Ennis 1, IH 45 Northbound Frontage Road.

Date of Installation: Aug., 1990 Instrument: Thermal Moisture sensor

Date of Measurement	Soil Suction beneath pavement (Bars) Depth, ft			
	1.50	3.33	5.50	7.00
09/22/90	0.215	--	-0.141	-0.366
10/26/90	-0.389	-0.389	0.046	-0.354
11/16/90	0.673	-0.246	-16.442	--
12/19/90	0.035	-0.397	-8.505	--
02/04/91	-0.351	0.415	-12.661	-13.075
03/05/91	-0.459	--	-10.469	--
04/05/91	--	--	--	13.283
06/06/91	-29.820	-0.770	-11.231	-25.905
07/22/91	-6.420	-0.667	-2.787	-22.637
12/05/91	--	-7.812	-30.859	--
01/29/92	--	-4.600	--	--
03/05/92	--	--	-10.696	--
04/28/92	-1.965	-0.913	-4.016	-47.356
06/11/92	-19.042	--	-9.173	-0.426
08/24/92	--	--	-15.111	-1.699

Table 29. In Situ Soil Suction Measurements at Ennis 2, IH 45 Northbound Frontage Road.

Date of Installation: Aug., 1990 Instrument: Thermal Moisture sensor

Date of Measurement	Soil Suction beneath pavement (Bars) Depth, ft			
	1.50	3.50	5.00	6.67
09/22/90	0.233	-0.745	-0.367	-0.014
10/26/90	--	--	--	--
11/16/90	-0.106	0.136	-0.075	-0.136
12/19/90	0.127	-0.015	0.339	0.461
02/04/91	0.034	0.229	-0.229	-3.402
03/05/91	1.089	1.489	-12.872	--
04/05/91	-19.595	--	-5.338	--
06/06/91	-0.282	-0.520	-8.791	-3.741
07/22/91	-1.124	-1.046	-0.858	-9.108

Table 30. In Situ Soil Suction Measurements Beneath Pavement at Wichita Falls 1, IH 44 Northbound

Date of Installation: April, 1989 Instrument: Thermocouple Psychrometer

Date of Measurement	Soil Suction (Bars) Depth, ft									
	3		5		8		12		15	
10/89	--	--	95.7	--	--	--	0.5	--	2.8	1.8
01/90	--	--	--	--	--	--	--	--	--	--
05/90	--	--	--	--	--	--	--	--	--	--
08/90	--	--	--	--	--	--	--	--	--	--
11/90	--	--	--	--	--	--	--	--	--	--
02/91	--	--	--	--	--	--	--	--	--	--
04/91	--	--	--	--	--	--	--	--	--	--
07/91	--	--	--	--	--	--	--	--	--	--
10/91	--	--	--	--	--	--	--	--	--	--
02/92	--	--	--	--	--	--	--	--	--	--
06/92	--	--	--	--	--	--	--	--	--	--

Table 31. In Situ Soil Suction Measurements Beneath Embankment at Wichita Falls 1, IH 44 Northbound

Date of Installation: April, 1989 Instrument: Thermocouple Psychrometer

Date of Measurement	Soil Suction (Bars) Depth, ft									
	1		3		6		10		13	
10/89	--	17.0	3.9	4.0	17.3	15.1	7.3	10.8	14.6	12.5
01/90	95.2	2.8	--	35.6	--	--	--	--	5.9	--
05/90	--	9.4	12.5	11.6	14.1	6.3	25.4	4.5	5.8	6.0
08/90	--	2.9	5.8	6.3	6.3	6.6	40.0	6.3	5.2	0.3
11/90	1.6	2.7	1.6	2.0	3.2	0.0	22.2	4.6	--	4.3
02/91	--	--	--	--	--	0.8	2.0	4.5	3.2	5.0
04/91	--	0.6	11.9	12.6	--	11.3	14.0	--	8.7	8.7
07/91	--	--	17.1	15.4	--	17.7	12.7	12.2	19.1	33.9
10/91	--	--	1.1	1.8	--	5.9	1.9	3.1	4.4	--
02/92	95.5	87.4	6.8	0.4	--	1.5	0.3	1.1	15.9	--
06/92	--	16.7	10.1	8.4	--	6.2	6.5	6.6	4.1	10.7

Table 32. In Situ Soil Suction Measurements Beneath Pavement at Wichita Falls 2, IH 44 Southbound

Date of Installation: April, 1989 Instrument: Thermocouple Psychrometer

Date of Measurement	Soil Suction (Bars) Depth, ft									
	3		5		8		12		15	
10/89	--	--	1.5	1.8	1.2	3.7	6.9	5.8	3.1	3.5
01/90	4.4	--	4.5	--	--	--	8.6	5.6	--	8.5
05/90	15.3	--	14.0	12.3	6.5	5.1	15.2	8.5	6.0	--
08/90	8.1	--	9.8	--	7.9	6.7	81.0	5.1	6.9	--
11/90	2.2	--	2.6	--	36.3	0.9	5.9	108.4	4.8	--
02/91	10.9	--	21.6	--	1.3	--	9.4	17.9	--	--
04/91	36.1	--	31.1	15.7	9.5	7.5	13.8	--	--	--
07/91	80.7	--	49.0	17.0	19.6	13.7	105.3	--	--	--
10/91	11.4	--	9.1	8.3	1.8	0.7	--	33.1	--	--
02/92	--	--	8.0	8.4	10.2	2.6	--	54.2	--	--
06/92	--	--	16.1	16.4	18.1	--	--	--	--	--

Table 33. In Situ Soil Suction Measurements Beneath Embankment at Wichita Falls 2, IH 44 Southbound

Date of Installation: April, 1989 Instrument: Thermocouple Psychrometer

Date of Measurement	Soil Suction (Bars) Depth, ft									
	1		3		6		10		13	
10/89	--	--	1.7	--	1.5	2.7	3.4	30.4	6.7	3.4
01/90	--	2.0	3.2	--	2.7	6.1	1.8	2.9	8.5	5.2
05/90	11.9	14.2	20.3	--	8.0	8.9	5.5	6.8	11.2	9.4
08/90	2.5	--	17.0	31.3	4.0	--	4.7	34.7	7.1	2.5
11/90	3.4	--	40.1	--	5.9	16.4	2.8	64.5	9.1	7.2
02/91	2.6	--	7.4	--	9.8	--	3.0	20.2	7.4	5.5
04/91	13.6	20.8	20.1	--	19.2	60.6	10.6	13.3	16.6	14.6
07/91	--	--	15.7	--	8.1	58.3	10.2	20.5	9.7	7.5
10/91	--	--	4.2	53.9	7.4	9.9	4.0	10.5	6.5	4.5
02/92	--	--	--	--	7.7	10.1	0.6	12.8	--	33.0
06/92	--	--	13.2	16.9	13.5	27.7	--	30.4	--	--

Table 34. In Situ Soil Suction Measurements Beneath Pavement at Snyder 1, US 84 Northbound

Date of Installation: June, 1989 Instrument: Thermocouple Psychrometer

Date of Measurement	Soil Suction (Bars) Depth, ft									
	3		5		8		12		15	
10/89	0.7	1.3	4.6	1.8	10.9	6.1	19.8	15.0	28.7	21.9
01/90	--	--	--	--	--	--	8.8	6.5	14.3	13.4
04/90	11.7	12.0	11.7	14.0	6.4	6.2	10.0	6.8	16.4	15.8
09/90	9.1	11.5	10.8	9.5	6.5	1.8	2.2	2.0	1.7	1.0
01/91	--	--	3.6	5.1	--	7.9	4.4	1.1	0.7	3.0
06/91	--	2.4	14.2	17.0	--	9.6	24.6	--	50.5	0.2
09/91	--	--	0.6	--	--	0.5	--	--	--	--
03/92	62.7	--	12.4	--	--	--	--	--	--	--
07/92	13.2	--	11.4	--	--	--	--	--	--	--

Table 35. In Situ Soil Suction Measurements Beneath Embankment at Snyder 1, US 84 Northbound

Date of Installation: June, 1989 Instrument: Thermocouple Psychrometer

Date of Measurement	Soil Suction (Bars) Depth, ft									
	2		4		7		11		14	
10/89	0.3	2.3	2.2	2.5	0.3	3.4	2.2	4.8	5.6	4.2
01/90	--	--	--	--	5.8	8.2	10.0	14.2	9.8	17.4
04/90	9.4	--	14.4	7.0	9.7	12.9	18.1	20.2	14.7	--
09/90	6.1	7.3	8.3	6.6	12.6	14.3	9.8	13.9	13.1	10.3
01/91	--	--	5.2	6.3	5.2	--	8.5	8.5	8.4	5.0
06/91	--	--	96.6	22.0	10.8	--	15.0	13.0	17.6	9.0
09/91	--	--	4.4	29.5	5.0	--	1.0	6.8	8.8	1.4
03/92	--	--	0.7	32.4	--	--	--	5.1	--	--
07/92	--	--	--	25.8	--	--	--	--	--	--

Table 36. In Situ Soil Suction Measurements Beneath Pavement at Snyder 2, US 84 Northbound

Date of Installation: Feb., 1991 Instrument: Thermocouple Psychrometer

Date of Measurement	Soil Suction (Bars) Depth, ft									
	3		5		8		12		15	
05/91	26.9	46.5	17.9	22.5	10.8	12.5	8.4	9.1	10.4	12.4
09/91	2.5	--	--	1.6	17.0	6.0	5.7	--	--	8.5
03/92	--	63.5	--	--	2.0	--	--	--	--	3.5
06/92	--	105.0	--	--	4.1	--	--	6.6	6.8	3.8

Table 37. In Situ Soil Suction Measurements Beneath Embankment at Snyder 2, US 84 Northbound

Date of Installation: Feb., 1991 Instrument: Thermocouple Psychrometer

Date of Measurement	Soil Suction (Bars) Depth, ft									
	2.5		4.5		7.5		11.5		14.5	
05/91	30.3	26.1	15.2	11.1	10.0	9.7	8.5	9.2	7.4	10.0
09/91	1.3	--	2.5	--	2.7	17.2	10.5	14.1	12.3	5.7
03/92	--	--	--	2.9	3.4	--	--	0.3	6.4	6.1
06/92	16.1	--	72.3	8.5	3.8	--	--	5.4	5.1	5.4

Table 38. In Situ Soil Suction Measurements Beneath Pavement at Snyder 3, US 84 Northbound

Date of Installation: Feb., 1991 Instrument: Thermocouple Psychrometer

Date of Measurement	Soil Suction (Bars) Depth, ft							
	3		5		8		12	
05/91	13.6	15.1	16.2	12.3	10.6	9.7	6.3	4.9
09/91	2.3	0.0	--	20.7	0.5	2.6	2.3	42.0
03/92	3.8	10.0	--	3.4	--	--	--	8.6
06/92	9.7	--	--	--	--	5.2	--	7.1

Table 39. In Situ Soil Suction Measurements Beneath Embankment at Snyder 3, US 84 Northbound

Date of Installation: Feb., 1991 Instrument: Thermocouple Psychrometer

Date of Measurement	Soil Suction (Bars) Depth, ft							
	2		4		7		11	
05/91	13.4	21.3	13.7	13.3	11.8	11.2	9.1	8.6
09/91	--	--	--	--	--	--	0.3	--
03/92	8.7	7.2	4.9	--	--	--	--	--
06/92	4.6	4.4	24.9	--	--	--	--	--

APPENDIX C

ROUGHNESS MEASUREMENTS

Table 40. Serviceability Index Measurements at Seguin, IH 10

	Date of Measurement	Inside Lane	Outside Lane
Barrier Section	Sept., 1989	4.7	4.8
	May, 1990	4.7	4.7
	Dec., 1990	4.6	4.6
	April, 1991	4.5	4.6
	July, 1991	4.5	4.7
	Jan., 1992	4.5	4.6
	July, 1992	4.4	4.6
Control Section	July, 1992	4.7	4.7

Table 41. International Roughness Measurements at Seguin, IH 10

	Date of Measurement	Inside Lane (in/mile)		Outside Lane (in/mile)	
		Right Wheel	Left Wheel	Right Wheel	Left Wheel
Barrier Section	Sept., 89	50	49	48	45
	May, 90	52	54	53	48
	Dec., 90	51	55	54	54
	April, 91	54	58	55	51
	July, 91	51	52	49	51
	Jan., 92	52	54	55	56
	July, 92	58	60	47	54
Control Section	July, 92	43	48	44	54

Table 42. Maximum Expected Bump Measurements at Seguin, IH 10

	Date of Measurement	Inside Lane (in)		Outside Lane (in)	
		Right Wheel	Left Wheel	Right Wheel	Left Wheel
Barrier Section	Sept., 89	0.42	0.45	0.38	0.40
	May, 90	0.30	0.32	0.31	0.30
	Dec., 90	0.42	0.44	0.44	0.43
	April, 91	0.43	0.46	0.43	0.41
	July, 91	0.46	0.37	0.52	0.36
	Jan., 92	0.47	0.48	0.43	0.58
	July, 92	0.59	0.57	0.59	0.59
Control Section	July, 92	0.43	0.46	0.53	0.57

Table 43. Serviceability Index Measurements at Converse, FM 1516

	Date of Measurement	Northbound Lane	Southbound Lane
Barrier Section	May, 1990	4.50	4.70
	Dec., 1990	4.30	4.60
	April, 1991	4.60	4.30
	July, 1991	4.30	4.60
	Jan., 1992	4.10	4.50
	July, 1992	3.90	4.30

Table 44. International Roughness Index Measurements at Converse, FM 1516

	Date of Measurement	Northbound Lane (in/mile)		Southbound Lane (in/mile)	
		Right Wheel	Left Wheel	Right Wheel	Left Wheel
Barrier Section	May, 90	82	56	60	44
	Dec., 90	86	60	65	48
	April, 91	68	51	90	60
	July, 91	87	61	68	49
	Jan., 92	97	62	76	51
	July, 92	111	70	86	54

Table 45. Maximum Expected Bump Height Measurements at Converse, FM 1516

	Date of Measurement	Northbound Lane (in)		Southbound Lane (in)	
		Right Wheel	Left Wheel	Right Wheel	Left Wheel
Barrier Section	May, 90	0.28	0.27	0.28	0.28
	Dec., 90	0.35	0.35	0.37	0.36
	April, 91	0.40	0.39	0.36	0.37
	July, 91	0.35	0.36	0.38	0.36
	Jan., 92	0.34	0.35	0.37	0.37
	July, 92	0.37	0.35	0.40	0.39

Table 46. Serviceability Index Measurements at Dallas, IH 635 Westbound

	Date of Measurement	Inside Lane	Center Lane	Outside Lane
Barrier Section	Nov., 90	4.20	3.70	3.60
	Mar., 91	4.00	3.50	3.50
	July, 91	4.16	3.68	3.60
	Jan., 92	4.00	3.60	3.50
	July, 92	3.80	3.40	3.40
Control Section	Nov., 90	3.30	2.40	2.90
	July, 91	3.29	2.44	2.95
	Jan., 92	3.30	2.50	2.80
	July, 92	3.10	2.70	3.10

Table 47. International Roughness Measurements at Dallas, IH 635 Westbound

	Date of Measurement	Inside Lane (in/mile)		Center Lane (in/mile)		Outside Lane (in/mile)	
		Right Wheel	Left Wheel	Right Wheel	Left Wheel	Right Wheel	Left Wheel
Barrier Section	Nov., 90	70	98	75	135	97	150
	Mar., 91	72	75	86	88	101	92
	July, 91	70	128	77	171	101	177
	Jan., 92	79	127	90	156	104	160
	July, 92	84	139	100	188	112	175
Control Section	Nov., 90	102	70	144	78	100	86
	July, 91	127	70	185	83	124	89
	Jan., 92	139	80	170	92	106	95
	July, 92	152	84	184	102	146	102

Table 48. Maximum Expected Bump Height Measurements at Dallas, IH 635 Westbound

	Date of Measurement	Inside Lane (in)		Center Lane (in)		Outside Lane (in)	
		Right Wheel	Left Wheel	Right Wheel	Left Wheel	Right Wheel	Left Wheel
Barrier Section	Nov., 90	0.32	0.25	0.42	0.36	0.50	0.35
	Mar., 91	0.33	0.31	0.43	0.38	0.50	0.45
	July, 91	0.37	0.27	0.44	0.39	0.51	0.42
	Jan., 92	0.34	0.25	0.43	0.48	0.53	0.44
	July, 92	0.40	0.37	0.45	0.54	0.54	0.53
Control Section	Nov., 90	0.27	0.31	0.41	0.37	0.35	0.46
	July, 91	0.27	0.33	0.46	0.42	0.40	0.50
	Jan., 92	0.34	0.33	0.54	0.40	0.49	0.53
	July, 92	0.44	0.39	0.55	0.41	0.49	0.50

Table 49. Serviceability Index Measurements at Dallas, IH 635 Eastbound

	Date of Measurement	Inside Lane	Center Lane	Outside Lane
Barrier Section	Jan., 92	3.1	3.4	2.8
	July, 92	3.2	2.8	2.6
Control Section	Jan., 92	3.6	2.8	2.7
	July, 92	3.0	2.4	2.7

Table 50. International Roughness Measurements at Dallas, IH 635 Eastbound

	Date of Measurement	Inside Lane (in/mile)		Center Lane (in/mile)		Outside Lane (in/mile)	
		Right Wheel	Left Wheel	Right Wheel	Left Wheel	Right Wheel	Left Wheel
Barrier Section	Jan., 92	140	131	119	150	142	187
	July, 92	110	122	147	121	153	144
Control Section	Jan., 92	105	111	154	173	139	139
	July, 92	145	123	171	138	165	121

Table 51. Maximum Expected Bump Height Measurements at Dallas, IH 635 Eastbound

	Date of Measurement	Inside Lane (in)		Center Lane (in)		Outside Lane (in)	
		Right Wheel	Left Wheel	Right Wheel	Left Wheel	Right Wheel	Left Wheel
Barrier Section	Jan., 92	0.37	0.38	0.35	0.65	0.49	0.88
	July, 92	0.44	0.45	0.50	0.44	0.57	0.51
Control Section	Jan., 92	0.29	0.29	0.47	0.47	0.49	0.47
	July, 92	0.42	0.33	0.49	0.38	0.61	0.35

APPENDIX D

ESTIMATED VERTICAL MOVEMENTS

Table 52. Vertical Movement for Cracked Soil with Deep Roots

Median Type	Drainage Condition	Location	Vertical Movement (cm) Depth of barrier (ft)			
			0	3	5	8
Paved	Normal	El Paso	1.96	1.79	1.66	1.54
		San Antonio	9.59	8.29	7.26	6.67
		Dallas	11.50	10.84	9.96	8.87
		Houston	9.27	9.10	8.68	7.82
		Port Arthur	9.26	9.13	8.72	7.86
	Slope	El Paso	1.91	1.78	1.65	1.52
		San Antonio	8.50	7.48	6.47	6.00
		Dallas	13.13	12.63	11.93	10.94
		Houston	10.60	9.84	9.04	8.16
		Port Arthur	10.45	9.79	9.01	8.01
	Ponded	El Paso	6.73	6.09	5.51	5.11
		San Antonio	13.82	12.81	12.33	12.18
		Dallas	16.59	16.40	16.04	15.57
		Houston	8.92	8.87	8.35	7.57
		Port Arthur	8.17	7.81	7.26	6.45
Sodded	Normal	El Paso	2.12	1.95	1.84	1.70
		San Antonio	9.62	8.57	7.66	7.10
		Dallas	11.58	11.01	10.28	9.39
		Houston	9.28	9.44	9.20	8.76
		Port Arthur	9.25	9.48	9.27	8.83
	Slope	El Paso	2.07	1.94	1.82	1.69
		San Antonio	8.58	7.76	6.86	6.34
		Dallas	12.71	12.66	11.91	11.10
		Houston	10.52	10.15	9.51	8.94
		Port Arthur	10.47	10.31	9.65	9.01
	Ponded	El Paso	8.35	7.43	6.40	5.68
		San Antonio	12.68	12.13	11.59	11.60
		Dallas	14.56	14.95	14.80	14.96
		Houston	8.74	8.97	8.77	8.25
		Port Arthur	8.15	8.10	7.87	7.29

Table 53. Vertical Movement for Medium Cracked Soil with Deep Roots

Median Type	Drainage Condition	Location	Vertical Movement (cm) Depth of barrier (ft)			
			0	3	5	8
Paved	Normal	El Paso	1.27	1.07	0.98	0.84
		San Antonio	5.63	4.56	3.87	3.43
		Dallas	8.27	6.74	5.64	4.41
		Houston	6.18	4.87	3.54	2.08
		Port Arthur	5.94	4.61	3.26	1.79
	Slope	El Paso	1.26	1.13	0.97	0.84
		San Antonio	4.77	4.02	3.64	3.53
		Dallas	10.86	9.24	8.37	7.55
		Houston	7.11	5.73	4.53	3.20
		Port Arthur	7.09	5.66	4.42	3.02
	Ponded	El Paso	2.88	2.77	2.47	2.27
		San Antonio	8.88	8.01	7.31	6.91
		Dallas	11.32	10.10	8.93	7.74
		Houston	6.66	5.30	3.93	2.37
		Port Arthur	5.86	4.49	3.10	1.50
Sodded	Normal	El Paso	1.29	1.15	0.98	0.83
		San Antonio	5.54	4.43	3.69	3.18
		Dallas	8.13	6.60	5.44	4.14
		Houston	6.36	5.01	3.66	2.12
		Port Arthur	6.14	4.80	3.40	1.86
	Slope	El Paso	1.29	1.14	0.97	0.83
		San Antonio	4.67	3.83	3.39	3.26
		Dallas	10.58	8.87	7.99	7.09
		Houston	7.13	5.72	4.46	3.05
		Port Arthur	7.17	5.72	4.43	2.95
	Ponded	El Paso	2.74	2.61	2.30	2.10
		San Antonio	8.55	7.68	6.96	6.55
		Dallas	11.19	9.97	8.74	7.48
		Houston	6.81	5.44	4.02	2.38
		Port Arthur	6.07	4.69	3.25	1.56

Table 54. Vertical Movement for Tight Soil with Shallow Roots

Median Type	Drainage Condition	Location	Vertical Movement (cm) Depth of barrier (ft)			
			0	3	5	8
Paved	Normal	El Paso	0.06	0.03	0.01	0.00
		San Antonio	1.63	1.58	1.57	1.56
		Dallas	2.72	2.82	2.50	2.50
		Houston	1.13	1.16	0.73	0.59
		Port Arthur	0.82	0.88	0.44	0.28
	Slope	El Paso	0.06	0.03	0.00	0.00
		San Antonio	1.61	1.56	1.55	1.53
		Dallas	4.31	4.59	4.42	4.41
		Houston	2.19	2.24	1.87	1.84
		Port Arthur	2.16	2.17	1.78	1.72
	Ponded	El Paso	1.18	1.26	1.18	1.18
		San Antonio	3.25	3.55	3.44	3.45
		Dallas	3.22	3.54	3.16	3.16
		Houston	1.05	1.11	0.69	0.53
		Port Arthur	0.63	0.67	0.23	0.06
Sodded	Normal	El Paso	0.05	0.03	0.00	0.00
		San Antonio	1.51	1.44	1.44	1.43
		Dallas	2.60	2.67	2.35	2.35
		Houston	1.10	1.12	0.69	0.55
		Port Arthur	0.81	0.86	0.41	0.26
	Slope	El Paso	0.05	0.02	0.00	0.00
		San Antonio	1.48	1.43	1.41	1.39
		Dallas	4.10	4.36	4.19	4.17
		Houston	2.09	2.13	1.75	1.72
		Port Arthur	2.06	2.07	1.67	1.62
	Ponded	El Paso	1.13	1.20	1.10	1.10
		San Antonio	3.20	3.48	3.36	3.37
		Dallas	3.17	3.46	3.07	3.08
		Houston	1.03	1.09	0.65	0.50
		Port Arthur	0.62	0.65	0.22	0.05

APPENDIX E

DESIGN AND CONSTRUCTION OF VERTICAL MOISTURE BARRIERS

DESIGN AND CONSTRUCTION OF VERTICAL MOISTURE BARRIERS

SITE INVESTIGATION

Site investigation is essential before installing vertical moisture barriers in pavements. Sufficient information must be obtained to enable a safe and economic design. The primary objectives of the investigation are:

1. to determine the sequence, thickness and lateral extent of the soil strata, and
2. to collect representative samples of the soils for identification, classification, and for use in laboratory tests to determine relevant soil parameters.

Before the start of the comprehensive site investigation, a study of available geological maps and U.S. Soil Conservation Service county soil survey reports should be made and an inspection of the site and the surrounding area should be made on foot. Valuable information regarding the nature of subsurface soil conditions can be obtained by examining existing excavations, river banks, quarries, and road or railway cuts.

In dry weather, the surface of expansive soils is characterized by deep cracking. Maximum crack depth in a subgrade soil is a very important parameter in the design of vertical moisture barriers in pavements on expansive soils. If the rooting depth of resident vegetation is known, an estimate for the crack depth can be made. Generally, grass roots cause cracks to a depth of 4-8 ft. Where trees are growing or have grown in the past, cracks penetrate to the depth of the root zone plus about 2 ft more. Root depths may be determined from

borings by logging the samples taken for root fibers. The depth of the last sample where fibers were still found is an estimate of the root depth. Existing structures should be examined for signs of damage due to soil movement. As the drainage pattern in the area affects the availability of water to the subgrade, the drainage condition of the area should also be obtained. Different longitudinal drainage conditions (normal, ponded, or slope) found along highway pavements are shown in Figure 129.

Based on the information obtained from the site visit, a comprehensive site investigation should be planned. Planning should include the determination of depth and location of borings. The number, location, and depth of boreholes should enable the basic soil layering structure of the site to be determined and significant irregularities in the subsurface conditions to be detected. The greater the degree of variability of the subsurface conditions, the greater the number of boreholes are required. Borings may be made in several stages. In the first stage, borings may be widely spaced. Based upon the findings from the initial borings, additional borings may be made between the initial borings to define the soil conditions in better detail. As a rule of thumb, borings should be placed every 100 m (or yards). They should be farther apart in uniform soils and closer together where the soil deposits are more variable. In order to carry out laboratory tests, it is recommended to collect Shelby tube soil samples at two foot intervals in all borings. Borings should be at least twice as deep as the expected depth of the moisture barrier.

For the samples collected from borings, the following laboratory tests should be carried out:

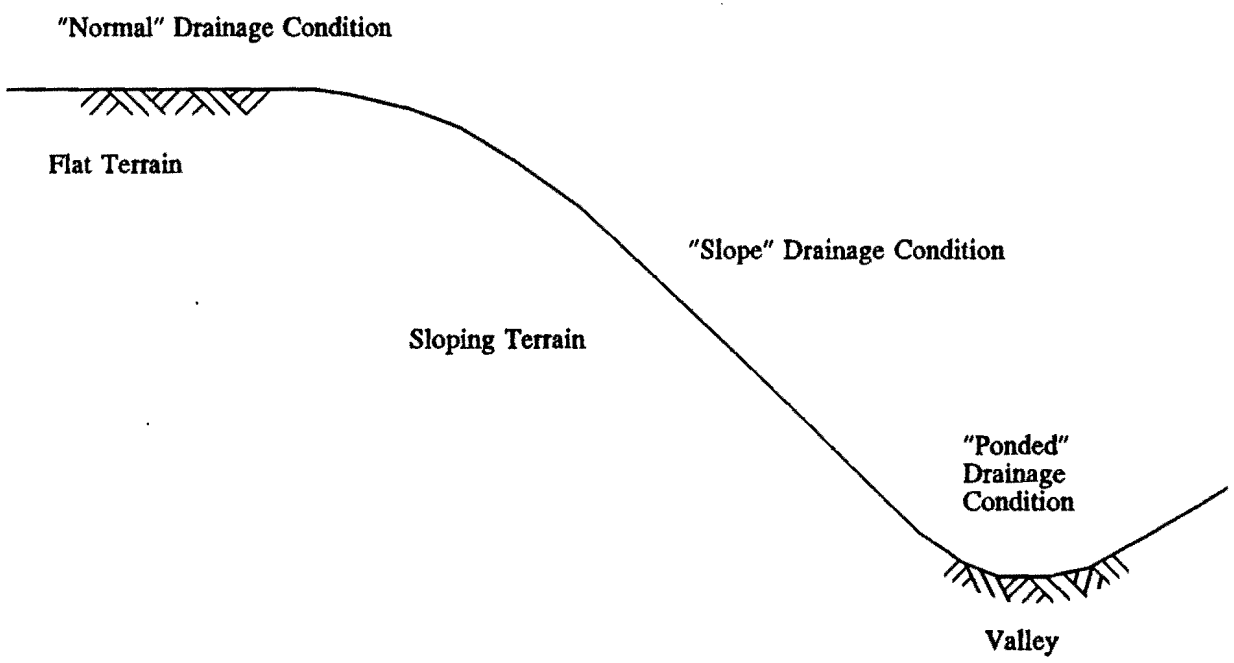

Figure 129. Types of Longitudinal Drainage Conditions along Highway Pavements

1. Atterberg limits,
2. percentage passing no. 200 sieve,
3. percent of fine clay (grain size less than 0.002 mm) from hydrometer analysis.,
4. filter paper suction,
5. specific gravity of soil particles for use in the hydrometer test,
6. dry density,
7. natural moisture content,
8. laboratory suction using pressure plate apparatus (optional), and
9. cation exchange capacity (optional).

After an investigation has been completed and the results of laboratory tests are available, the subsurface conditions discovered in each borehole should be summarized in the form of a borehole log. The log is prepared with reference to a vertical scale. The following details should be shown in a borehole log:

1. location, boring number, date of boring, and elevation of the ground surface at the boring and datum used;
2. date started and completed and interruptions;
3. name of driller and soils engineer or technician;
4. any unusual conditions noted or any other conditions observed which might be pertinent;
5. a detailed description of each stratum and the levels of strata boundaries;
6. the level at which boring was terminated; and
7. results of laboratory or in situ tests.

In order to identify the locations where moisture barriers are effective, longitudinal profiles showing the three soil types (cracked or pervious, moderately cracked, and tight) should be drawn along the length of the project. A method of identifying these soil conditions is given below in this appendix. In reducing the development of roughness in pavements, vertical moisture barriers are effective only when the subgrade soil is moderately cracked (when the unsaturated permeability ranges between 0.00005 and 0.001 cm^2/sec). In cracked or highly pervious subgrade soils (when the unsaturated permeability is greater than 0.001 cm^2/sec) or tight subgrade soils (when the unsaturated permeability is less than 0.00005 cm^2/sec) vertical moisture barriers are not effective. Moisture barriers should be placed only where moderately cracked soils are shown on the longitudinal soil profile drawn along the length of the project.

METHOD OF ANALYSIS

1. Perform simple linear regression for the data obtained from laboratory suction tests using percentage gravimetric water content (as a decimal) as the independent variable and soil suction (pF) as the dependent variable and estimate the slope of the straight line. If the laboratory suction results are not available, the following equation can be used to estimate the slope of the straight line:

$$S = -20.288 + 0.1551\ (LL) - 0.1167\ (PI) + 0.0684\ (\#200) \quad (34)$$

where,

S = Slope of the straight line (suction-water-content

slope). This should be a negative number which ranges between 0 and -20.

LL = Liquid limit, in percent (a number between 0 and 100).

PI = Plasticity index, in percent (a number between 0 and 100).

#200 = Percentage passing the no. 200 sieve (a number between 0 and 100).

2. Estimate the activity and the cation exchange activity of the soils using the following relationships:

Activity = PI/% fine clay

Cation Exchange activity = CEC/% fine clay

where,

PI = plasticity index,

CEC = cation exchange capacity, and

% fine clay = % passing 0.002 mm size/% passing #200.

Cation exchange capacity can be obtained directly from the cation exchange capacity test or from the following relationship:

$$CEC = (PL\%)^{1.17} \text{ meq/100 gm} \quad (35)$$

where,

PL = plastic limit, in percent.

3. Plot the activity and cation exchange activity of soils on McKeen's chart for the prediction of the suction compression index (SCI) and read the corresponding values of the suction compression index of soils with 100% fine clay content. The McKeen's chart is shown in Figure 130 and the values of SCI for each region in the chart is given in Table 55. Obtain the actual suction compression

index for each soil sample by multiplying the suction compression index obtained from the chart by the fine clay percentage (as a decimal) of each soil sample.

Table 55. SCI Values from McKeen's Chart

Region	SCI
I	0.220
II	0.163
III A	0.096
III B	0.096
IV A	0.061
IV B	0.061
V A	0.033
V B	0.033

4. Estimate the diffusion coefficient from the following relationship:

$$\alpha = 0.0029 - 0.000162(S) - 0.0122(SCI) \quad (36)$$

where,

α = diffusion coefficient (cm^2/sec),

S = suction-water-content slope (a negative number), and

SCI = suction compression index (a positive number between 0 and 0.22).

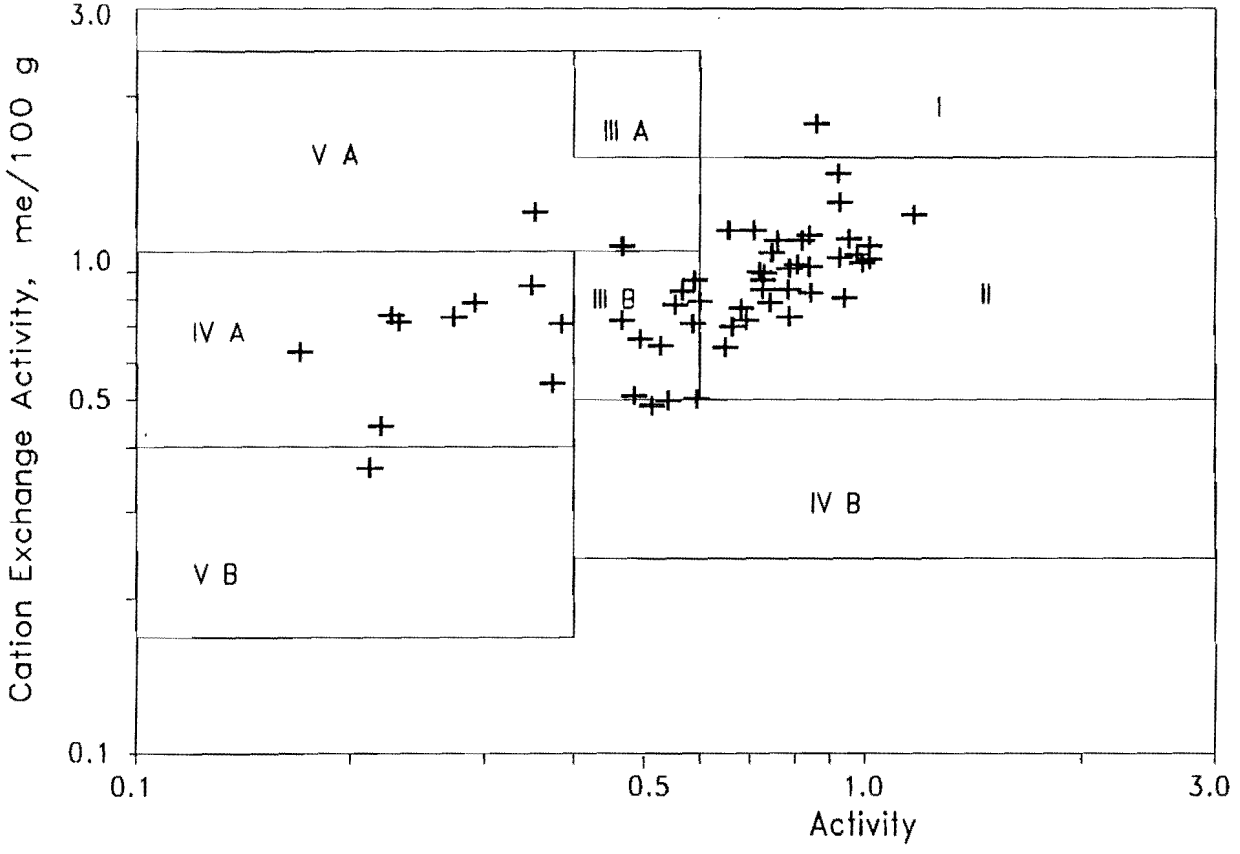

Figure 130. McKeen's Chart for the Prediction of Suction Compression Index

5. Estimate the unsaturated permeability from the following relationship:

$$P = \frac{\alpha \gamma_d}{|S| \gamma_w} \qquad (37)$$

where,

α = diffusion coefficient (cm^2/sec),

γ_w = density of water,

γ_d = dry density of soil,

$|S|$ = absolute value of the suction-water-content slope, and

P = unsaturated permeability (cm^2/sec).

6. Determine the soil type (cracked or highly permeable, medium cracked or moderately permeable, or tightly closed cracks or minimally permeable) based on the estimated unsaturated permeability. The ranges of unsaturated permeability for each soil type are given in Table 56.

Table 56. Unsaturated Permeability in Different Soil Types

Soil Type	Unsaturated Permeability (cm^2/sec)
Cracked or pervious	> 0.001
Medium cracked	0.00005 - 0.001
Tight	< 0.00005

7. Vertical moisture barriers are not effective in tight or cracked subgrade soils under any of the drainage conditions. They are effective in medium cracked soils in all climates and under all

drainage conditions except for the following two conditions:

1. extremely dry climates, and
2. semi-arid climates under "ponded" drainage conditions.

8. In locations where vertical moisture barriers are effective, the depth of the barrier should be greater than or at least equal to the depth of the root zone. Where gravel or sand seams are present, vertical moisture barriers should go below those seams.
9. Using the subgrade soil investigation report and longitudinal soil profiles, determine the locations where moisture barriers are effective and the depth of the barrier needed for each location and provide vertical moisture barriers accordingly. However, it is not recommended to provide vertical moisture barriers less than 0.25 miles long.

GUIDELINES FOR THE CONSTRUCTION OF VERTICAL MOISTURE BARRIERS

1. The barrier should be placed along the edge of the paved surface of the roadway. The barrier should normally be 8 ft (2.4 m) deep. A greater depth may be required by site conditions revealed by the site investigation.
2. The fabric barrier should be placed at the inside edge of the trench excavated at the edge of the paved surface of the roadway. The trench should be backfilled with a graded material. The top one foot of the trench should consist of base materials or lean concrete.
3. Sand has been found to be a poor backfill material because it tends to settle after being placed, leaving a void beneath the trench cap. A good test for a candidate backfill material is to

place it in a concrete cylinder mold and shake it. If it reduces volume due to the shaking, it will leave a void and should not be used. Lightweight aggregate has been found to be an acceptable backfill material in the Dallas district (District 18).

4. An impermeable asphalt concrete layer should be placed over the pavement and it should be extended beyond the barrier.
5. Construction joints including the lane-shoulder joint in the asphalt concrete layer should be properly sealed so that water does not penetrate to the subgrade from the surface.
6. Proper drainage should be maintained in the drainage ditches beside the roadway. In roadway sections where frequent maintenance is required to provide proper drainage, side ditches may be paved with concrete.
7. Whenever a crack appears in the pavement surface, it should be sealed immediately.